Charge dependent flow, early magnetic field and chiral magnetic effect in heavy ion collisions at ALICE

Shi Qiu

The XVth Quark Confinement and the Hadron Spectrum Conference, 1/8/2022

Content of the talk

- Probe electromagnetic field
  - Charge-dependent directed flow
    - Inclusive hadron measurements
    - Heavy flavor measurements (D^0 & $\overline{D}^0$)
  - Hyperon Polarization
- Searches for chiral anomalies
  - Chiral magnetic effect studies
    - Mix harmonic
    - Event shape engineering

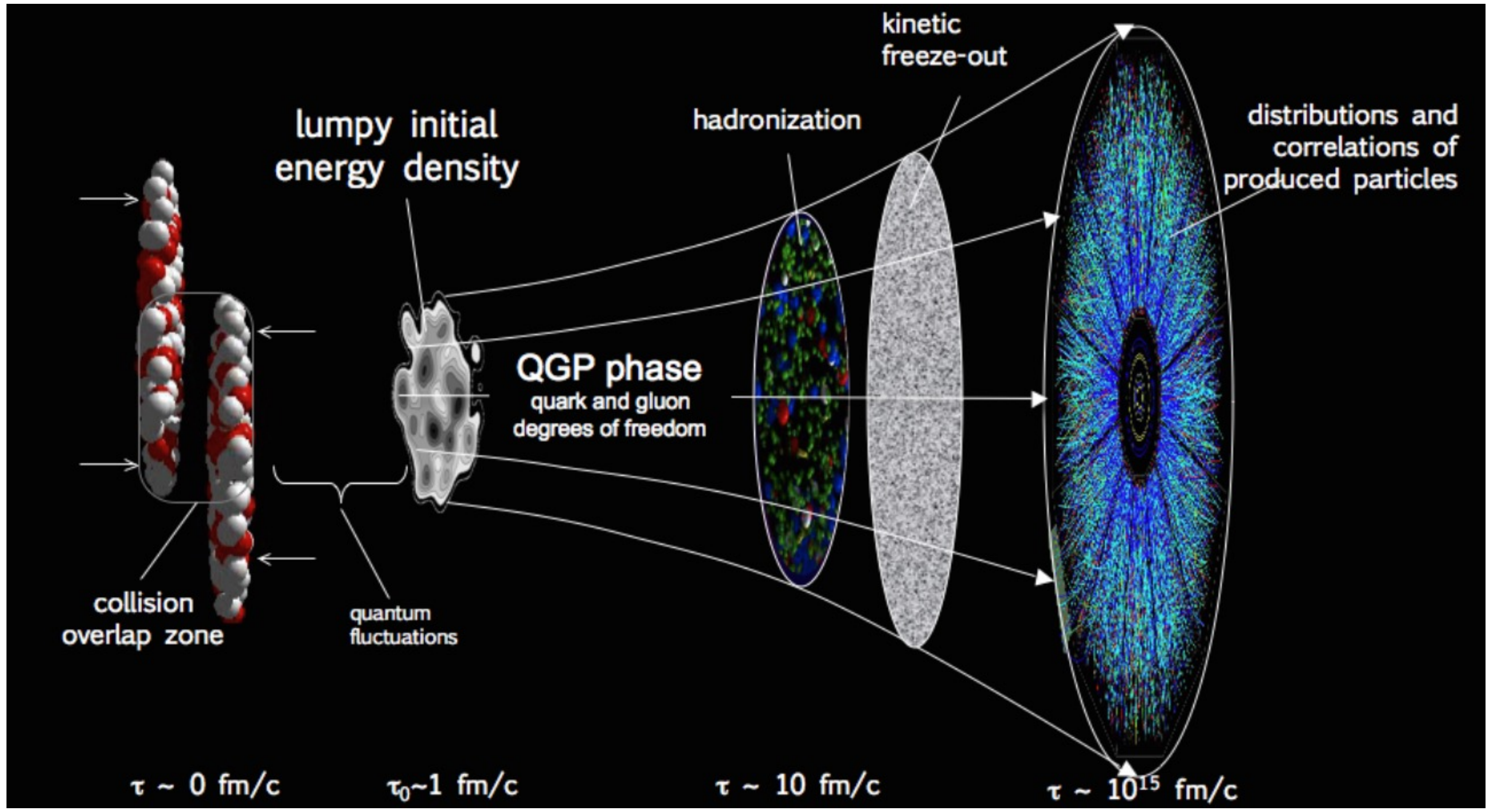

A Large Ion Collider Experiment

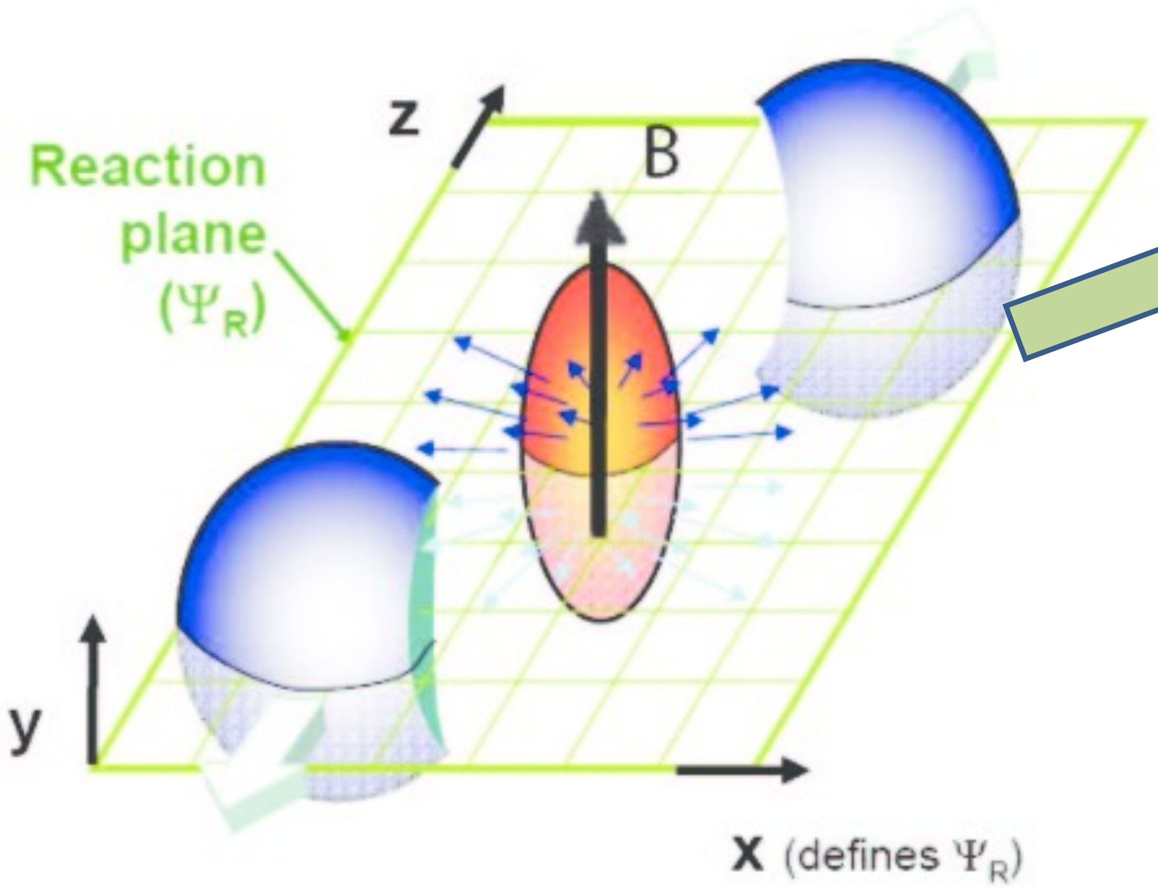

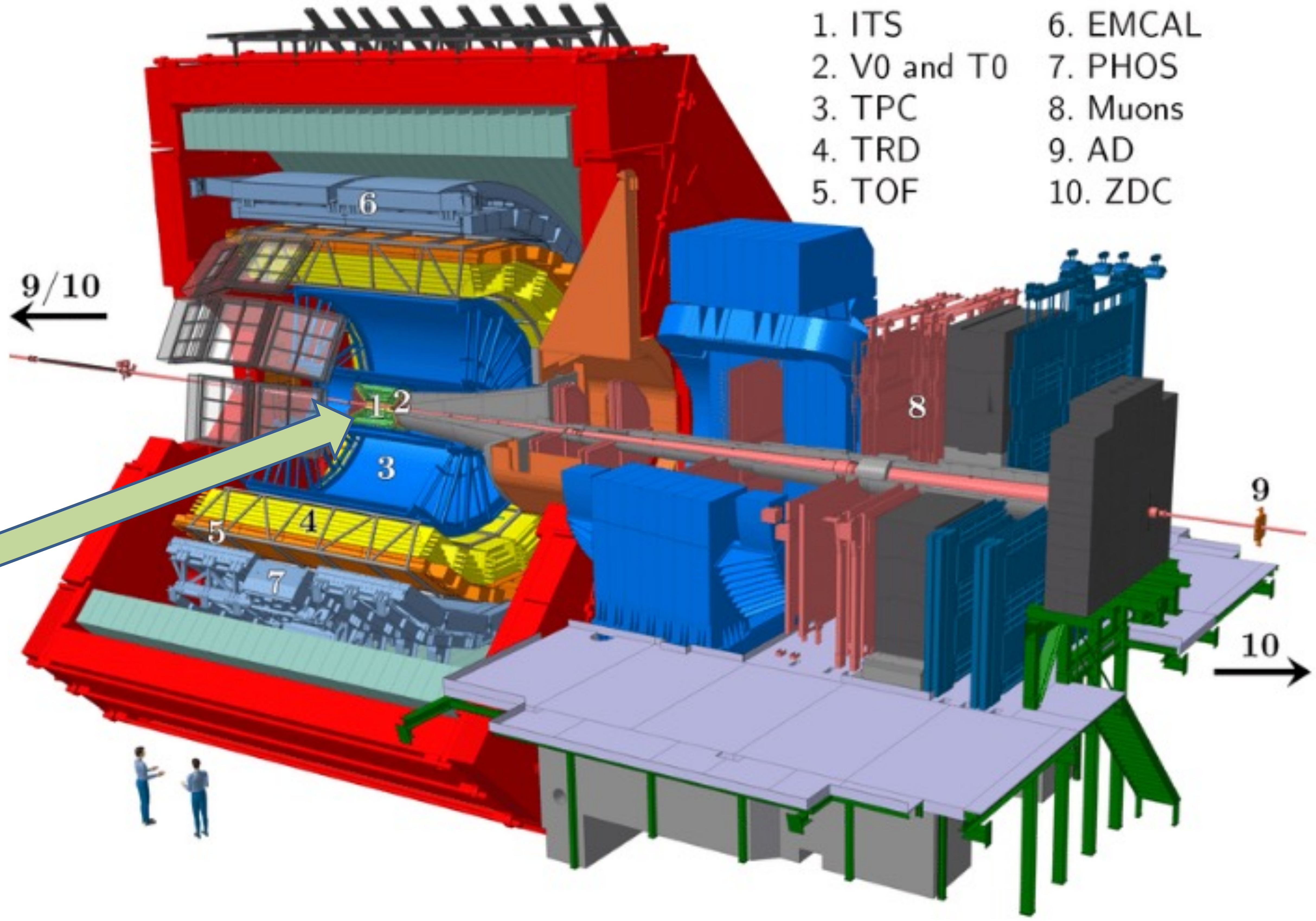

A Large Ion Collider Experiment

- ITS: semiconductor detector measuring charged particle traversing its segments ($|\eta| < 0.9$)

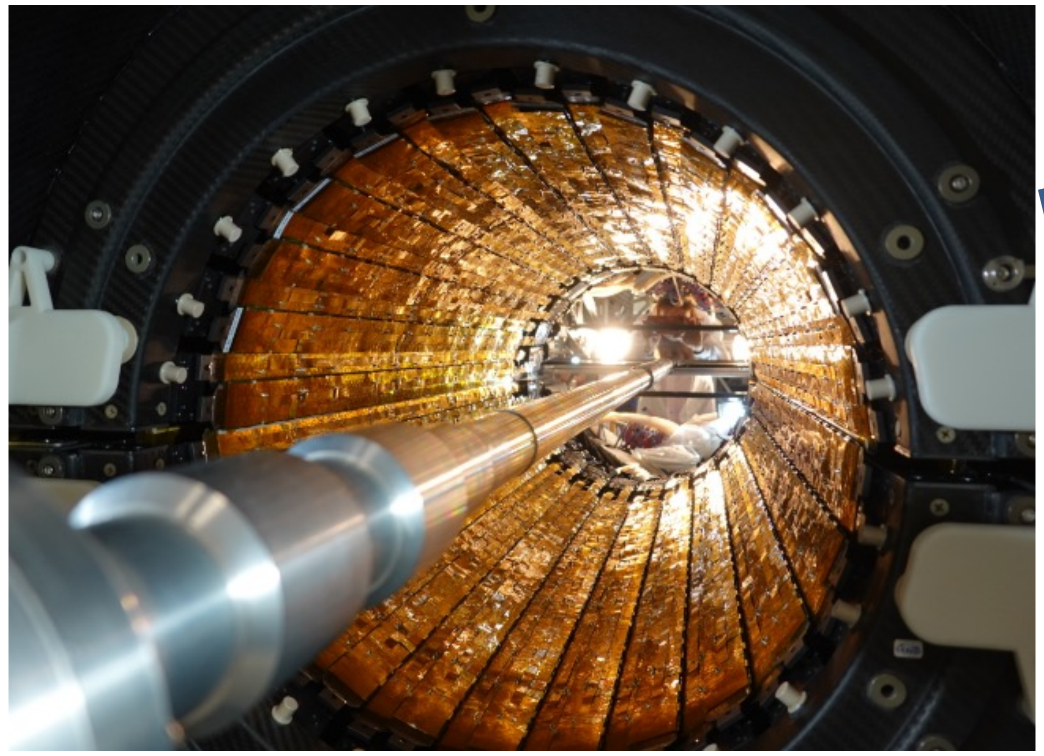

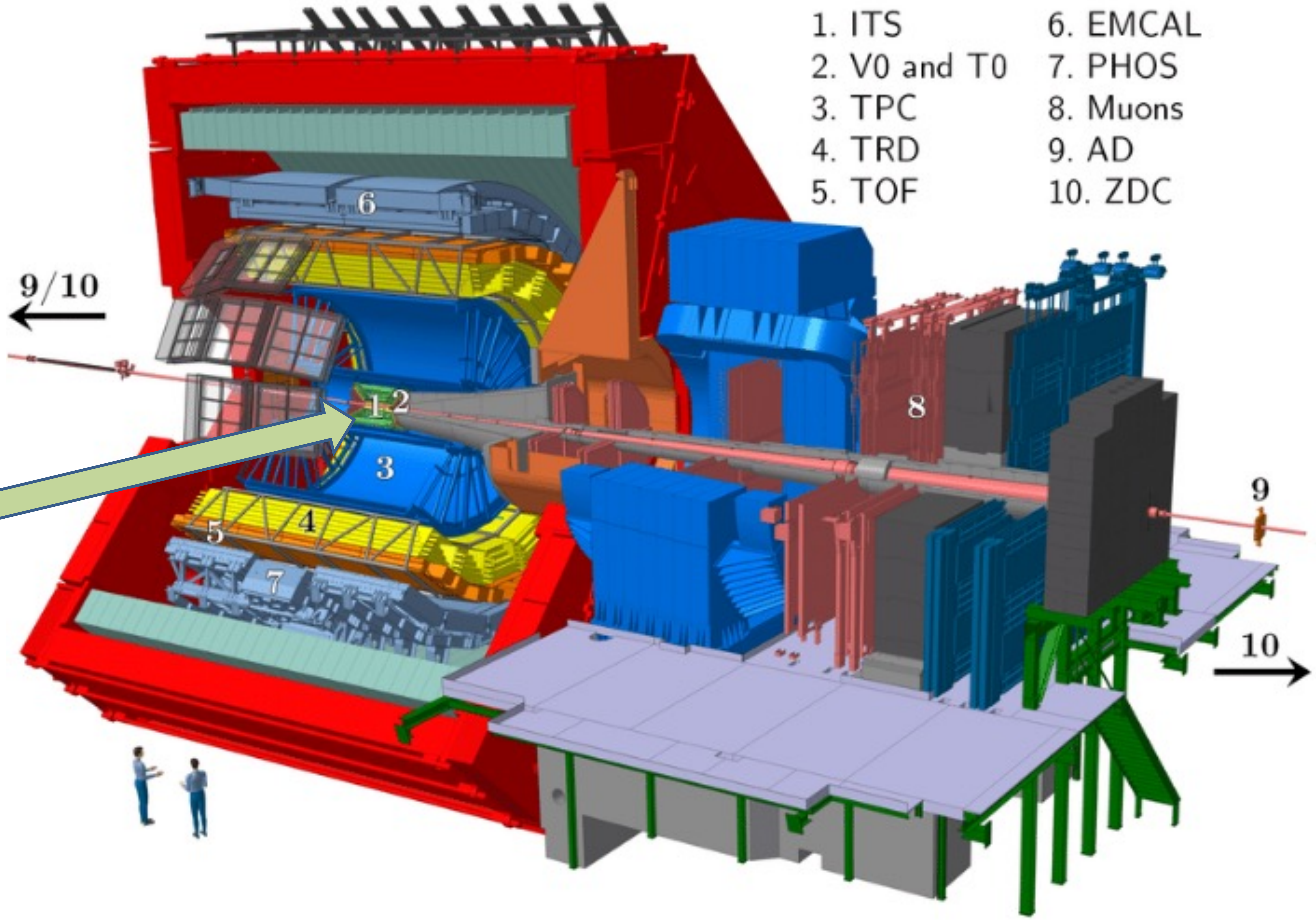

A Large Ion Collider Experiment

- ITS: a semiconductor detector measuring charged particle traversing its segments ($|\eta| < 0.9$)
- TPC: cylindrical gas detector used to reconstruct tracks and identify the particle species ($|\eta| < 0.9$)

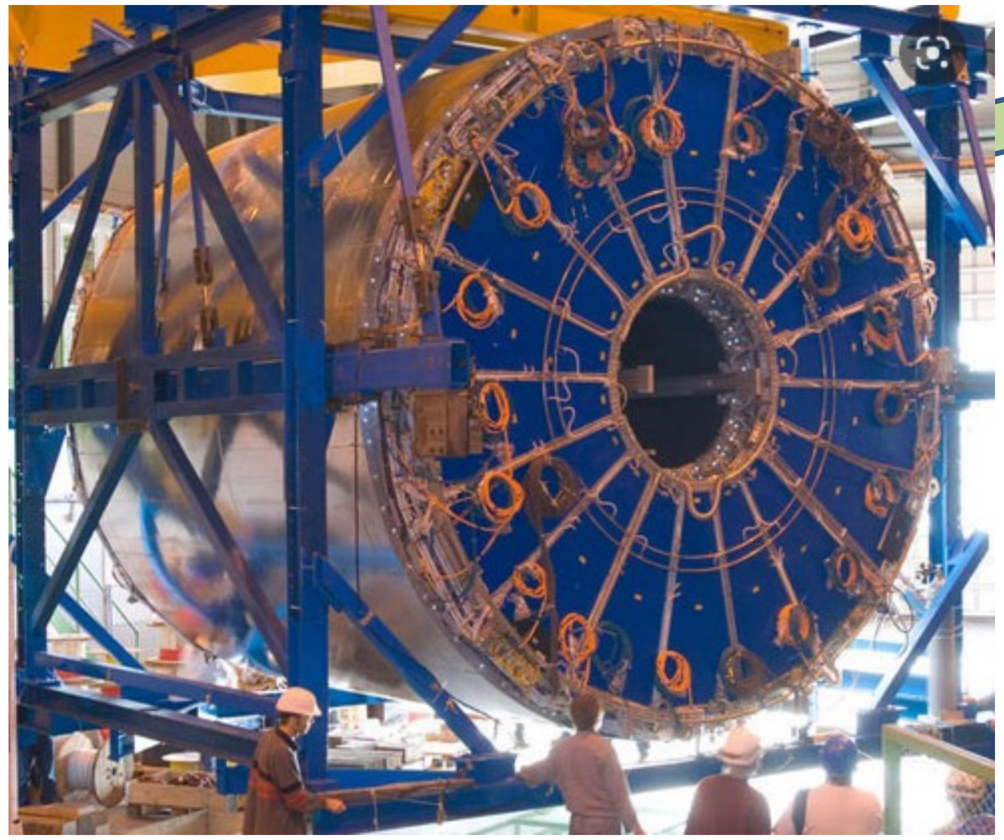

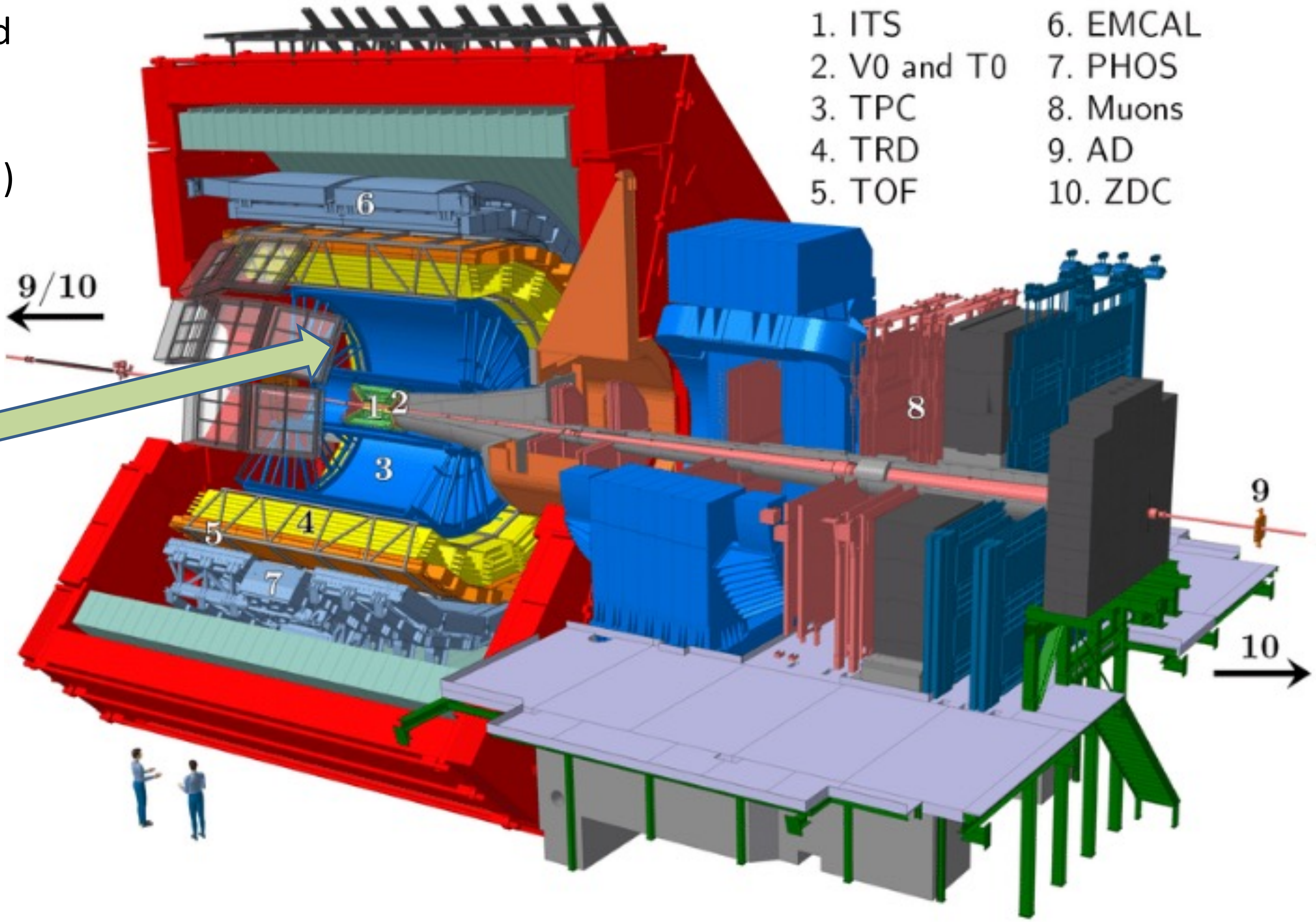

A Large Ion Collider Experiment

- ITS: a semiconductor detector measuring charged particle traversing its segments ($|\eta| < 0.9$)
- TPC: cylindrical gas detector used to reconstruct tracks and identify the particle species ($|\eta| < 0.9$)
- V0: two cylindrical scintillators located at opposite sides of the interaction point ($\mathrm{V0C}$: $2.8 < |\eta| < 5.1$, $\mathrm{V0A}$: $-3.7 < |\eta| < -1.7$)

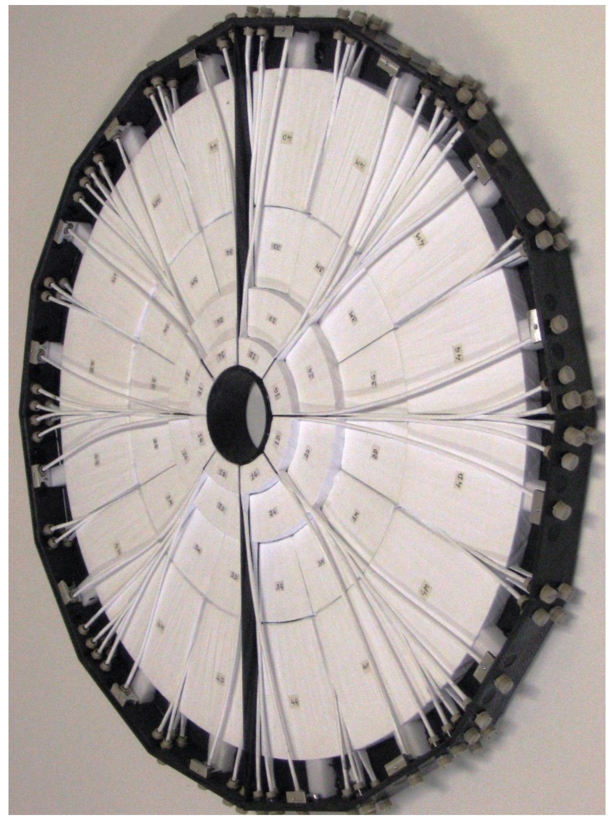

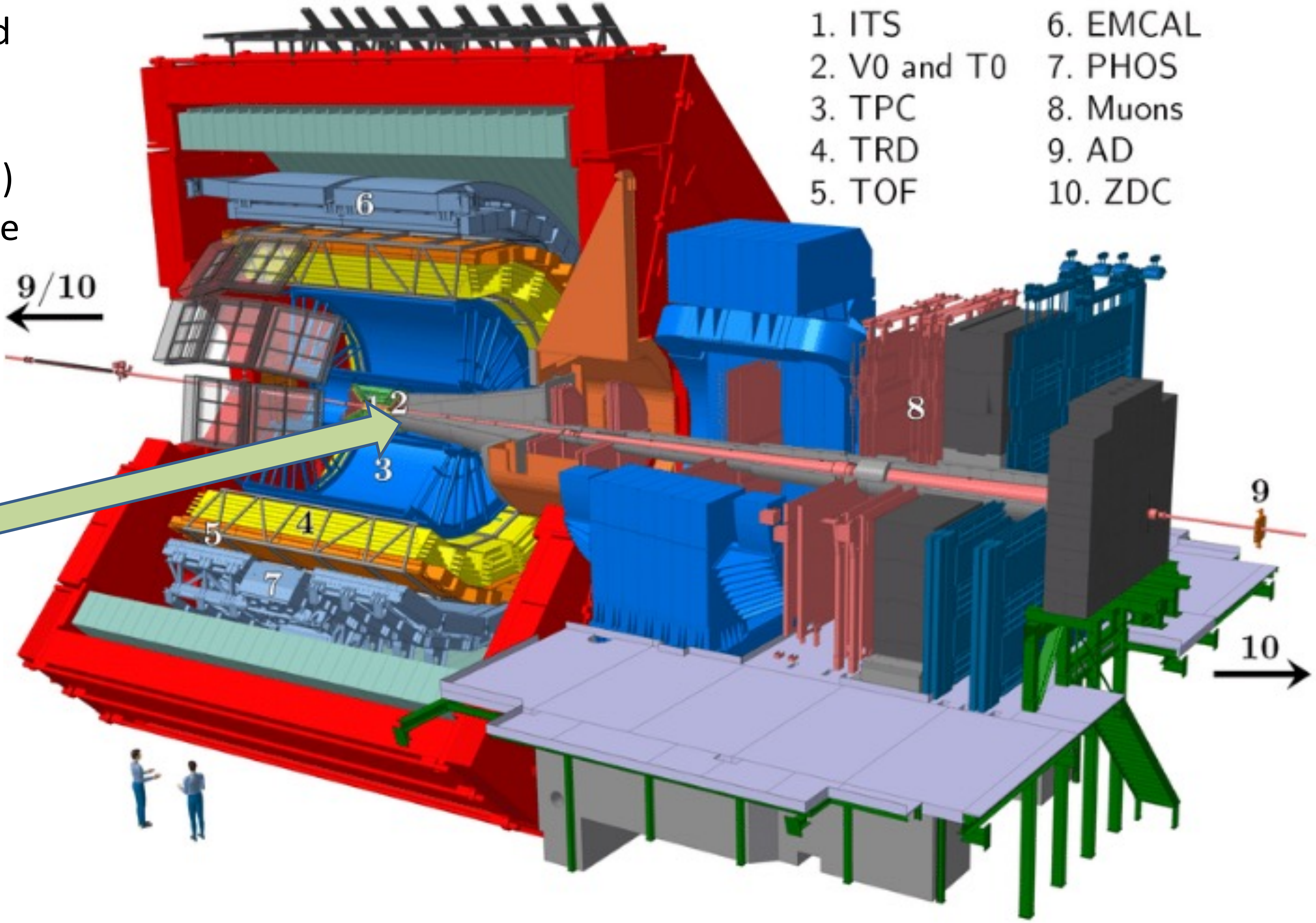

A Large Ion Collider Experiment

- ITS: a semiconductor detector measuring charged particle traversing its segments ($|\eta| < 0.9$)
- TPC: cylindrical gas detector used to reconstruct tracks and identify the particle species ($|\eta| < 0.9$)
- V0: two cylindrical scintillators located at opposite sides of the interaction point ($\mathrm{V0C}:\ 2.8 < \eta < 5.1, \mathrm{V0A}: -3.7 < \eta < -1.7$)
- ZDC: hadronic calorimeters located at beam rapidities ($4.8 < |\eta| < 5.7$)

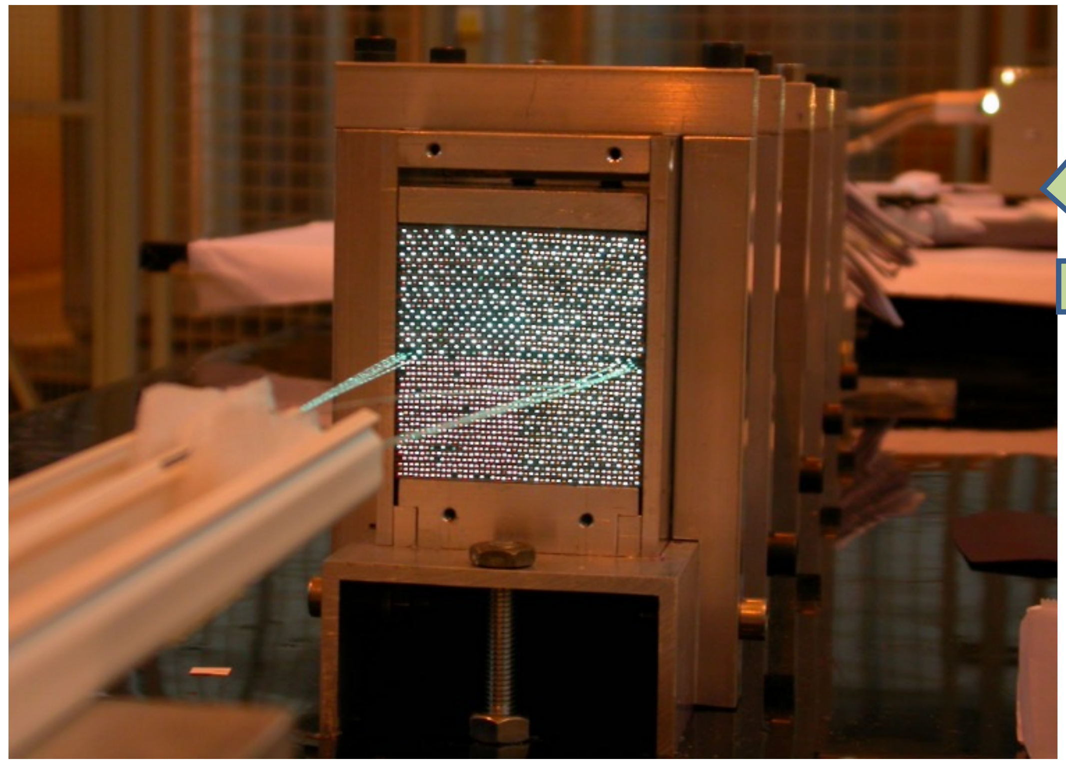

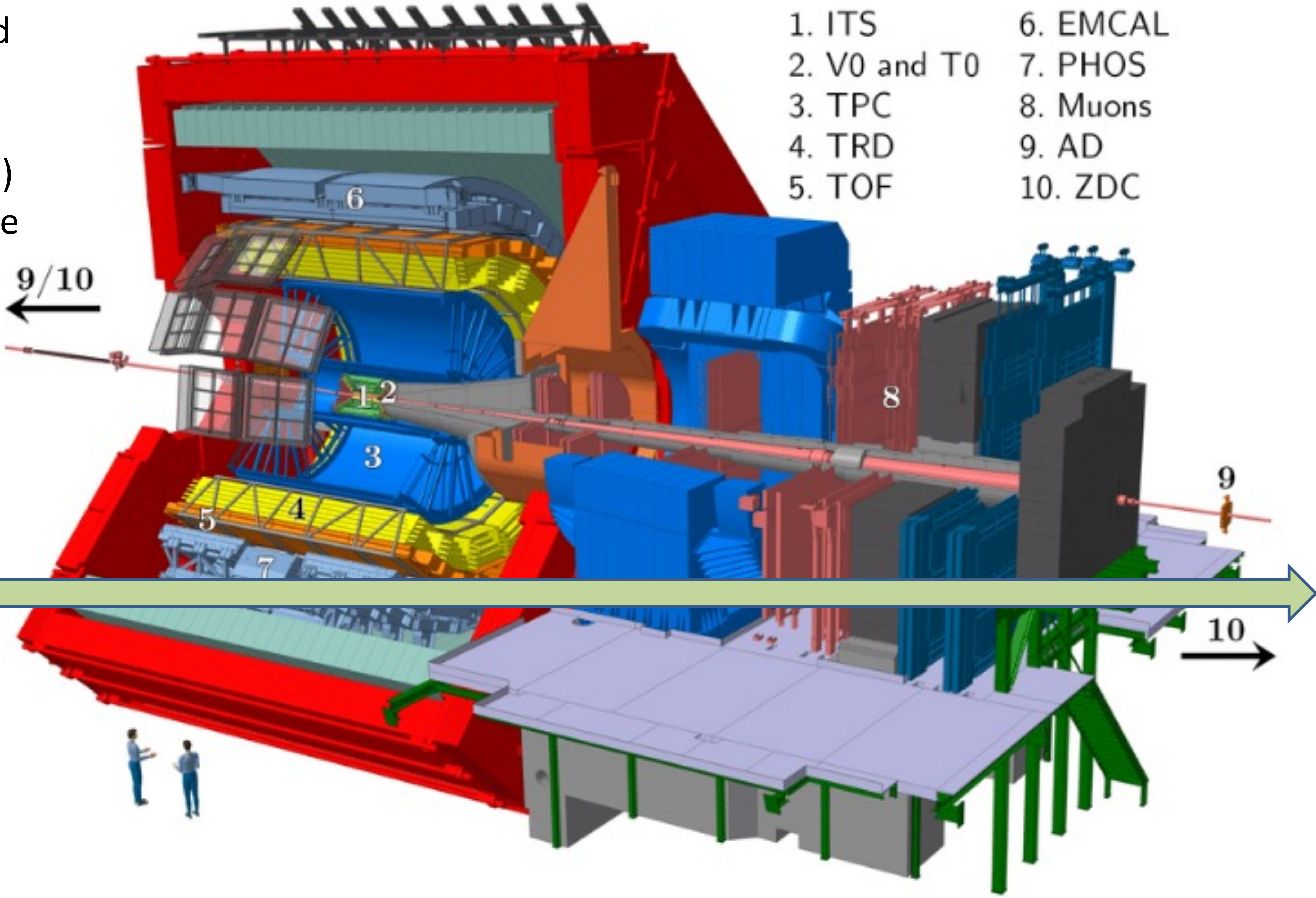

A Large Ion Collider Experiment

- ITS: a semiconductor detector measuring charged particle traversing its segments ($|\eta| < 0.9$)
- TPC: cylindrical gas detector used to reconstruct tracks and identify the particle species ($|\eta| < 0.9$)
- V0: two cylindrical scintillators located at opposite sides of the interaction point ($\mathrm{V0C}:\ 2.8 < |\eta| < 5.1, \mathrm{V0A}: -3.7 < |\eta| < -1.7$)
- ZDC: hadronic calorimeters located at beam rapidities ($4.8 < |\eta| < 5.7$)

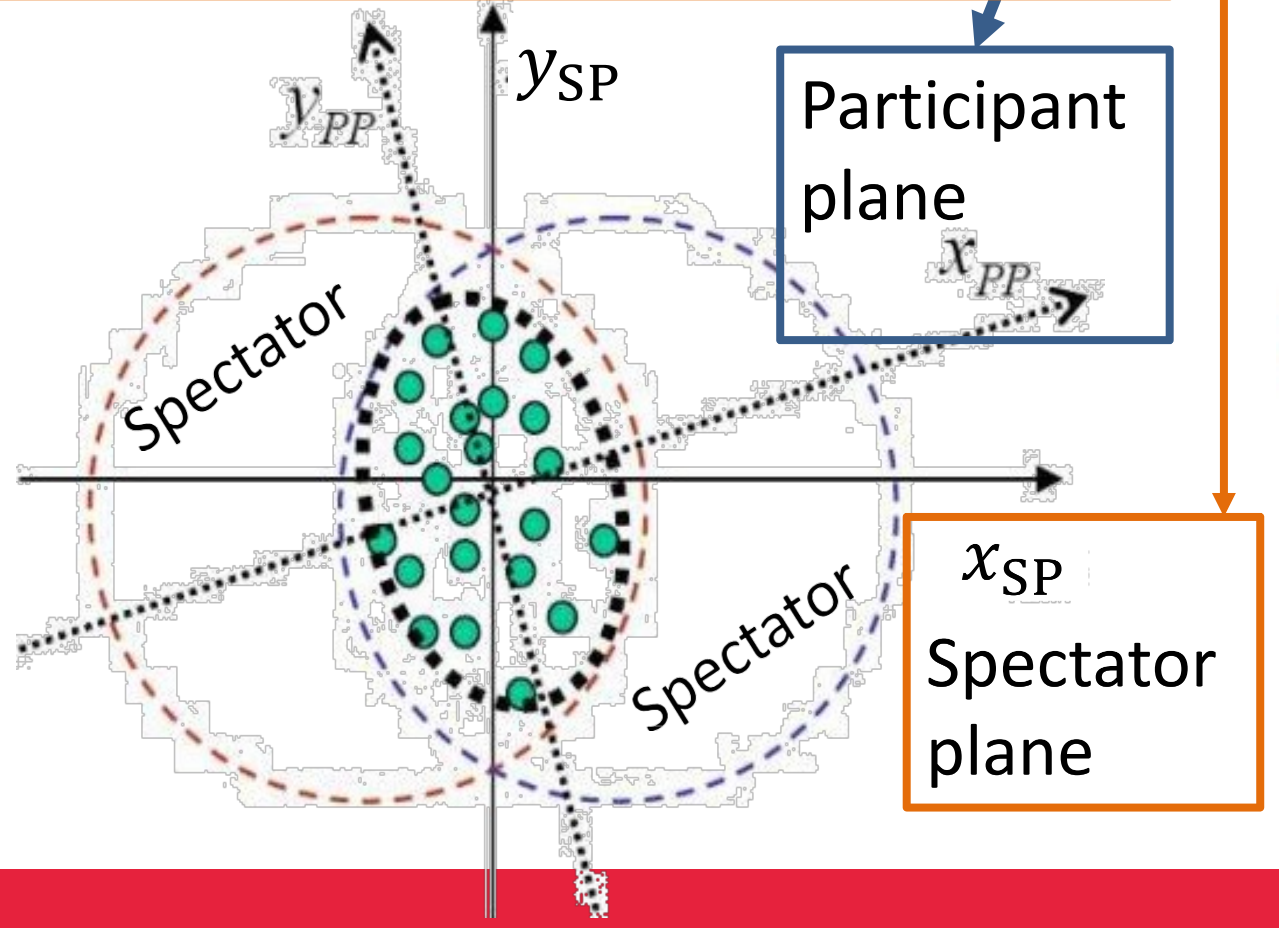

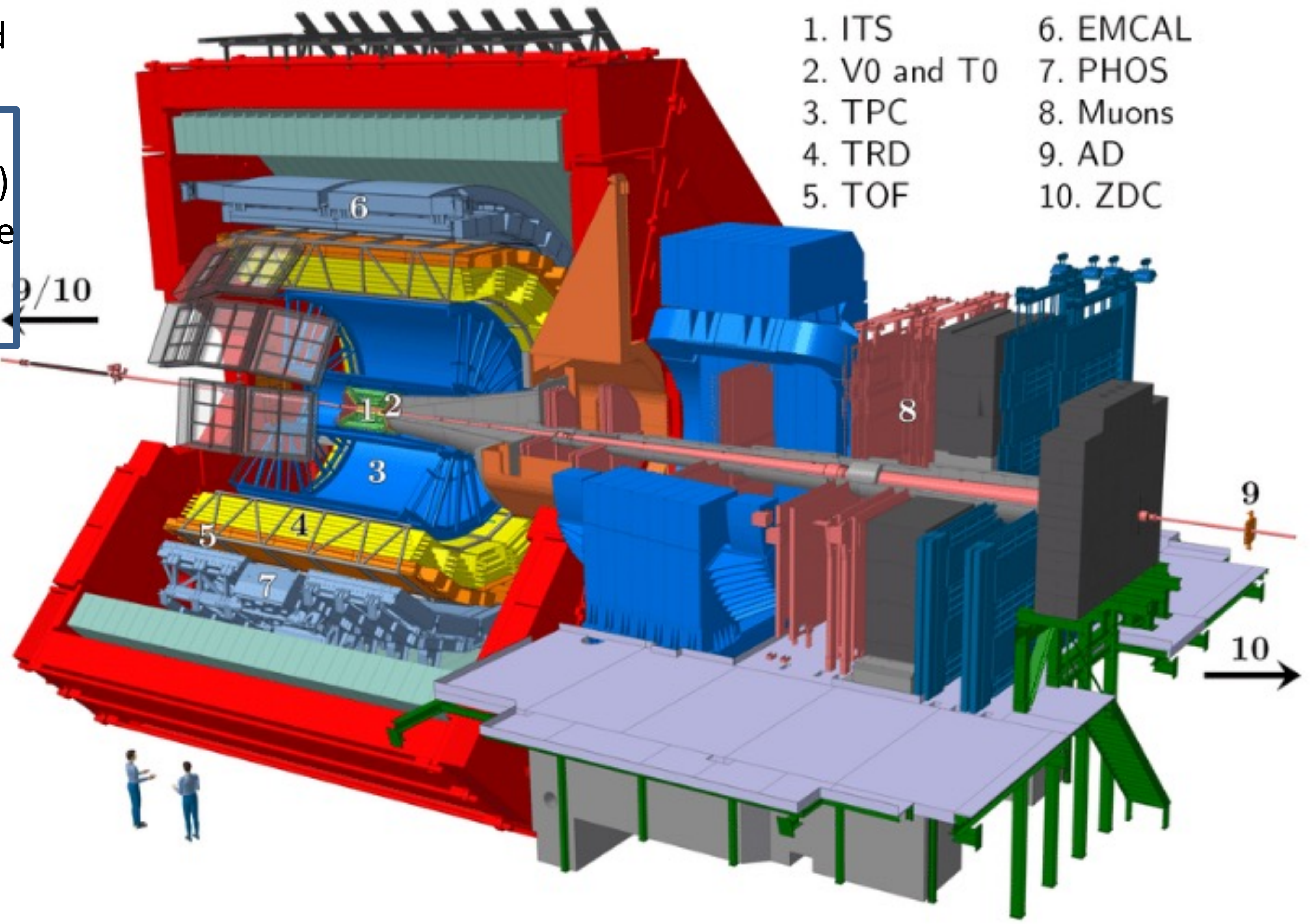

Electromagnetic field in heavy-ion collisions

- Complicated interplay of E and B fields gives rise to four types of currents
  - **Faraday current**: induced current from the decrease of the B field in the medium

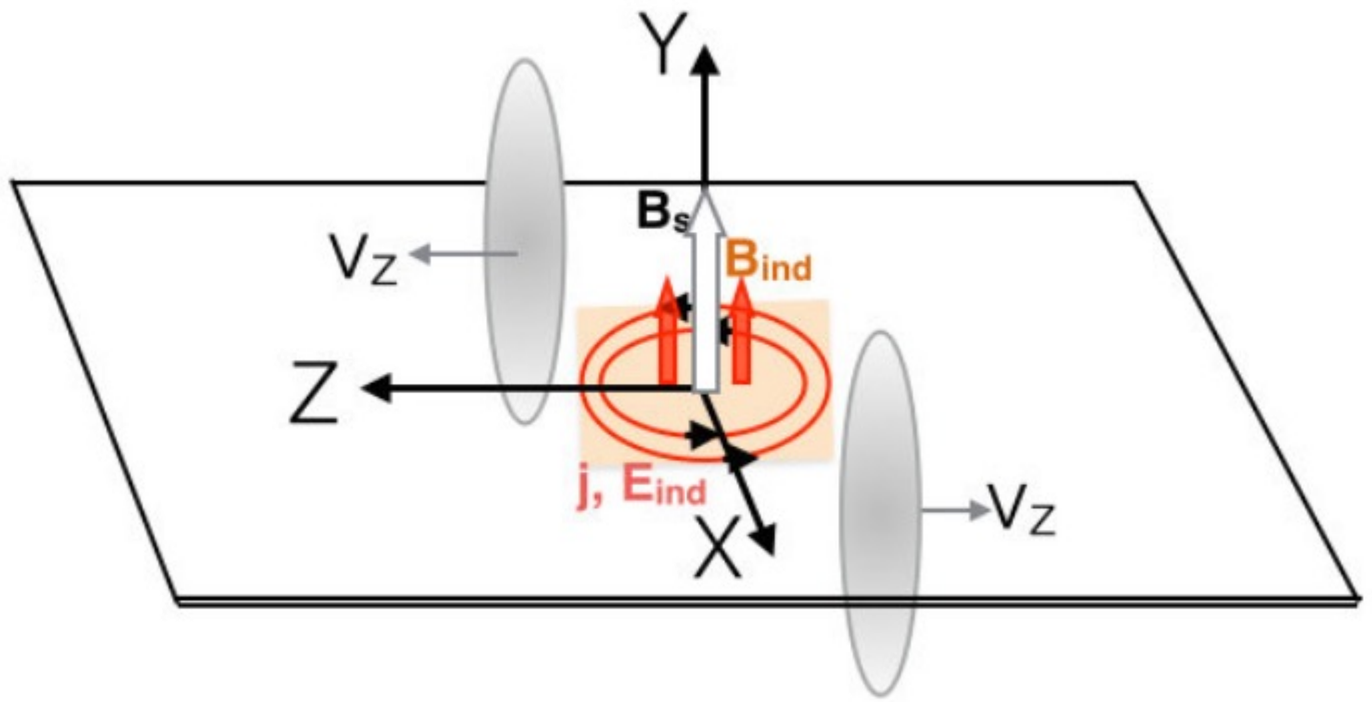

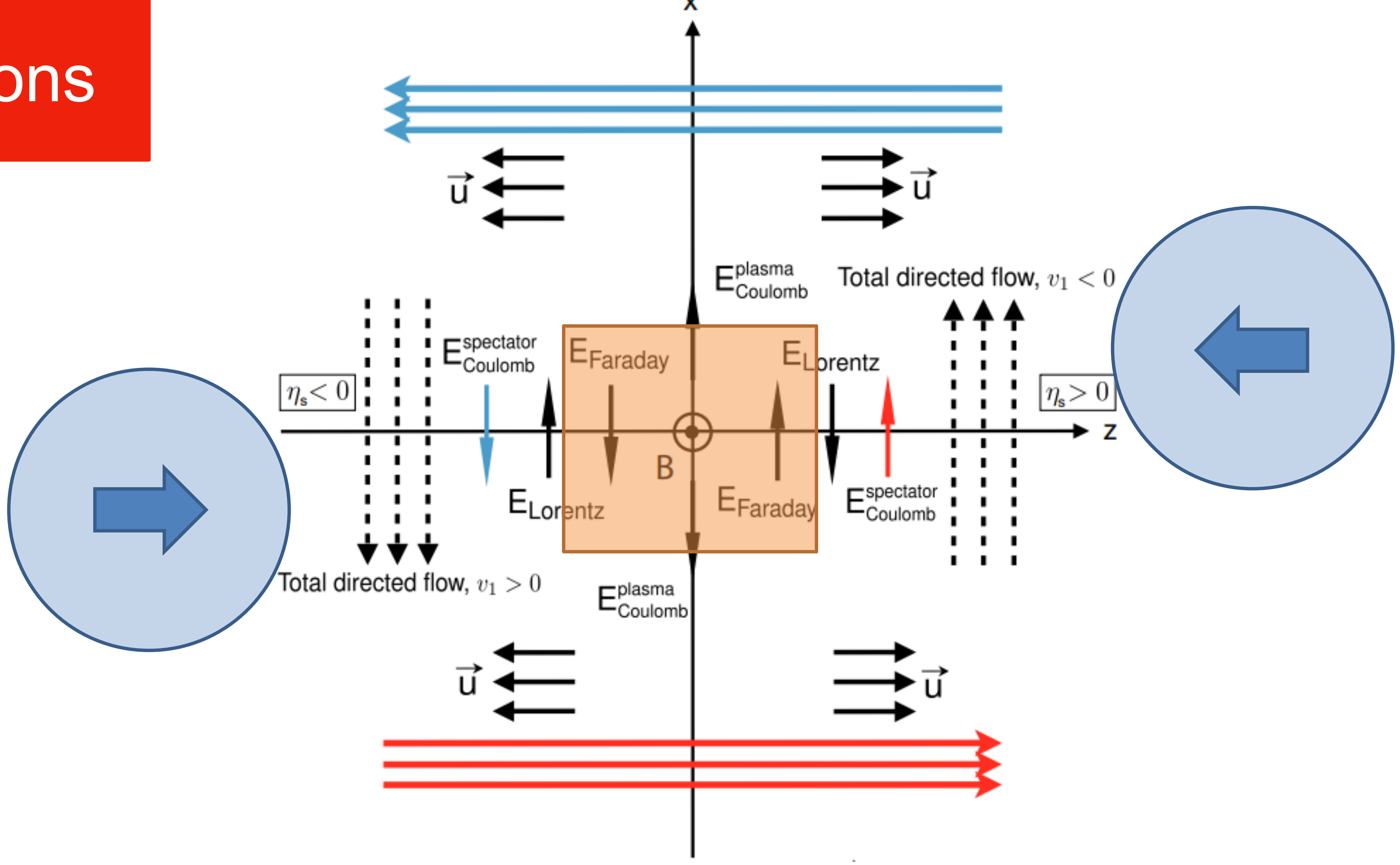

Electromagnetic field in heavy-ion collisions

- Complicated interplay of E and B fields gives rise to four types of currents
  - **Faraday current**: induced current from the decrease of the B field in the medium
  - **Lorentz current**: conducting medium expanding in longitudinal direction ($\vec{u}$) experiences Lorentz force result in an electric current perpendicular to $\vec{u}$ and $\vec{B}$ (Hall effect)

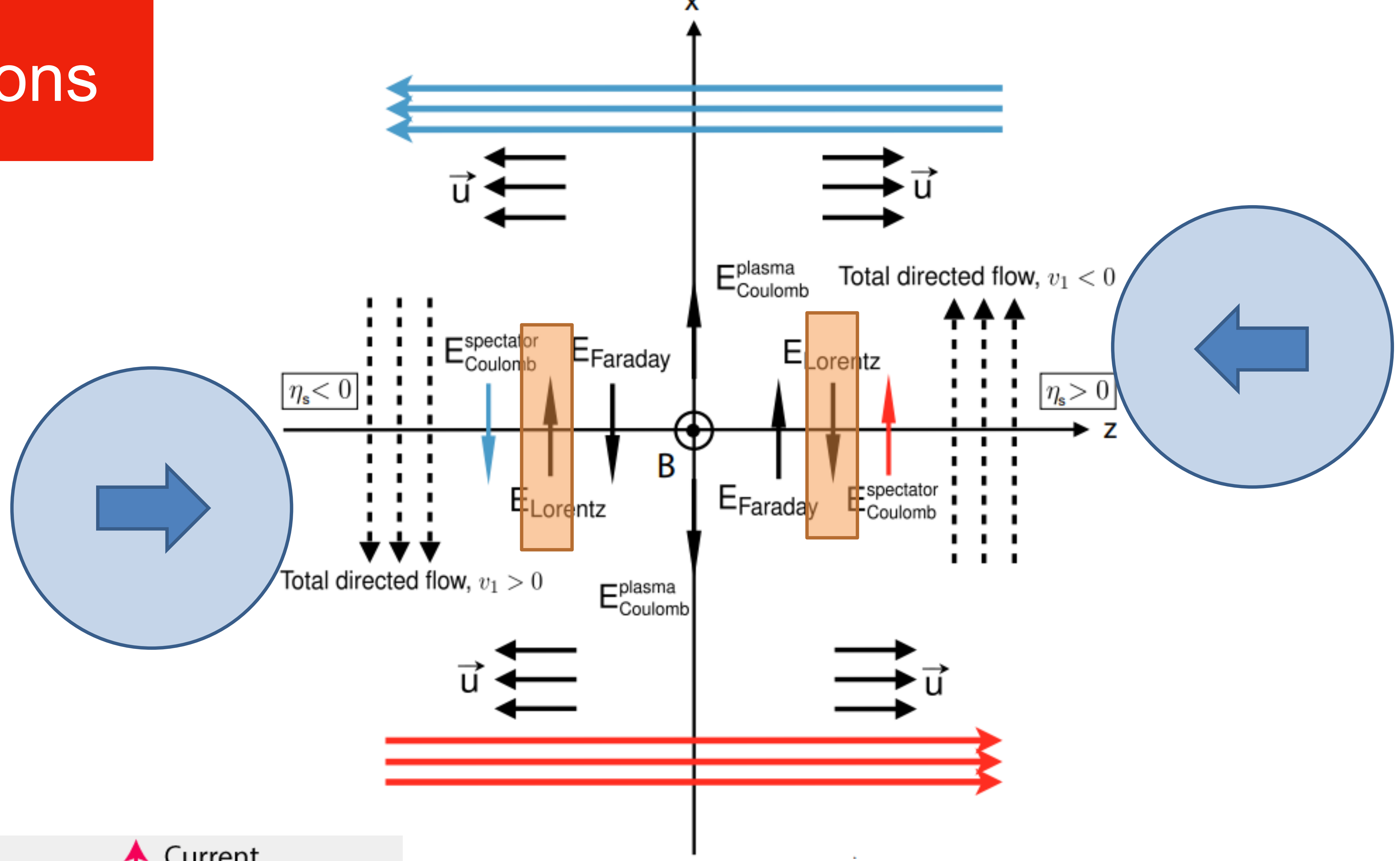

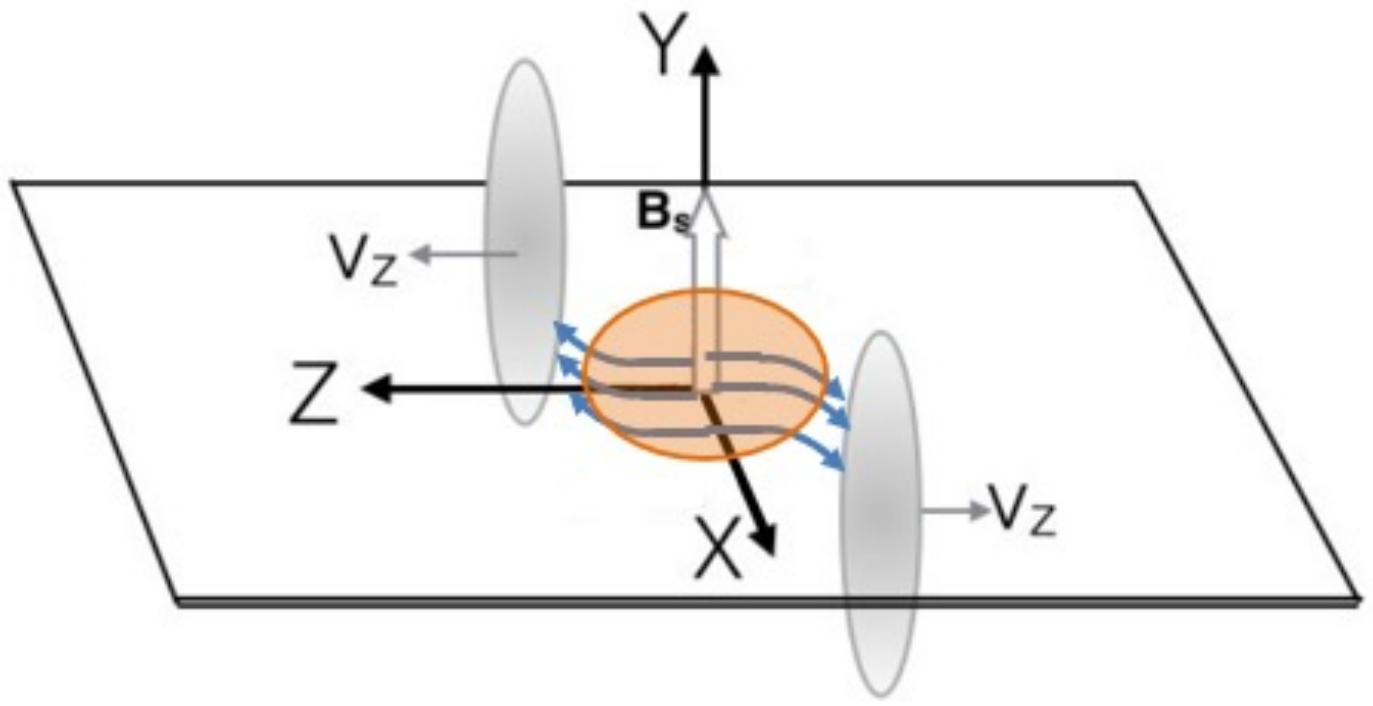

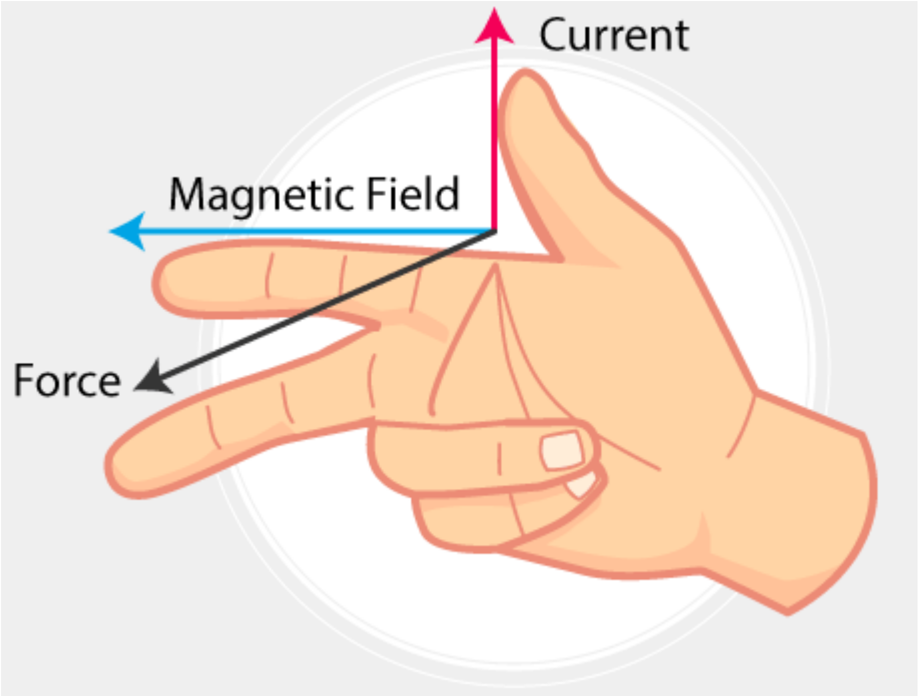

Electromagnetic field in heavy-ion collisions

- Complicated interplay of E and B fields gives rise to four types of currents
  - **Faraday current**: induced current from the decrease of the B field in the medium
  - **Lorentz current**: conducting medium expanding in longitudinal direction ($\vec{u}$) experiences Lorentz force result in an electric current perpendicular to $\vec{u}$ and $\vec{B}$ (Hall effect)
  - **Coulomb current**: positively charged spectators passing the collision zone exerts an electric force on charged plasma

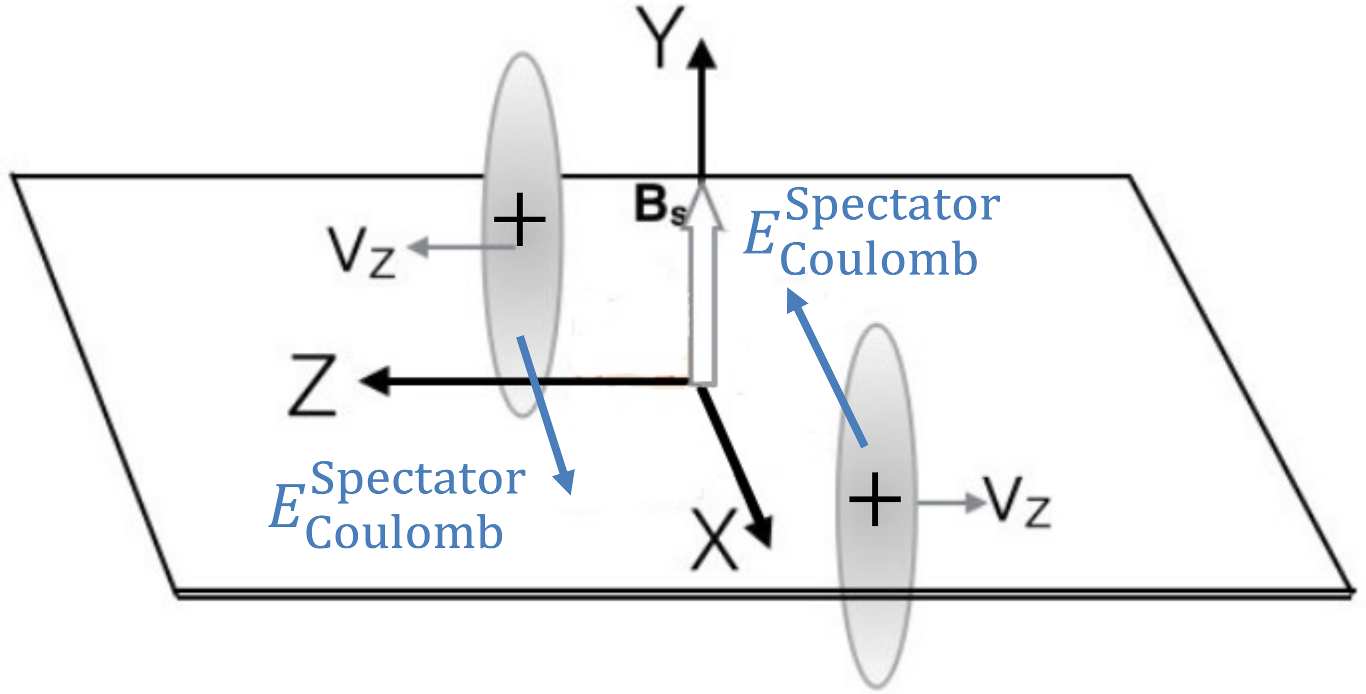

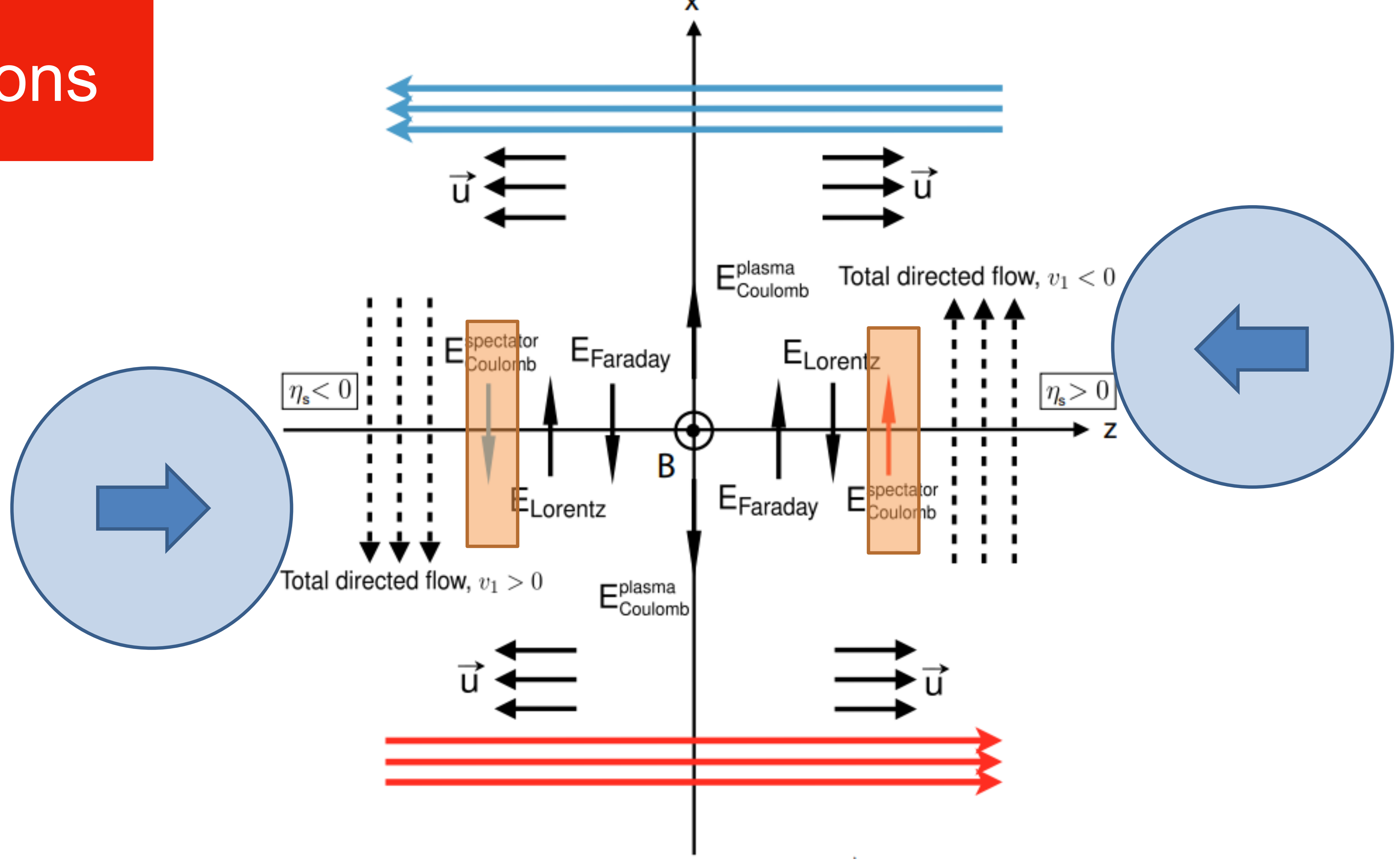

Electromagnetic field in heavy-ion collisions

- Complicated interplay of E and B fields gives rise to four types of currents
  - **Faraday current**: induced current from the decrease of the B field in the medium
  - **Lorentz current**: conducting medium expanding in longitudinal direction ($\vec{u}$) experiences Lorentz force result in an electric current perpendicular to $\vec{u}$ and $\vec{B}$ (Hall effect)
  - **Coulomb current**: positively charged spectators passing the collision zone exerts an electric force on charged plasma
  - **Plasma current**: the net positive charge in the plasma creates an outward E field

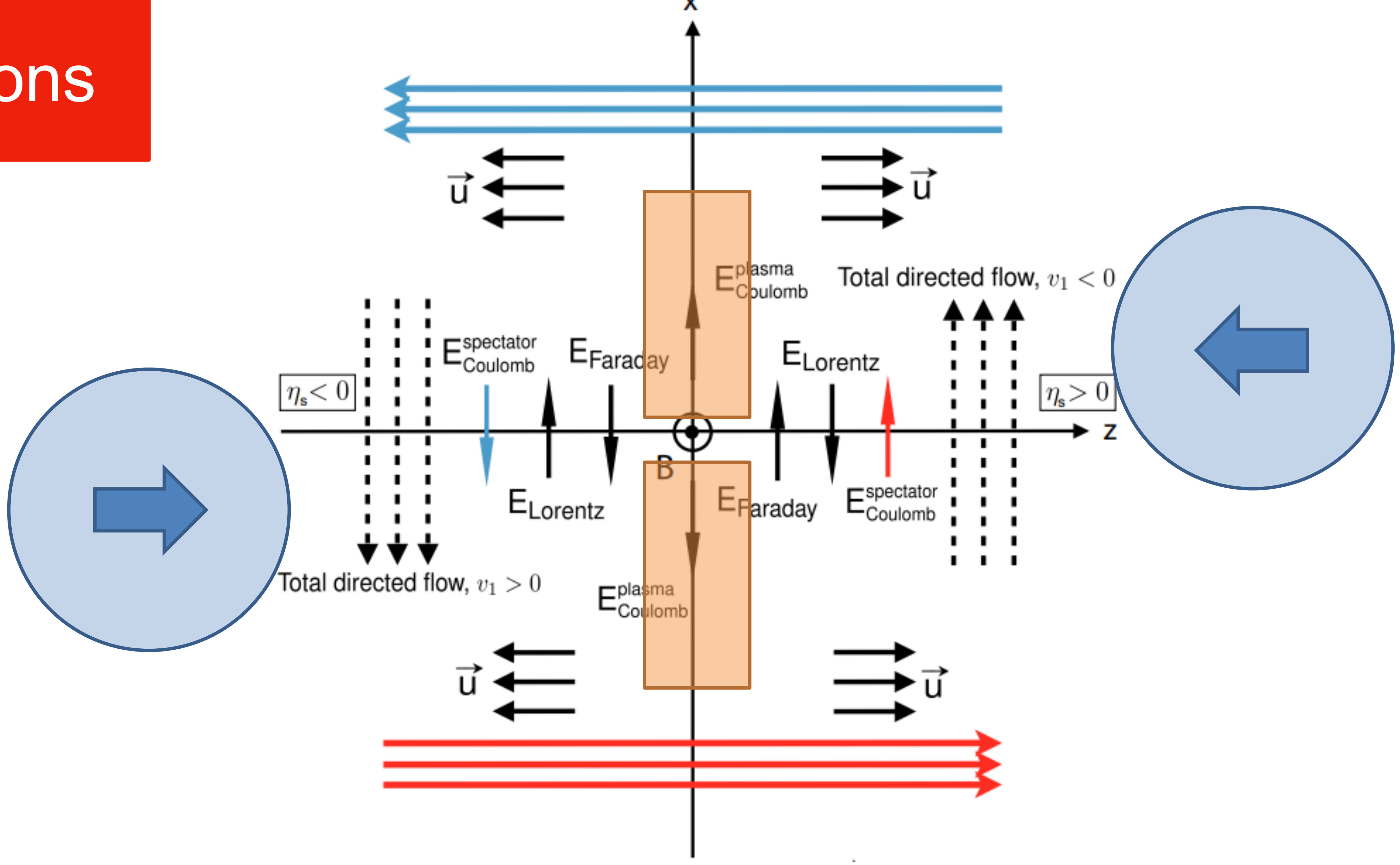

Nikhef

Electromagnetic field in heavy-ion collisions

- Complicated interplay of E and B fields gives rise to four types of currents
  - **Faraday current**: induced current from the decrease of the B field in the medium
  - **Lorentz current**: conducting medium expanding in longitudinal direction ($\vec{u}$) experiences Lorentz force result in an electric current perpendicular to $\vec{u}$ and $\vec{B}$ (Hall effect)
  - **Coulomb current**: positively charged spectators passing the collision zone exerts an electric force on charged plasma
  - **Plasma current**: the net positive charge in the plasma creates an outward E field
- First three effects result in a charge-odd directed flow Δv_1
- Fourth effect results in a non-trivial radial and elliptic flow

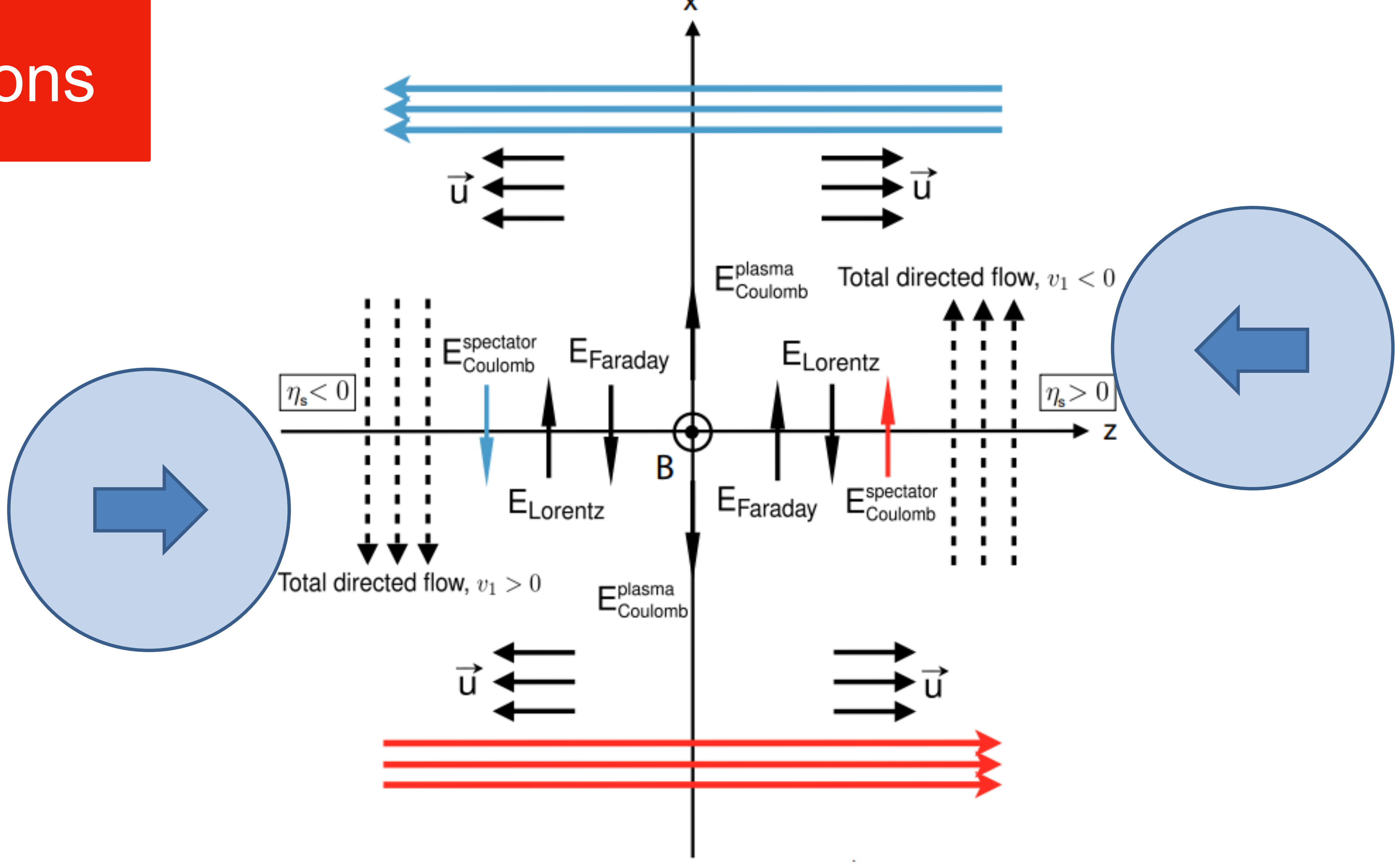

Electromagnetic field in heavy-ion collisions

Phys. Rev. Lett. 111, 172001 (2013)

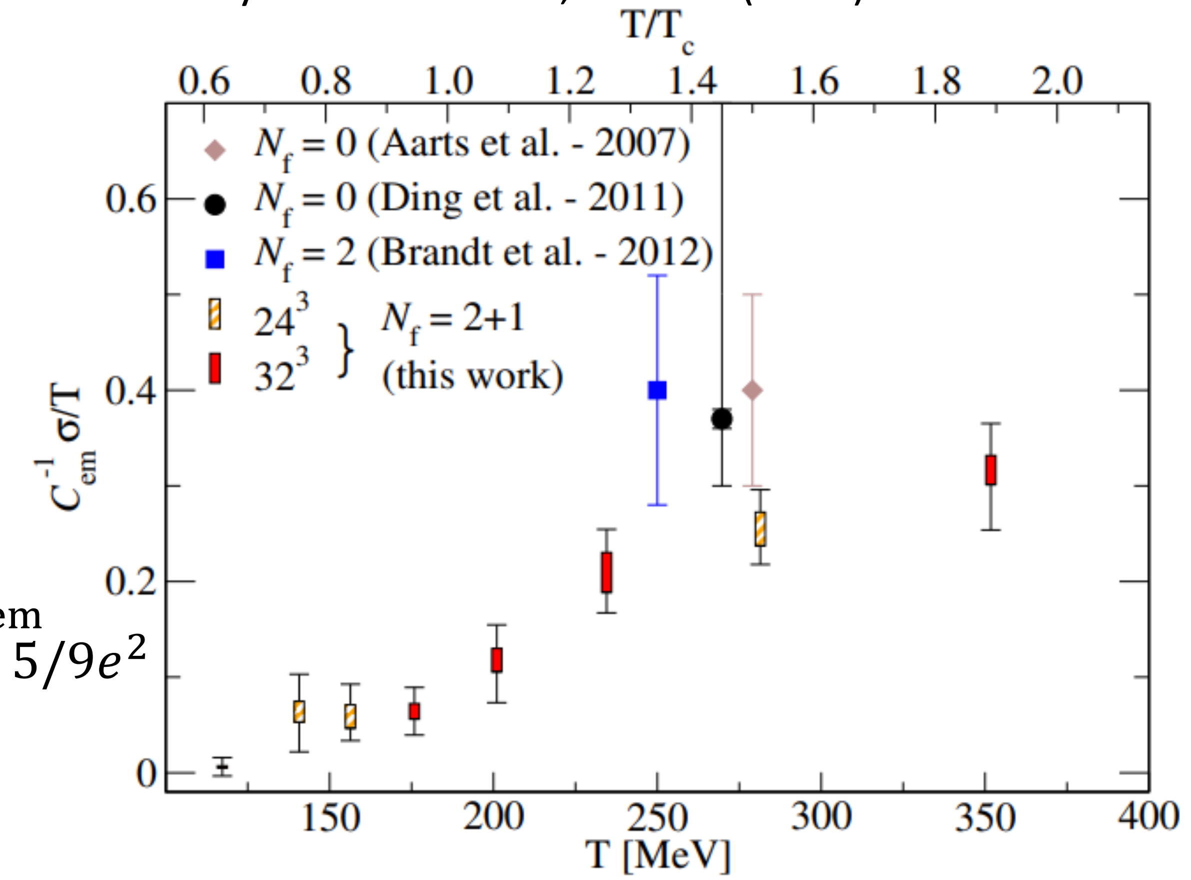

$C_{\text{em}} = 5/9e^2$

Phys. Rev. C 85, 044907 (2012)

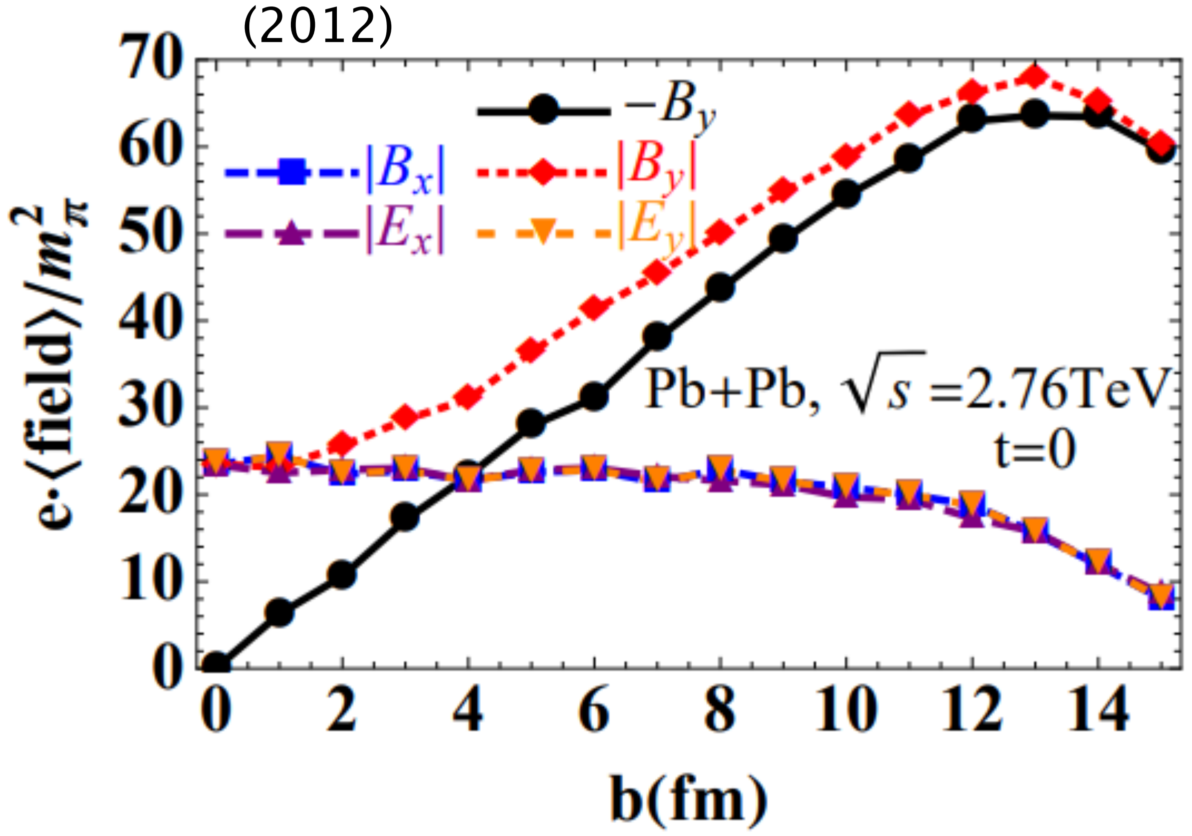

- Lattice QCD calculation suggests that the conductivity (σ) of QGP drops as the plasma cools.
- $\tau_{\text{decay}} \propto \sigma$ (τ_{decay} time constant of the magnetic field)

- EM field at t = 0 and r = 0, the centre of the collision region. B_y increases for more peripheral collisions

Electromagnetic field in heavy-ion collisions

Phys. Rev. Lett. 111, 172001 (2013)

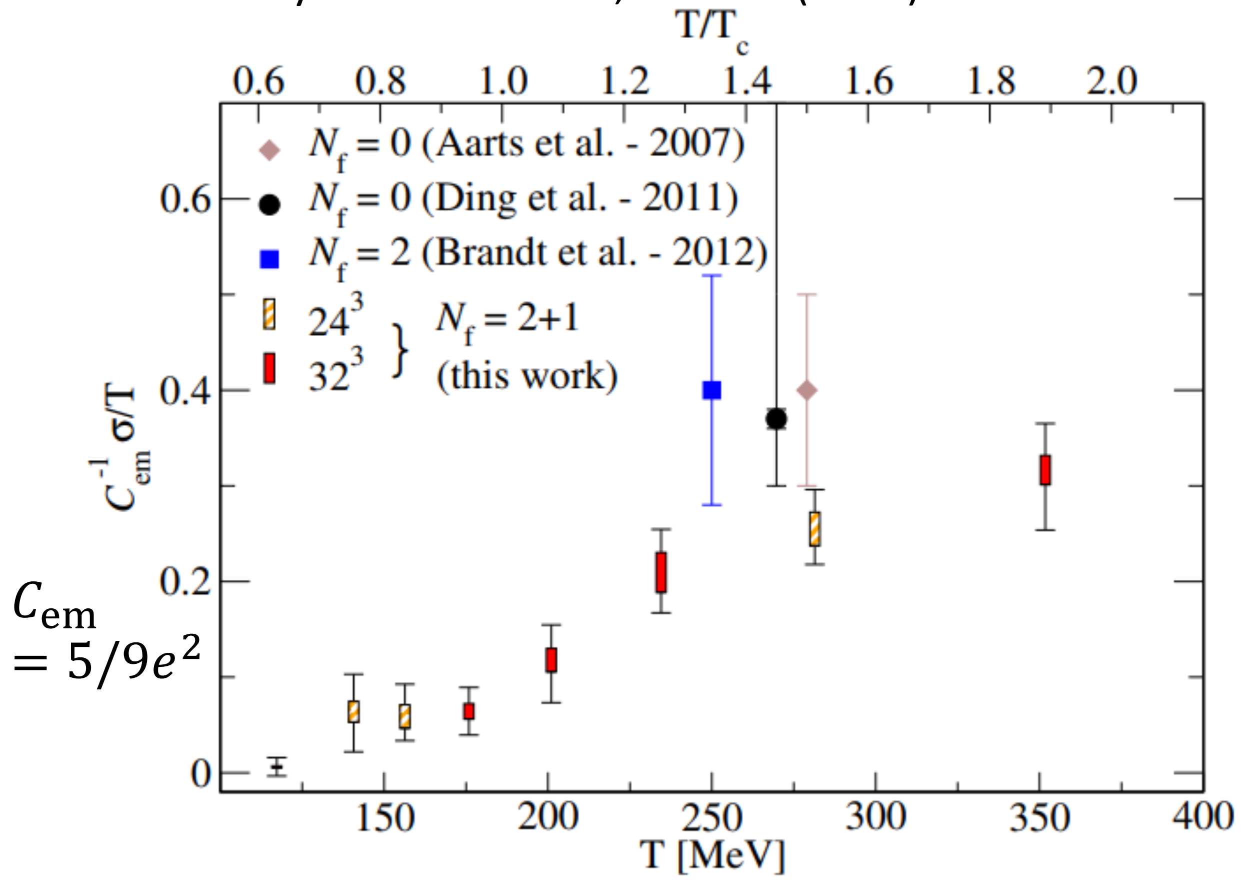

Phys. Rev. C 85, 044907 (2012)

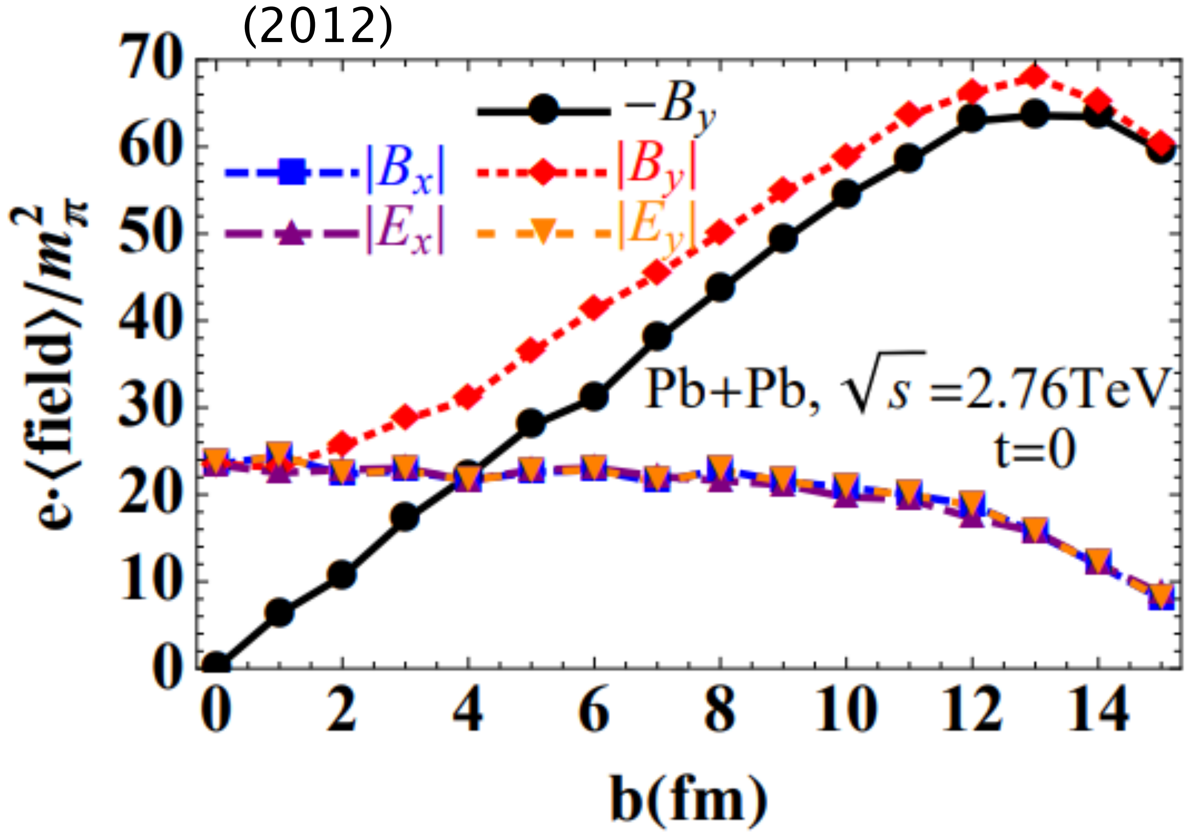

Phys. Rev. C 85, 044907 (2012)

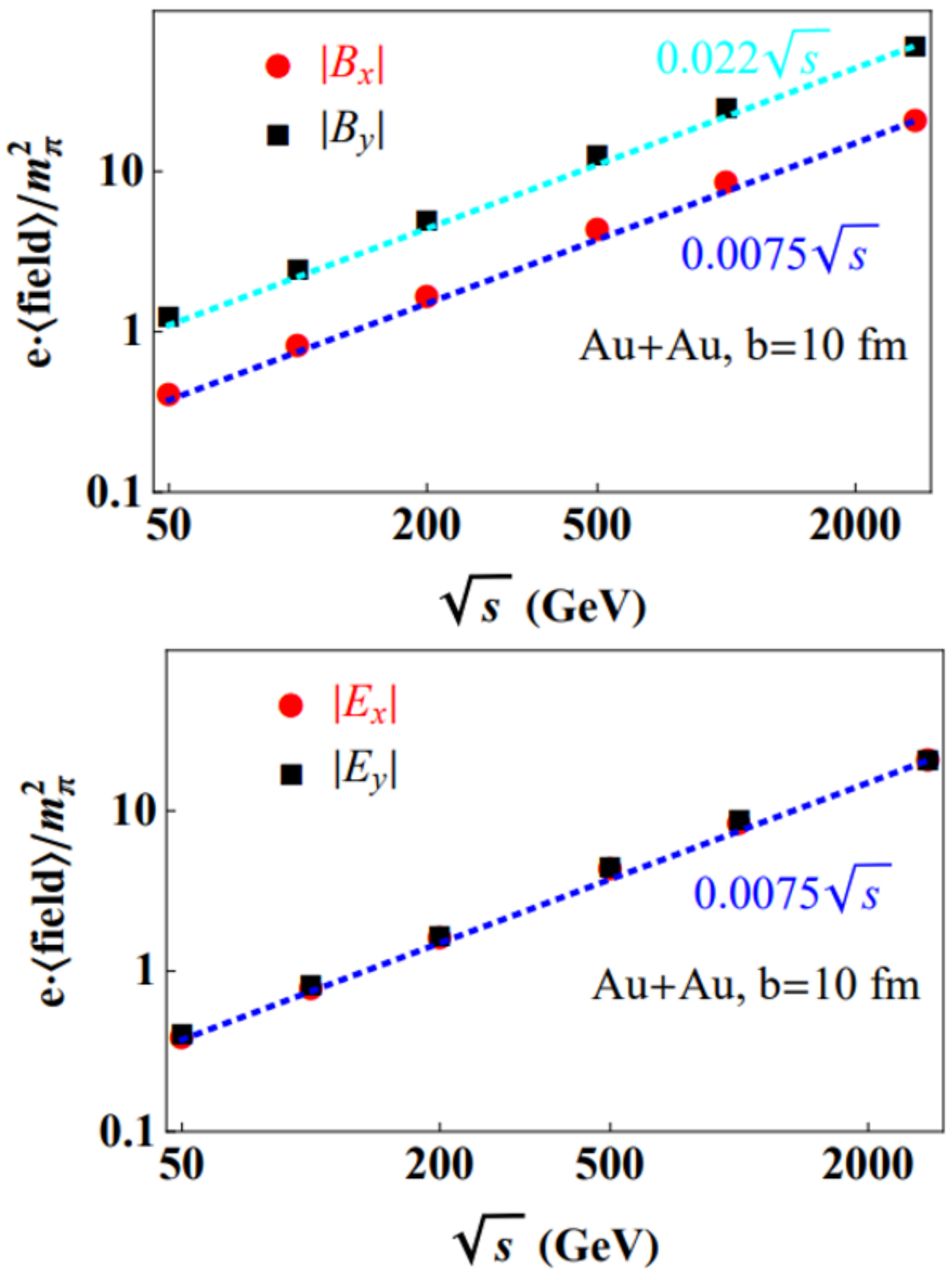

- Lattice QCD calculation suggests that the conductivity (σ) of QGP drops as the plasma cools.
- $\tau_{\text{decay}} \propto \sigma$ (τ_{decay} time constant of the magnetic field)

- EM field at t = 0 and r = 0, the centre of the collision region. B_y increases for more peripheral collisions

- Higher $\sqrt{s}$ leads to higher E and B field

Electromagnetic field in heavy-ion collisions

Phys. Rev. Lett. 111, 172001 (2013)

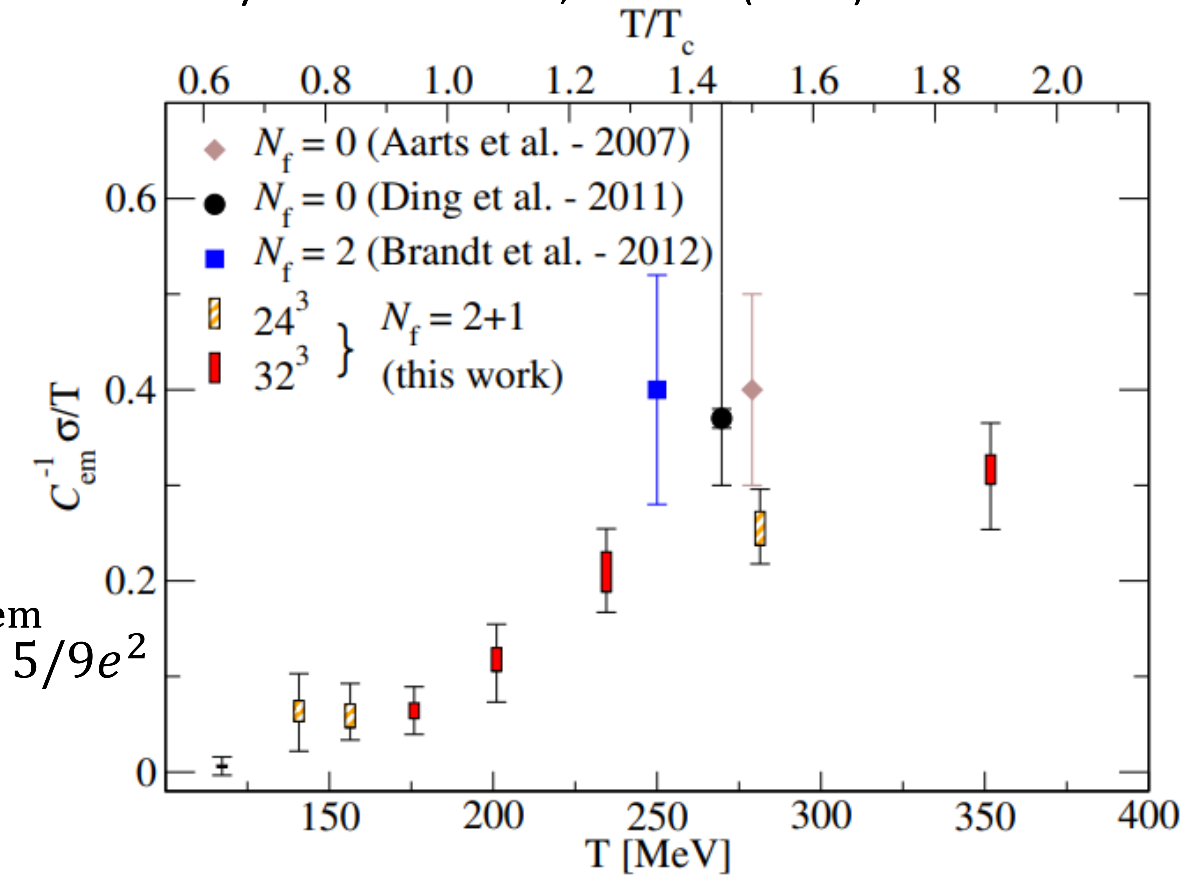

$C_{\text{em}} = 5/9e^2$

- Lattice QCD calculation suggests that the conductivity (σ) of QGP drops as the plasma cools.
- $\tau_{\text{decay}} \propto \sigma$ (τ_{decay} time constant of the magnetic field)

Phys. Rev. C 85, 044907 (2012)

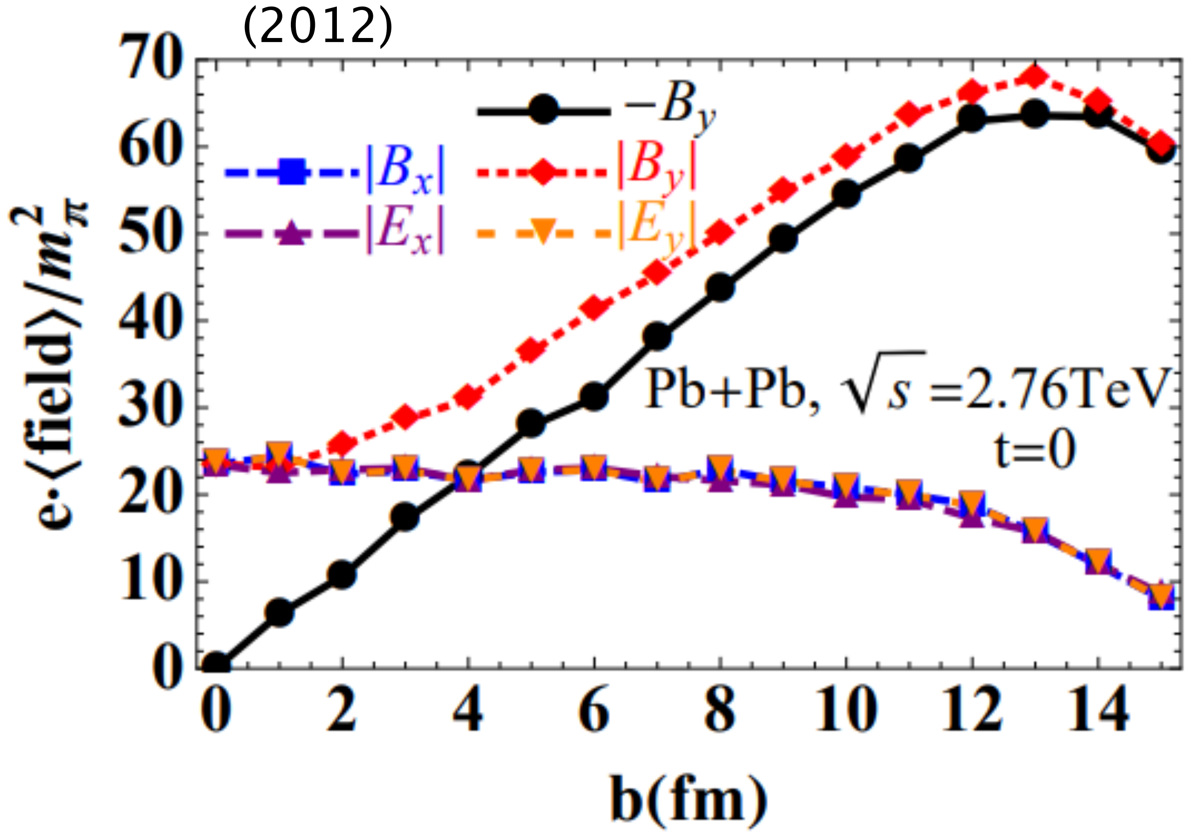

- EM field at t = 0 and r = 0, the centre of the collision region. B_y increases for more peripheral collisions

Phys. Rev. C 85, 044907 (2012)

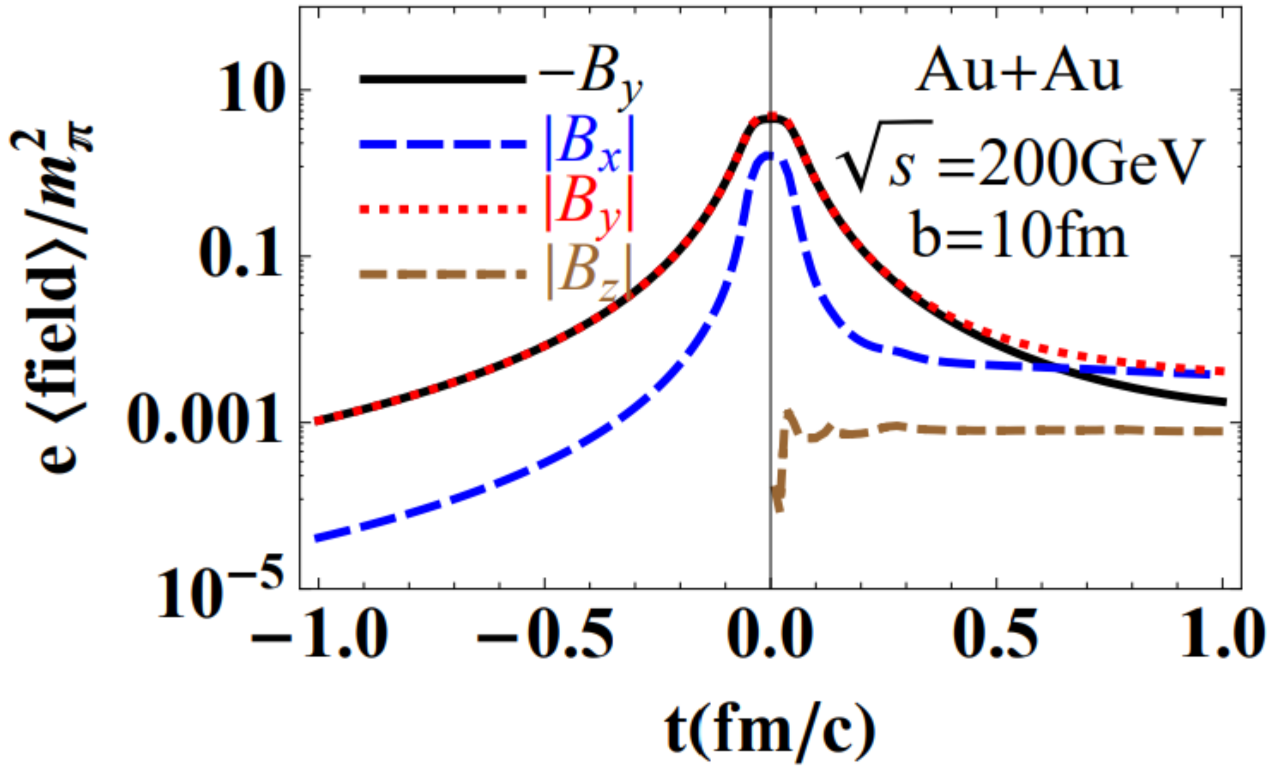

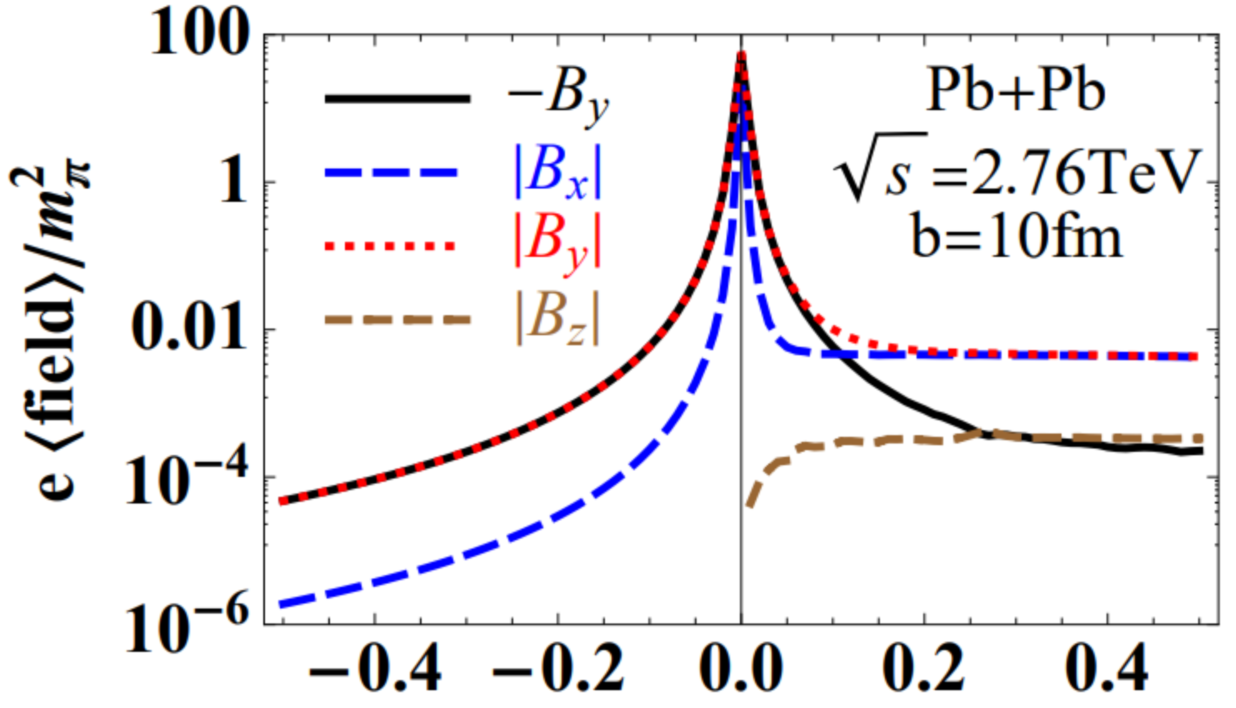

- Lifetime of the B field is shorter at 2.76 TeV than at 200 GeV.
- Lifetime of QGP at ALICE is $\sim 10\ \text{fm/c}$[1]

[1] Phys. Lett. B 696 (2011) 328

Charge-dependent directed flow

- Produced particle azimuthal distribution relative to the collision-spectator plane is directly sensitive to the presence of the electromagnetic fields
- The particle (α) azimuthal distribution:

$$\frac{dN}{d\varphi_\alpha} \sim 1 + 2\sum_n v_{n,\alpha} \cos[n(\varphi_\alpha - \Psi_{\mathrm{RP}})]$$

- ALICE uses the scalar-product [1] method

$$v_1 = \frac{\langle u_x Q_x^{A,C} + u_y Q_y^{A,C} \rangle}{\sqrt{|\langle Q_x^A Q_x^C + Q_y^A Q_y^C \rangle|}}$$

where $\boldsymbol{u} = (\cos\varphi, \sin\varphi)$ and $\boldsymbol{Q}^{A,C}$ is the flow vector for ZDC at A and C side.

- $\Delta v_1 = v_1(h^+) - v_1(h^-)$
- ALICE inclusive hadron measurements

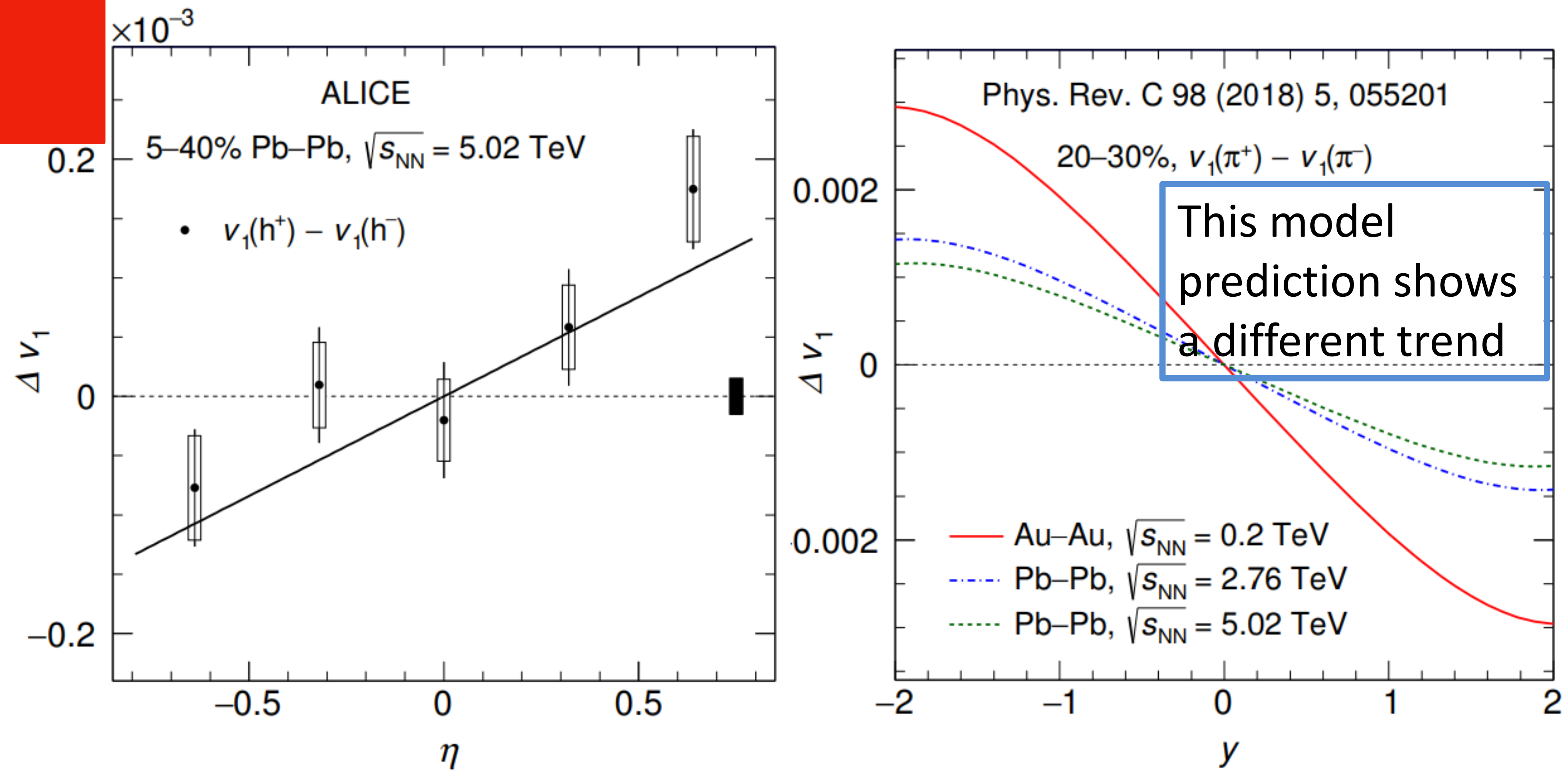

[1] Phys.Rev. C87 (2013) 044907

Charge-dependent directed flow

- Produced particle azimuthal distribution relative to the collision-spectator plane is directly sensitive to the presence of the electromagnetic fields
- The particle (α) azimuthal distribution:

$$\frac{dN}{d\varphi_\alpha} \sim 1 + 2\sum_n v_{n,\alpha}\cos[n(\varphi_\alpha - \Psi_{\mathrm{RP}})]$$

- ALICE uses the scalar-product [1] method

$$v_1 = \frac{\langle u_x Q_x^{A,C} + u_y Q_y^{A,C}\rangle}{\sqrt{|\langle Q_x^A Q_x^C + Q_y^A Q_y^C\rangle|}}$$

where $\boldsymbol{u} = (\cos\varphi, \sin\varphi)$ and $\boldsymbol{Q}^{A,C}$ is the flow vector for ZDC at A and C side.

- $\Delta v_1 = v_1(h^+) - v_1(h^-)$
- ALICE inclusive hadron measurements
- ALICE Heavy-flavor measurements on D^0 ($c\bar{u}$) and $\overline{D}^0$ ($\bar{c}u$
  - Charm quarks produced early in the hard process experience more effect from EM field leading to a larger gradient ($0.49 \pm 0.17(\mathrm{stats}) \pm 0.06(\mathrm{syst.})$)

[1] Phys.Rev. C87 (2013) 044907

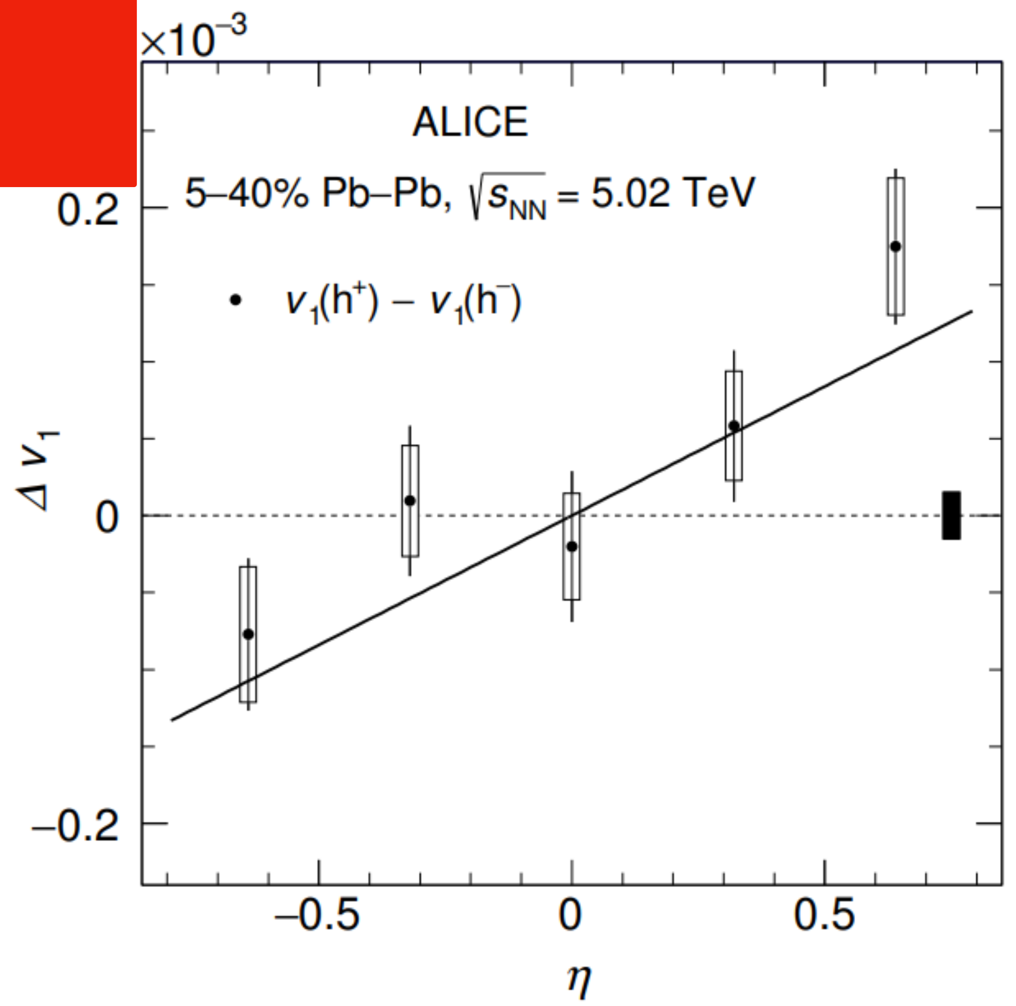

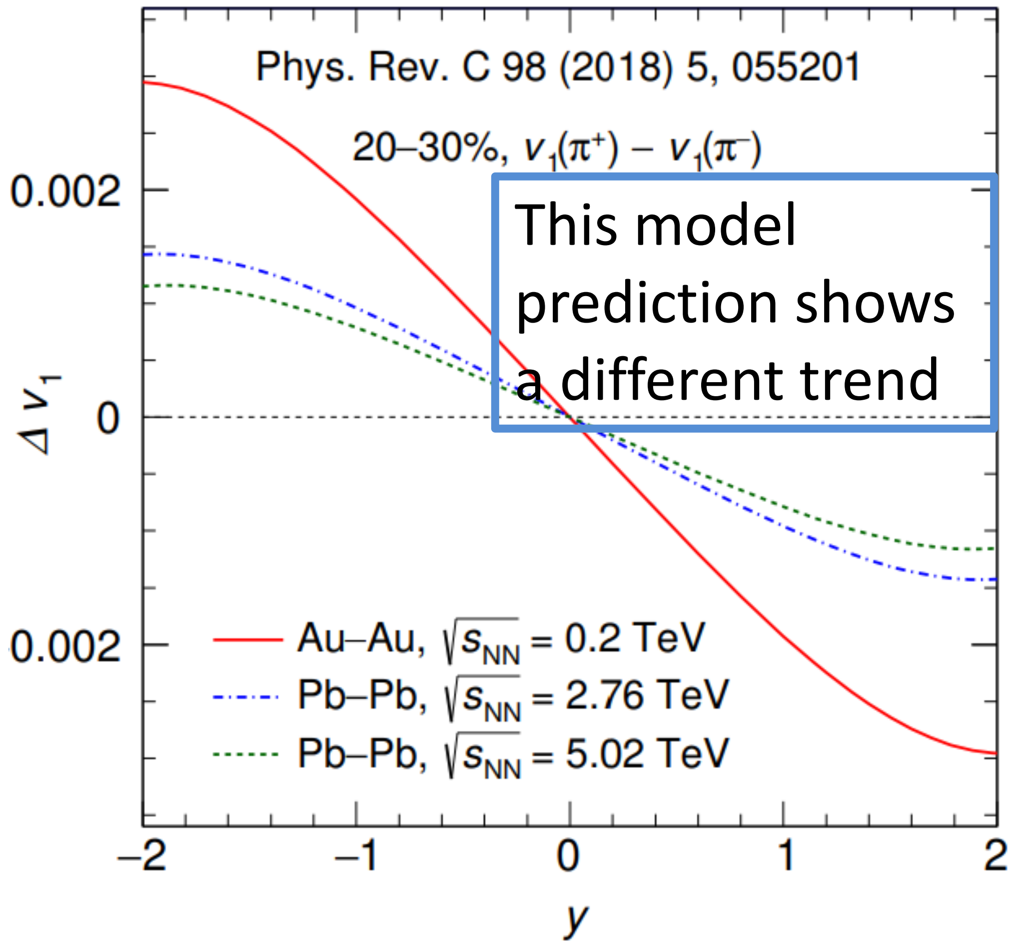

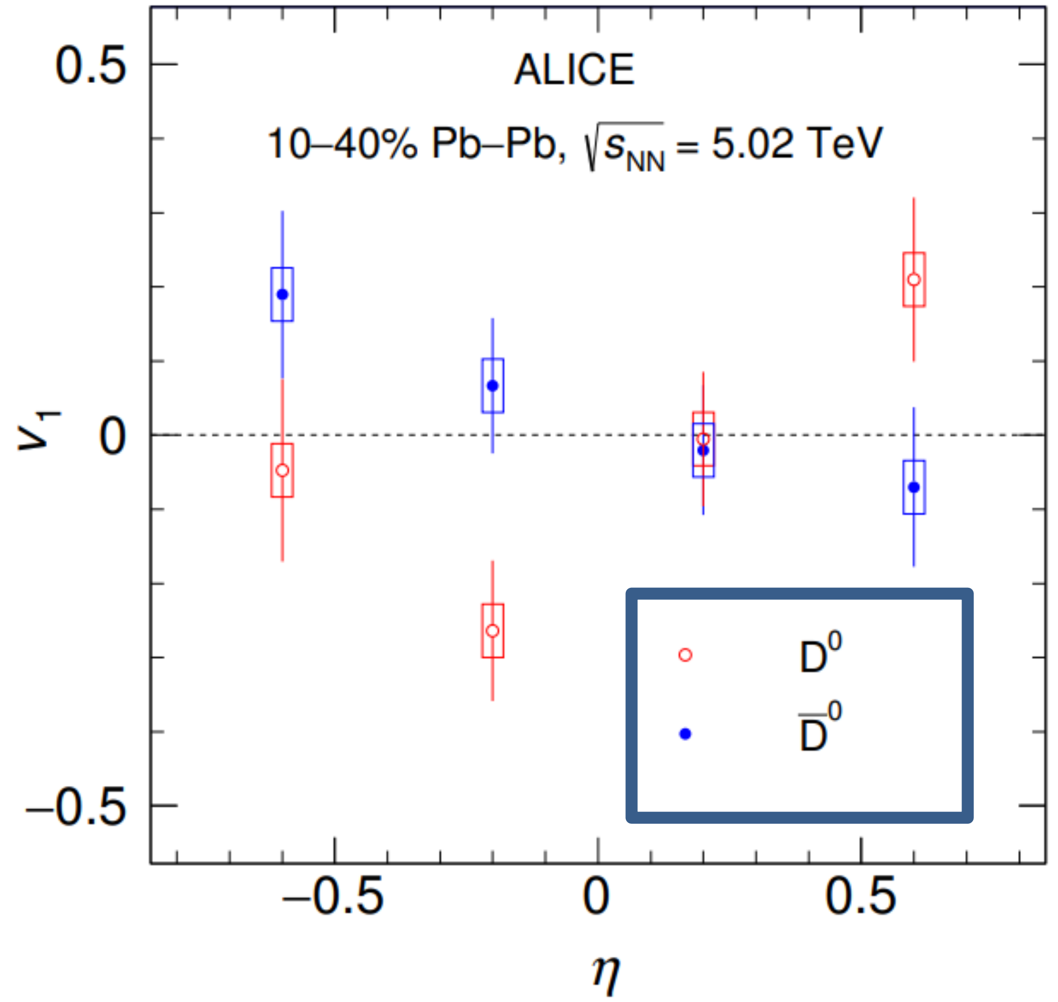

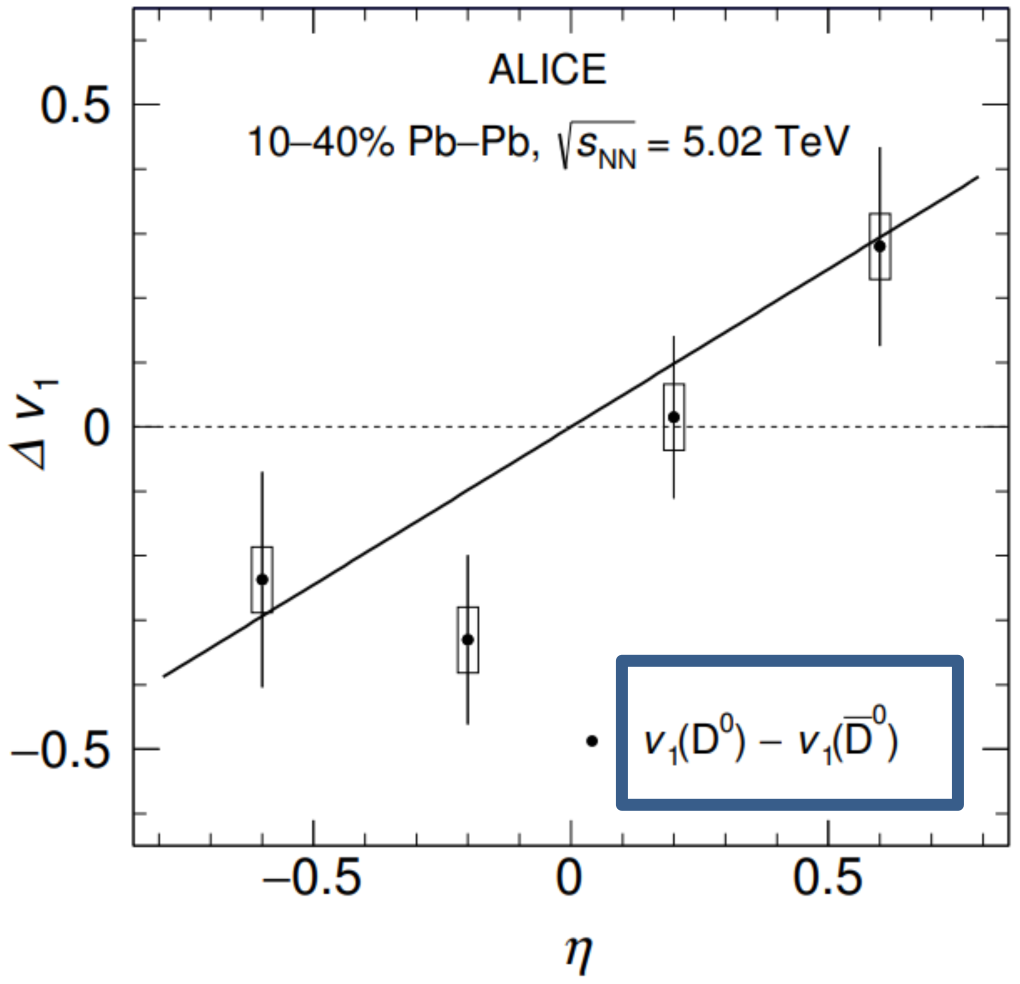

Charge-dependent directed flow

- Measurement of Δv_1 at RHIC energy shows a slope of $-0.011 \pm 0.034(\text{stat.})$ $\pm\, 0.020(\text{syst.})$
- The larger slope of Δv_1 of D mesons at LHC might indicate a stronger effect of the Lorentz force relative to the Coulomb one
- Predictions for the dependence of the Δv_1 for the D meson is almost flat for two choice of drag $\gamma^{[1]}$ from the matter
- Recent model calculation using a magnetic field with a slower time evolution and with a lifetime of about 0.4 fm/c can reproduce the measurement

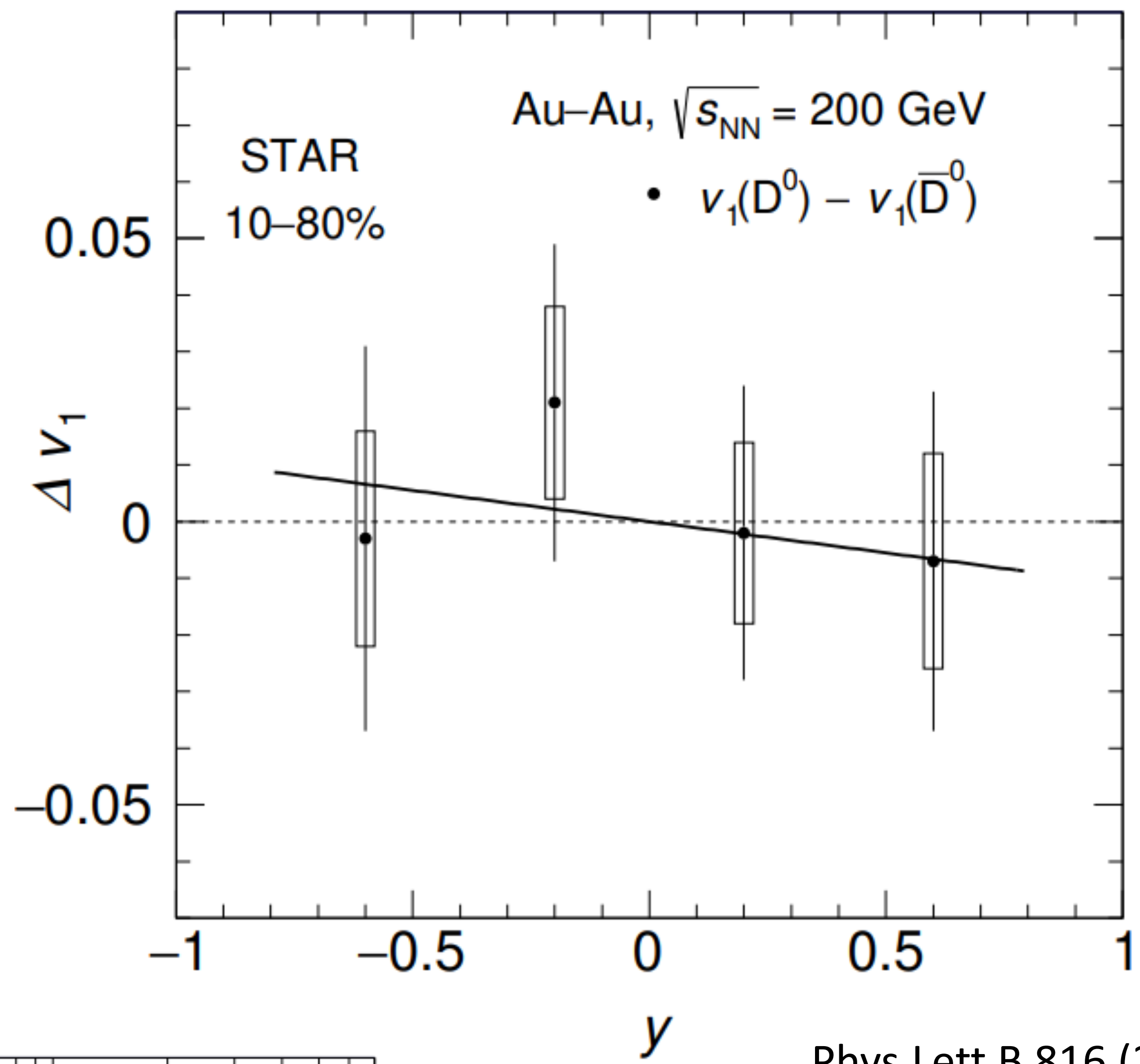

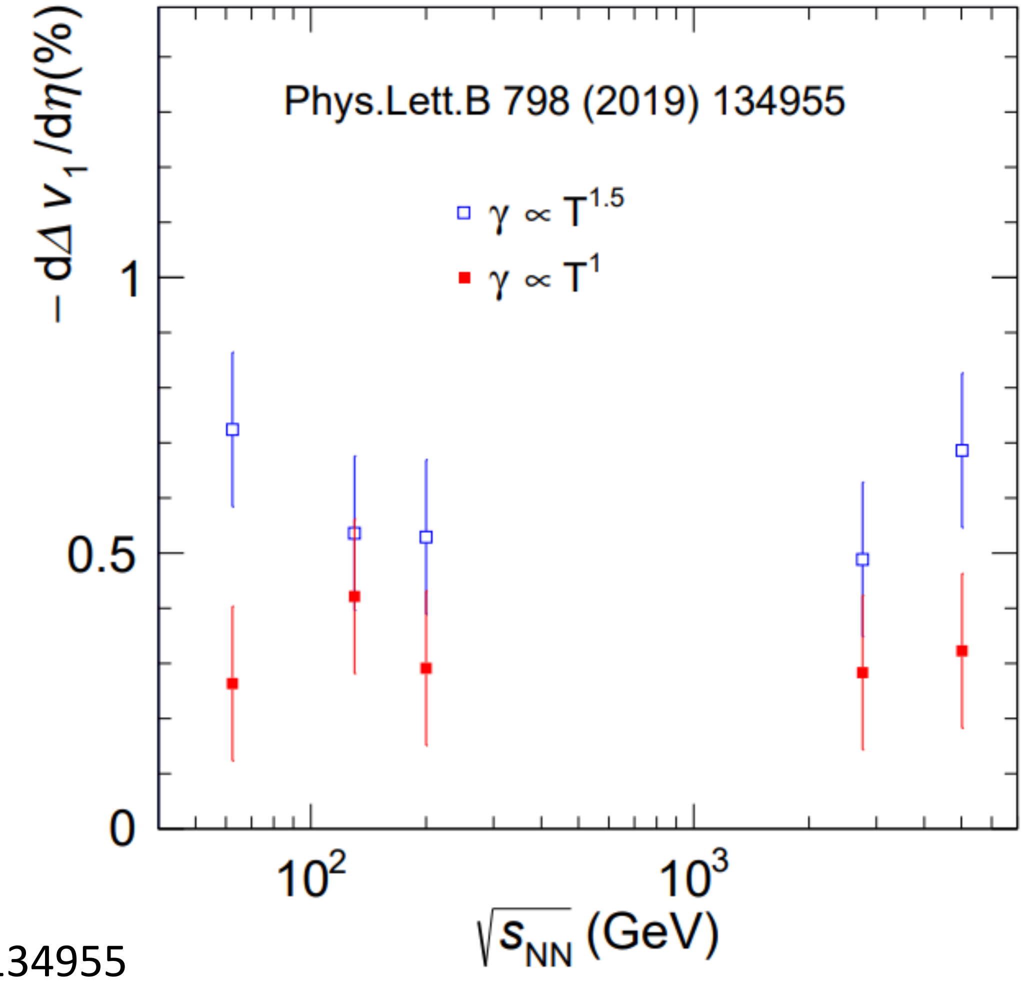

Phys.Lett B 816 (2021) 136271

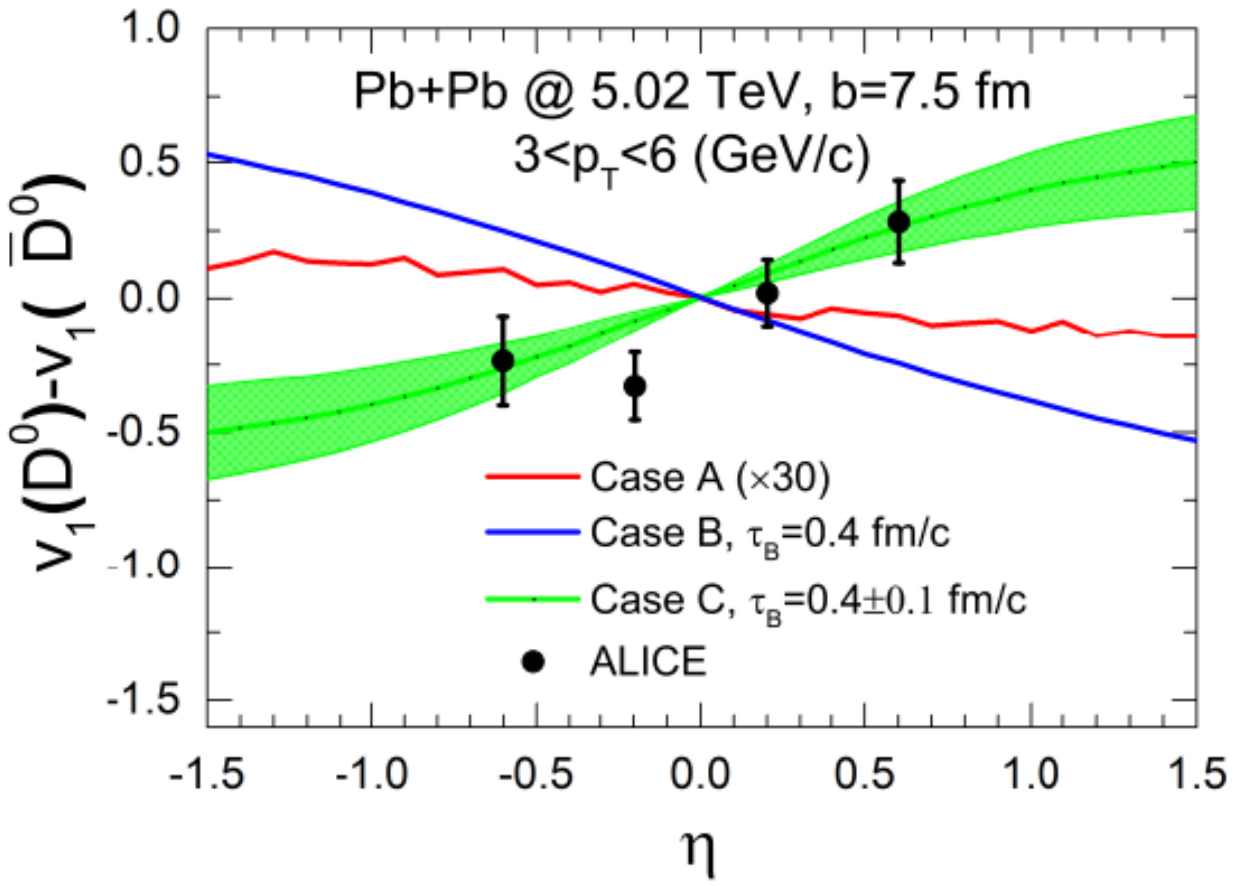

[1] More discussion on drag vs. Lorentz force, see Phys.Lett.B 798 (2019) 134955

Hyperon polarization

- Global polarization: spin alignment along the initial angular momentum
- Two contributions to the global polarization:
  - Magnetic field align particles’ and antiparticles’ spin oppositely due to the opposite sign of magnetic moment

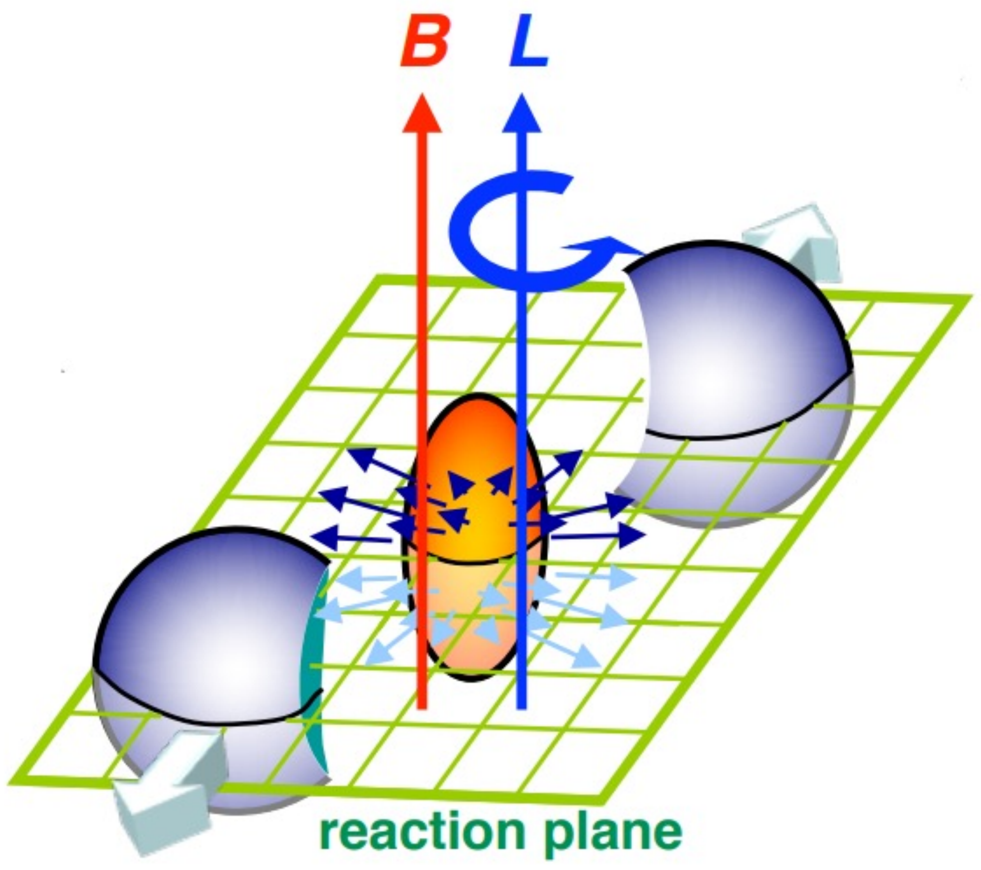

Hyperon polarization

- Global polarization: spin alignment along the initial angular momentum
- Two contributions to the global polarization:
  - Magnetic field align particles' and antiparticles' spin oppositely due to the opposite sign of magnetic moment
  - Large vorticity expected due to velocity difference along beam direction. Orbital angular momentum is transferred to particle spin equally for particles and antiparticles

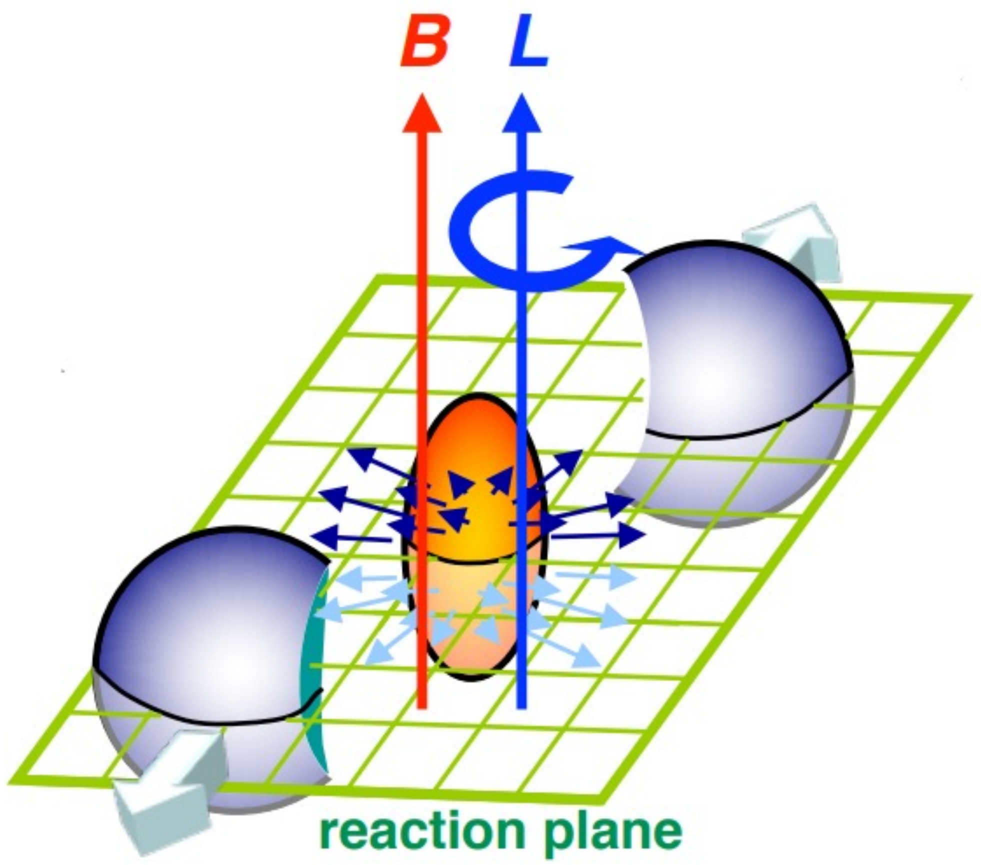

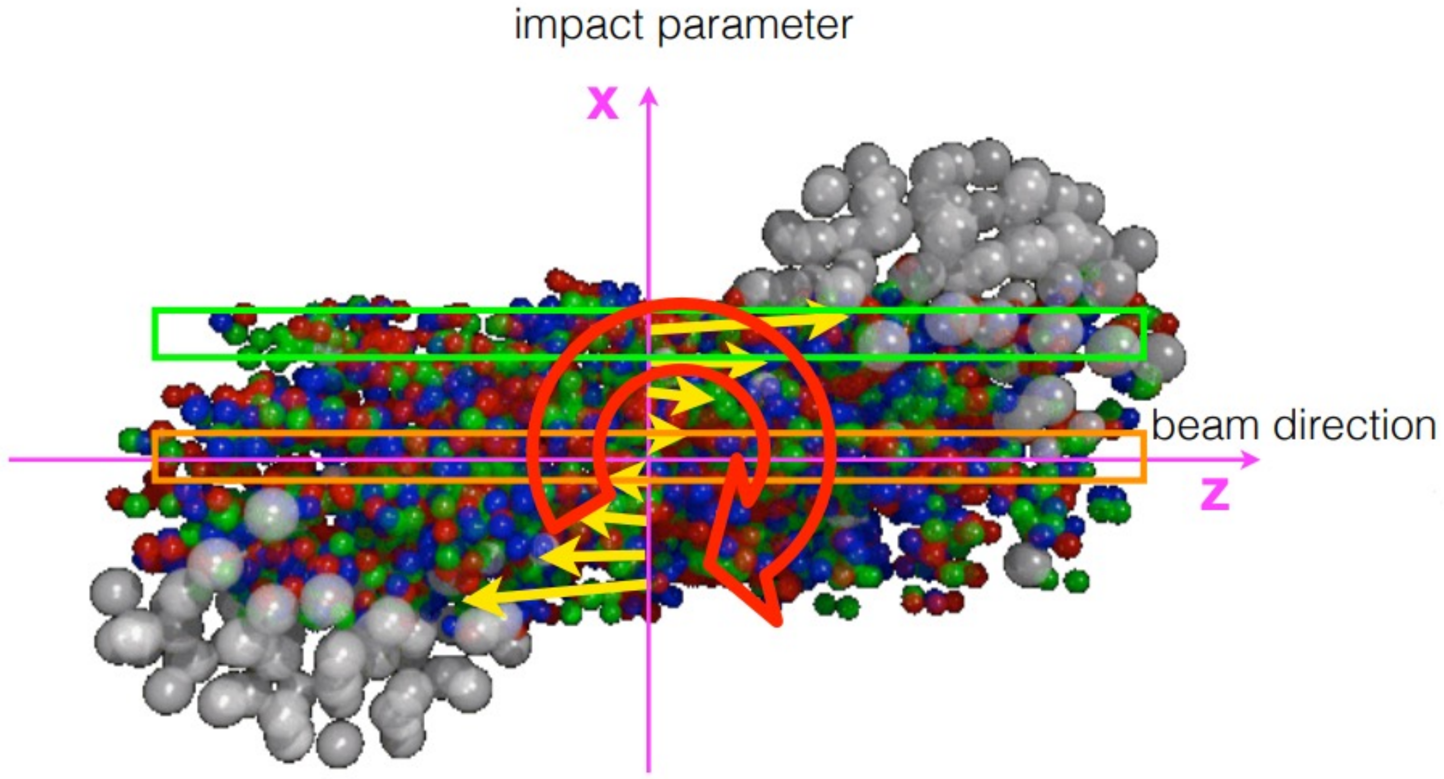

Hyperon polarization

- Global polarization: spin alignment along the initial angular momentum
- Two contributions to the global polarization:
  - Magnetic field align particles' and antiparticles' spin oppositely due to the opposite sign of magnetic moment
  - Large vorticity expected due to velocity difference along beam direction. Orbital angular momentum is transferred to particle spin equally for particles and antiparticles
- How to measure?
  - Λ ($\overline{\Lambda}$) decays dominantly into $p+\pi$. Protons are emitted preferentially in the direction of the Λ ($\overline{\Lambda}$) spin
- The global polarization is given by

$$P_H = -\frac{8}{\pi\alpha_H}\frac{\langle\sin(\phi_p^* - \Psi_{SP})\rangle}{R_{\mathrm{SP}}^{(1)}}$$

$$\Lambda \rightarrow p + \pi^-$$

(BR: 63.9%, c τ ~7.9 cm)

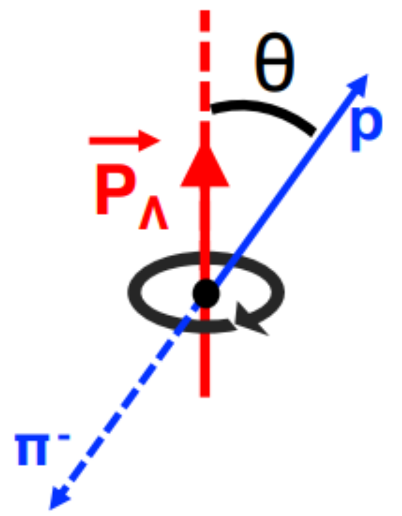

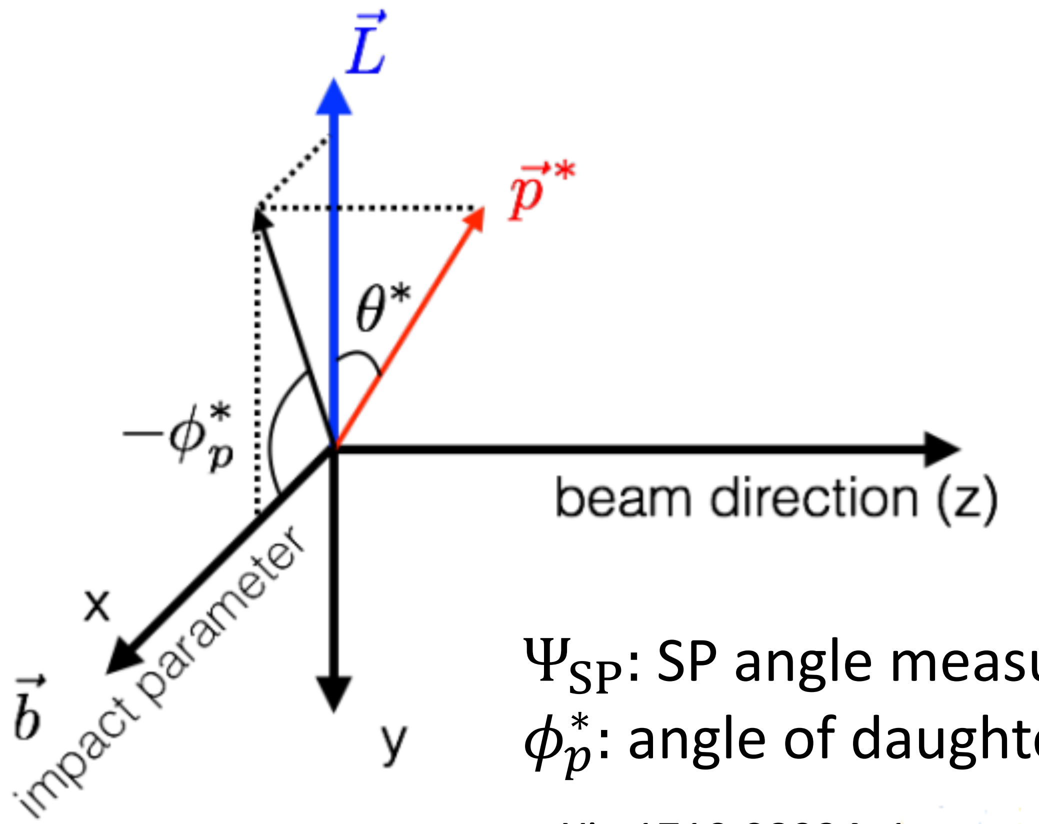

Ψ_{SP}: SP angle measured by ZDC

ϕ_p^*: angle of daughter proton in Λ rest frame

arXiv:1710.08934v1

Hyperon polarization

- Global polarization: spin alignment along the initial angular momentum
- Two contributions to the global polarization:
  - Magnetic field align particles' and antiparticles' spin oppositely due to the opposite sign of magnetic moment
  - Large vorticity expected due to velocity difference along beam direction. Orbital angular momentum is transferred to particle spin equally for particles and antiparticles
- How to measure?
  - Λ ($\overline{\Lambda}$) decays dominantly into $p + \pi$. Protons are emitted preferentially in the direction of the Λ ($\overline{\Lambda}$) spin
- The global polarization is given by

$$P_H = -\frac{8}{\pi \alpha_H} \frac{\langle \sin(\phi_p^* - \Psi_{SP}) \rangle}{R_{\mathrm{SP}}^{(1)}}$$

Phys. Rev. C 101, 044611 (2020)

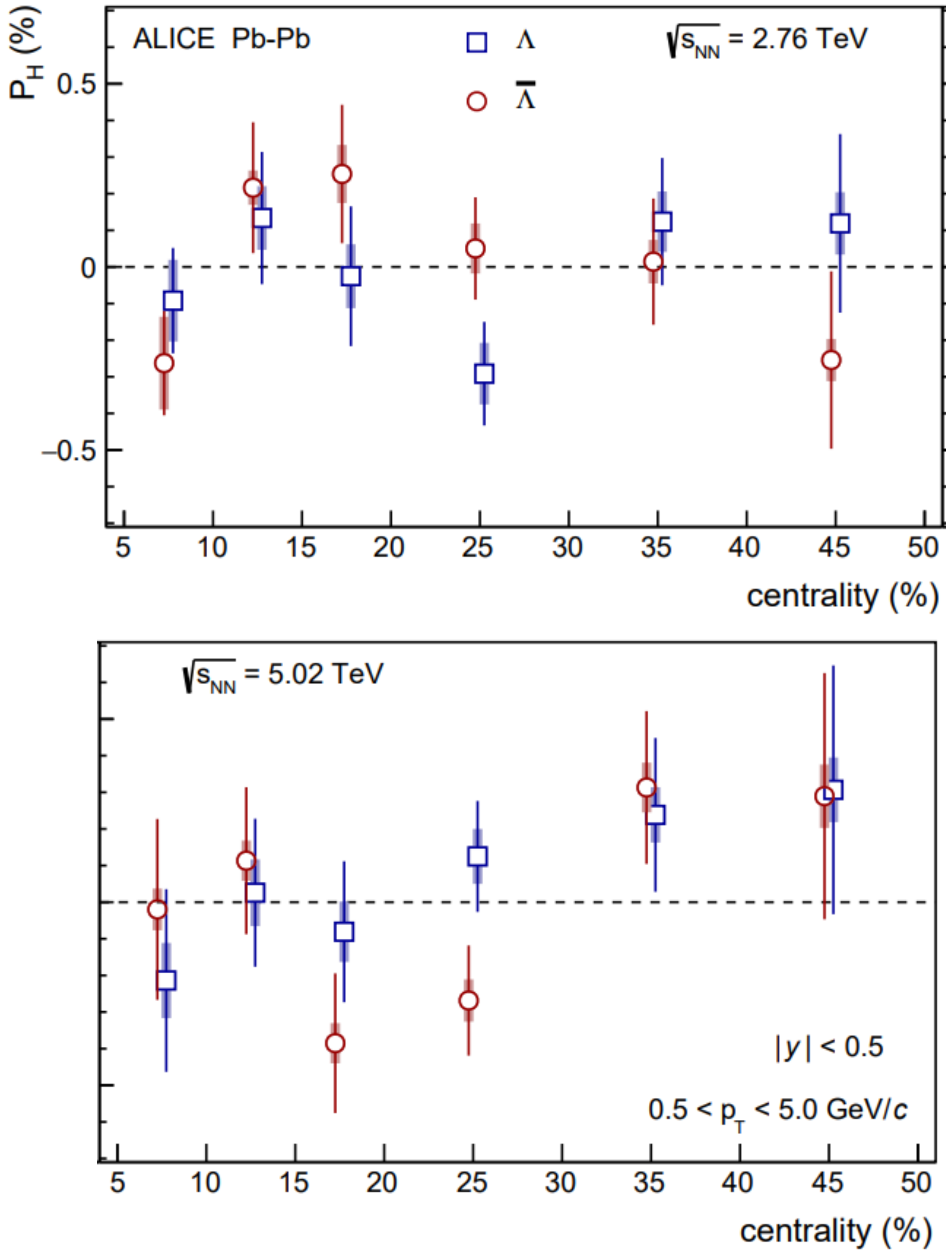

Hyperon polarization

- Confirms the observed earlier trend of the global polarization decrease with increasing $\sqrt{s_{NN}}$
- The magnitude of B field at kinetic freeze-out can be probed by $\Lambda - \overline{\Lambda}$ splitting:

$$P_\Lambda \approx \frac{0.5\omega}{T} \boxed{+\frac{|\mu_\Lambda|B}{T}}, P_{\overline{\Lambda}} \approx \frac{0.5\omega}{T} \boxed{-\frac{|\mu_\Lambda|B}{T}}$$

$$\Rightarrow P_\Lambda - P_{\overline{\Lambda}} \approx \frac{2|\mu_\Lambda|B}{T}$$

- More data (100x more) in the high luminosity LHC run will help to test the predicted splitting of P_Λ and $P_{\overline{\Lambda}}$ better

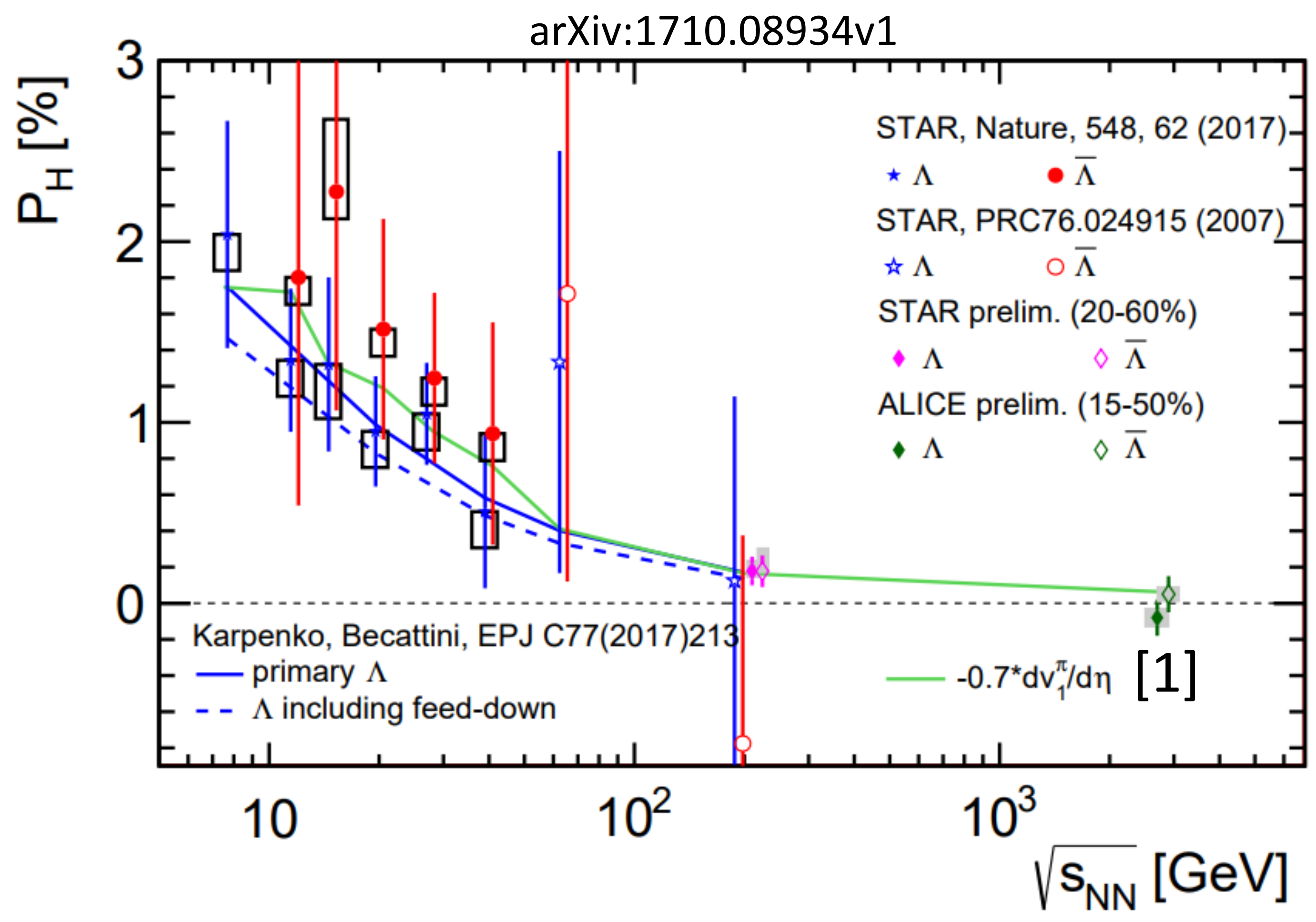

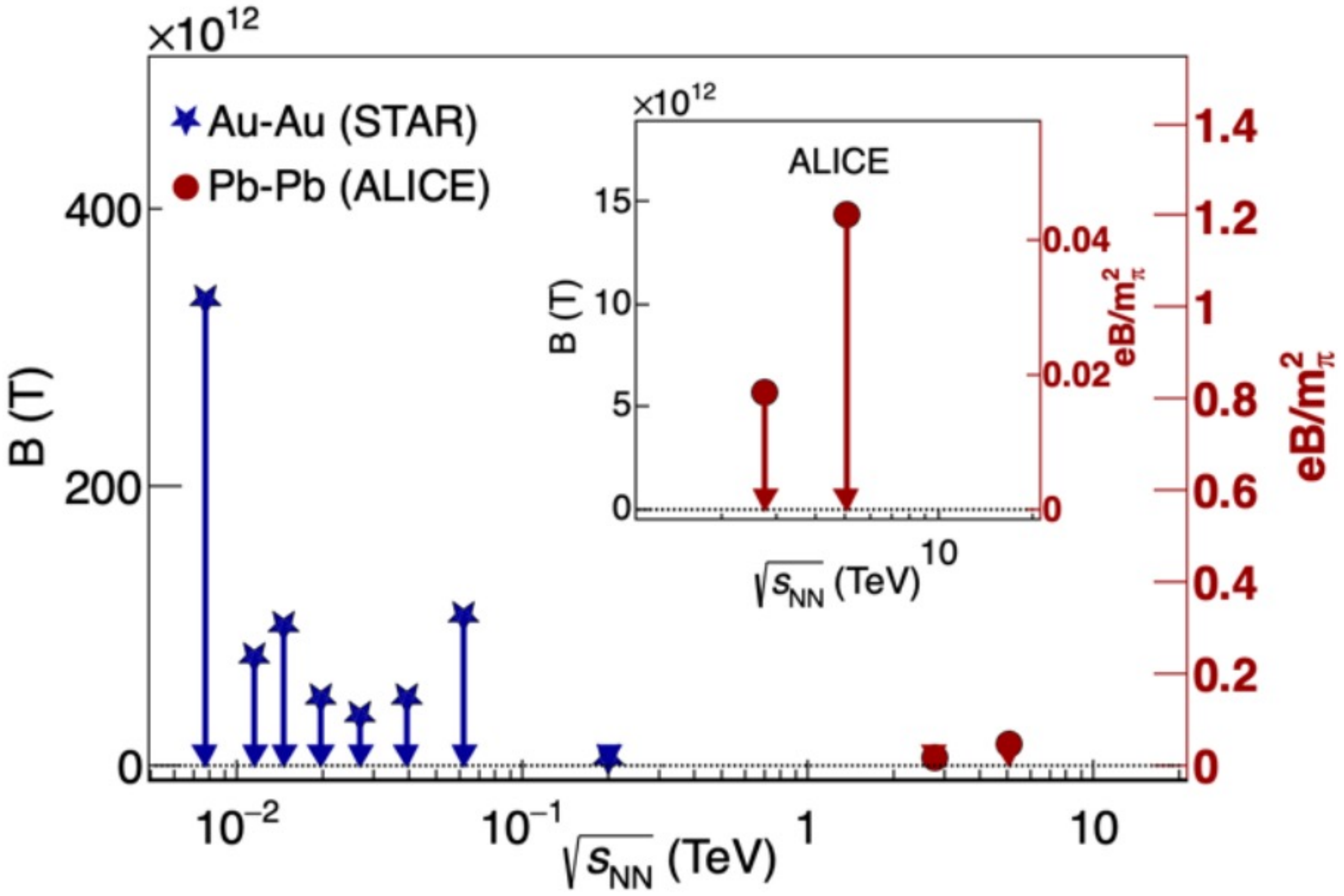

[1] Advances in High Energy Physics, vol. 2016, Article ID 2836989

Chiral magnetic effect

- CME: The generation of electric current along an external magnetic field induced by chirality imbalance.

Chiral magnetic effect

- CME: The generation of electric current along an external magnetic field induced by chirality imbalance.

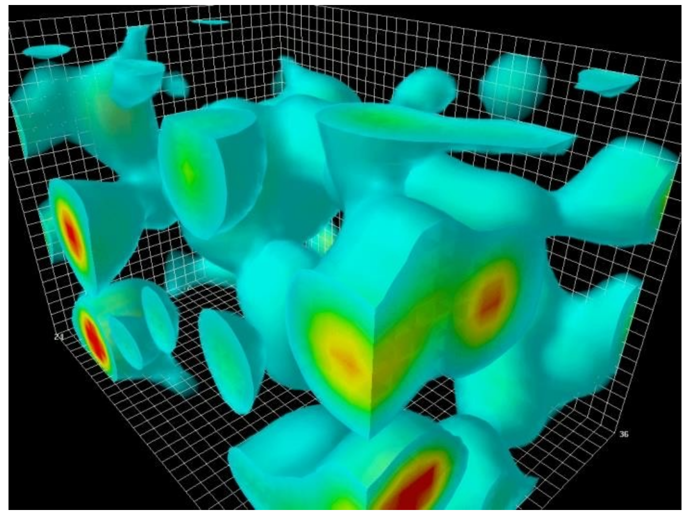

Non-trivial QCD vacuum structure

Red: momentum
Blue: spin

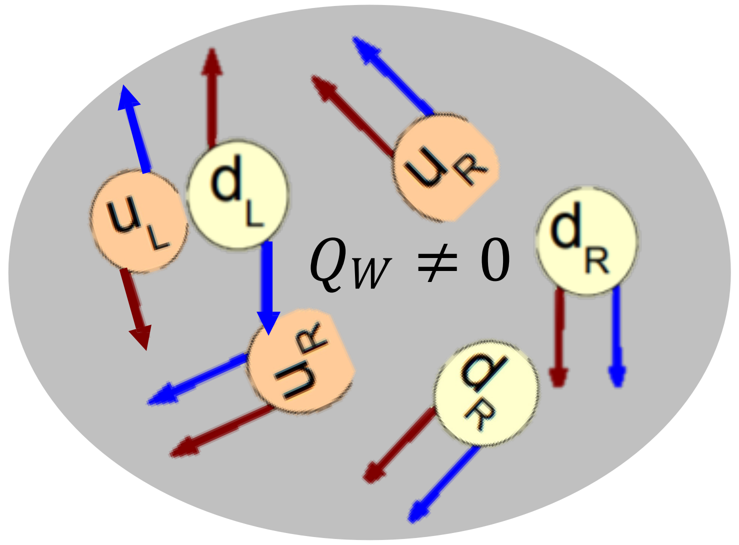

Chirality imbalance

Chiral magnetic effect

- CME: The generation of electric current along an external magnetic field induced by chirality imbalance.

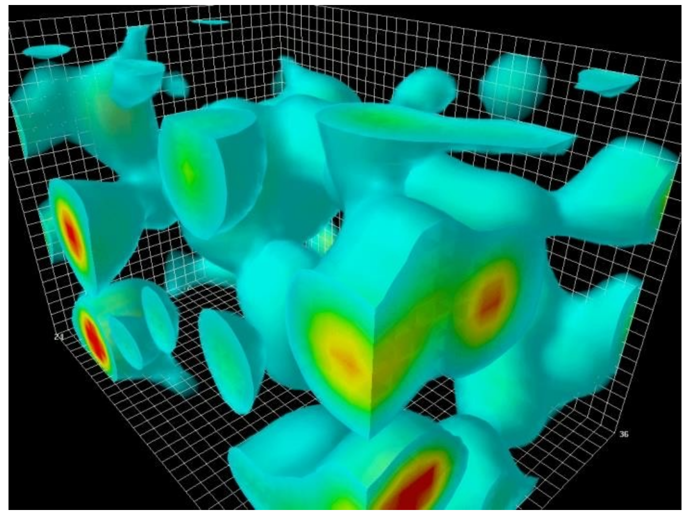

Non-trivial QCD vacuum structure

Red: momentum
Blue: spin

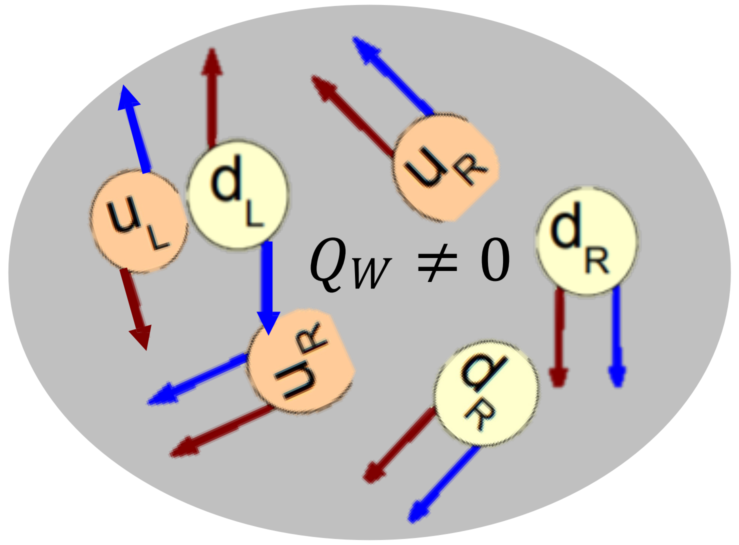

Chirality imbalance

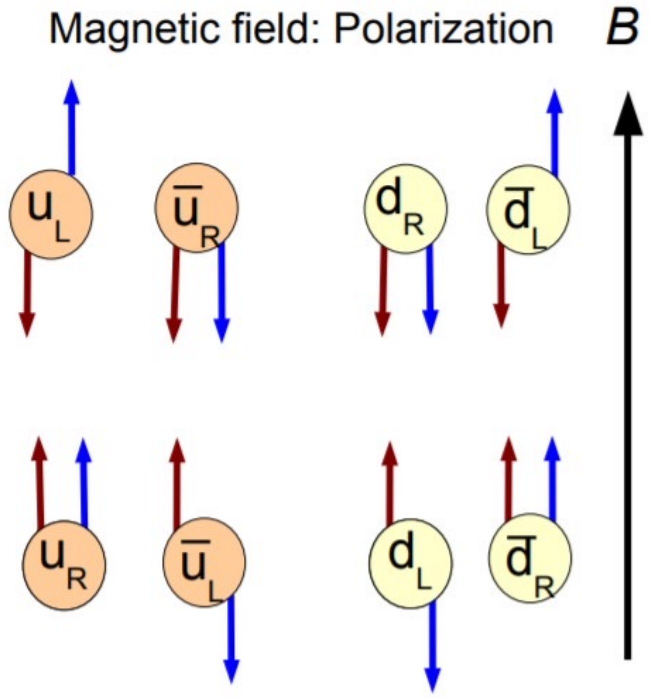

Under B field, LH quarks have $\vec{p}$ opposite to RH quarks

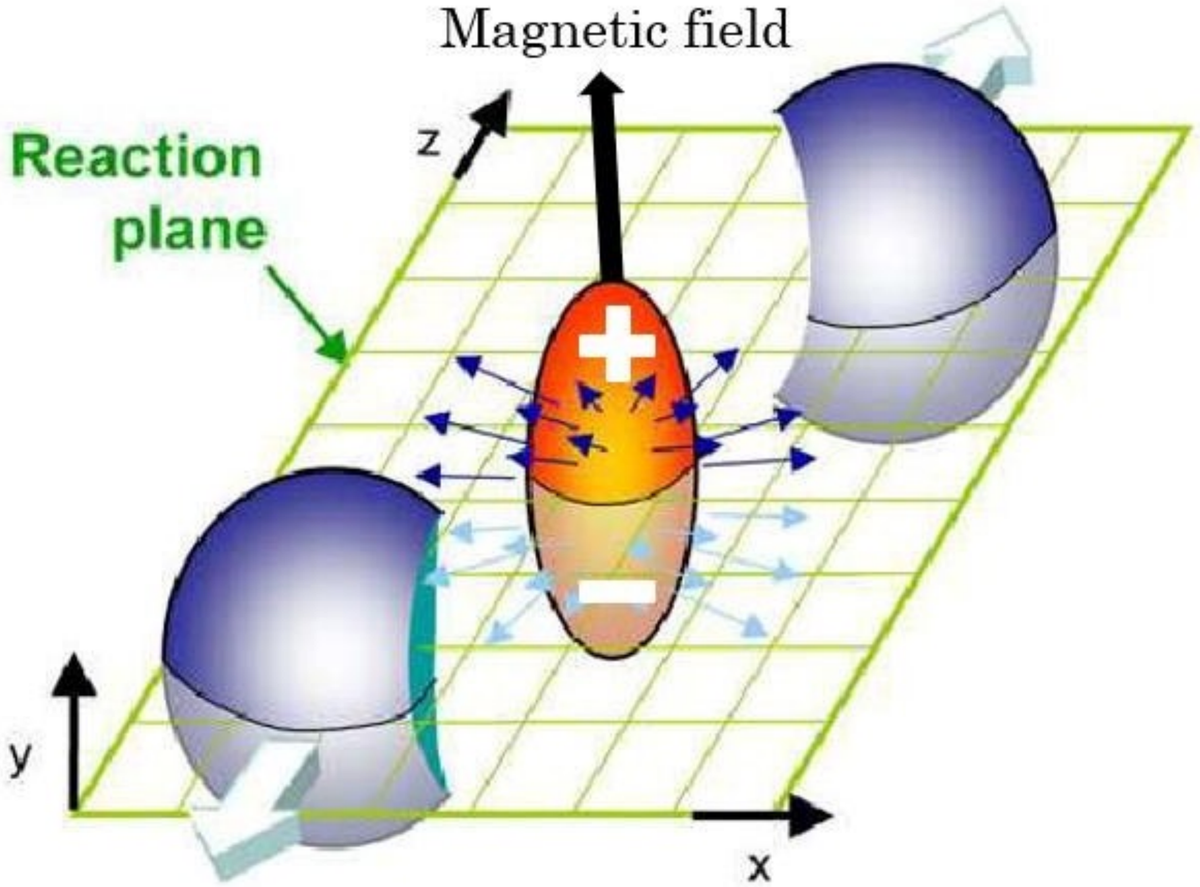

Current along B field

- Discovery of the CME implies: chiral symmetry restoration, local P/CP violation that may solve the strong CP problem

Chiral magnetic effect

- The commonly used $\Delta\gamma$ observable

$$\gamma_{\alpha\beta} = \langle\cos(\varphi_\alpha + \varphi_\beta - 2\Psi_{\mathrm{RP}})\rangle$$
$$\gamma_{\pm\mp} > 0, \gamma_{\pm\pm} < 0$$
$$\Delta\gamma = \gamma_{\pm\mp} - \gamma_{\pm\pm} > 0$$

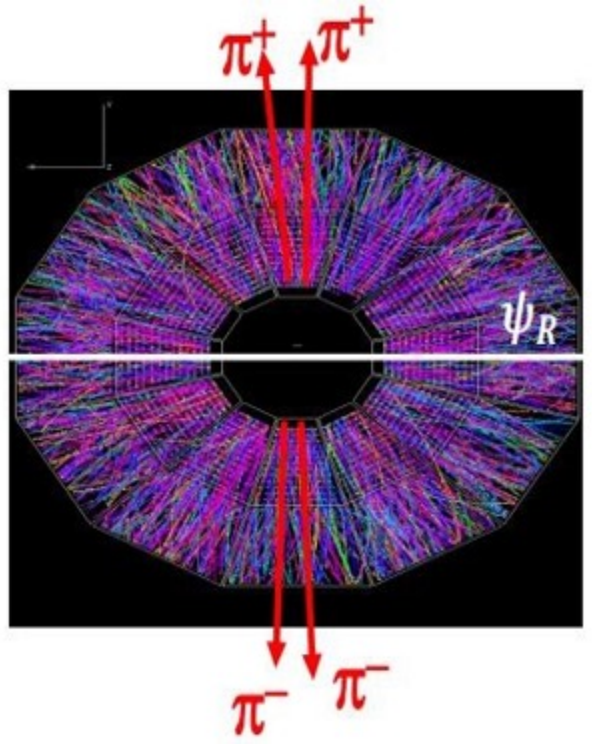

Chiral magnetic effect

- The commonly used $\Delta\gamma$ observable
$$\gamma_{\alpha\beta} = \langle\cos(\varphi_\alpha + \varphi_\beta - 2\Psi_{\mathrm{RP}})\rangle$$
$$\gamma_{\pm\mp} > 0, \gamma_{\pm\pm} < 0$$
$$\Delta\gamma = \gamma_{\pm\mp} - \gamma_{\pm\pm} > 0$$
- ALICE previous measurement showed that $\Delta\gamma$ significantly > 0.

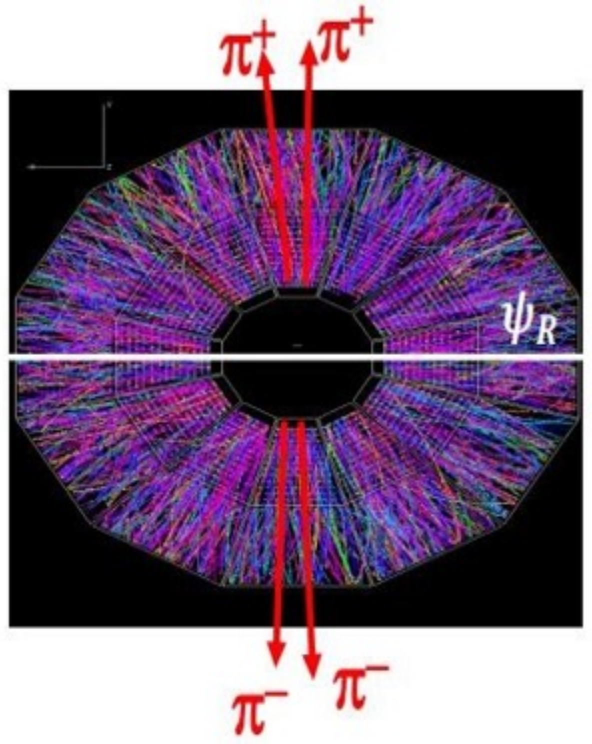

JHEP 09 (2020) 160

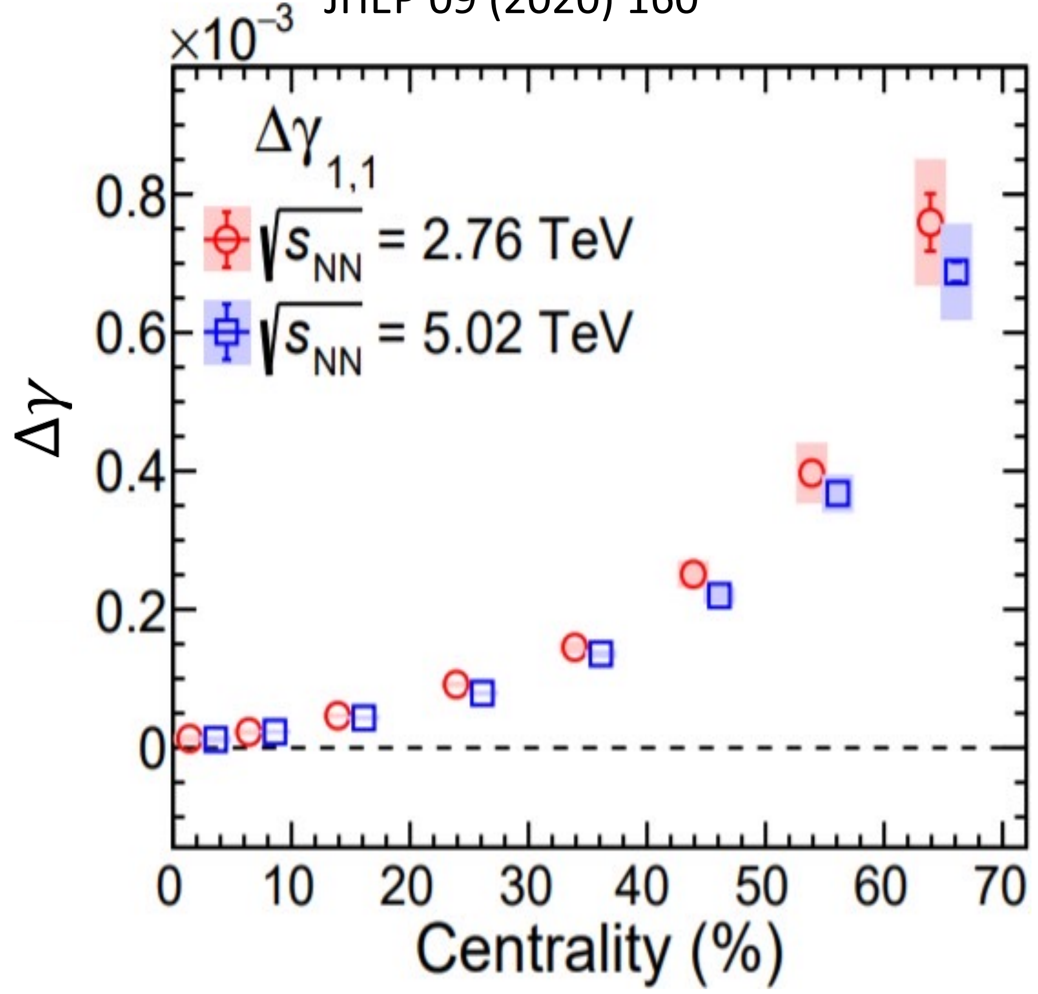

Chiral magnetic effect

- The commonly used $\Delta\gamma$ observable

$$\gamma_{\alpha\beta} = \langle \cos(\varphi_\alpha + \varphi_\beta - 2\Psi_{\mathrm{RP}}) \rangle$$
$$\gamma_{\pm\mp} > 0, \gamma_{\pm\pm} < 0$$
$$\Delta\gamma = \gamma_{\pm\mp} - \gamma_{\pm\pm} > 0$$

- ALICE previous measurement showed that $\Delta\gamma$ significantly > 0.
- However, $\Delta\gamma$ is heavily contaminated by local charge conservation (LCC) and resonance decays, mainly coupled with elliptic flow (noted as v_2)
    - e.g. $\rho^0 \to \pi^+\pi^-$, more OS pairs align in the Ψ_{RP} than B direction
- Similar value of γ observed in small system (no CME expected, pPb) confirming that the background is huge

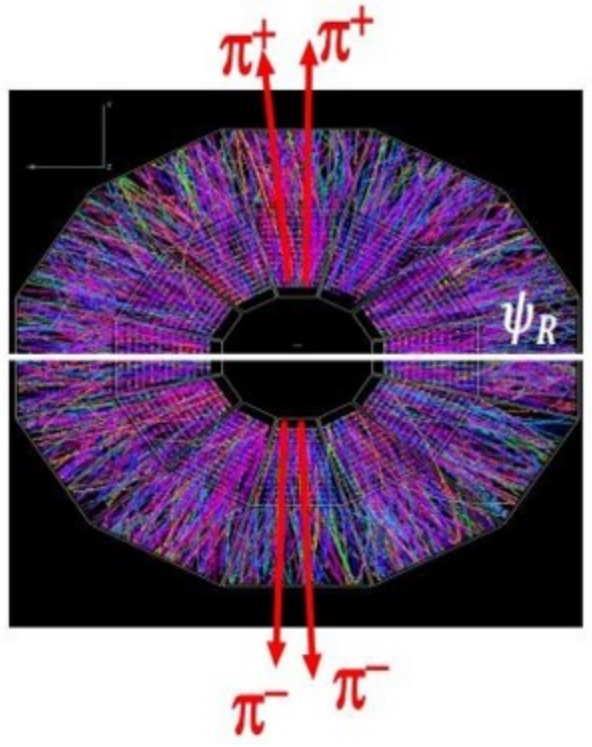

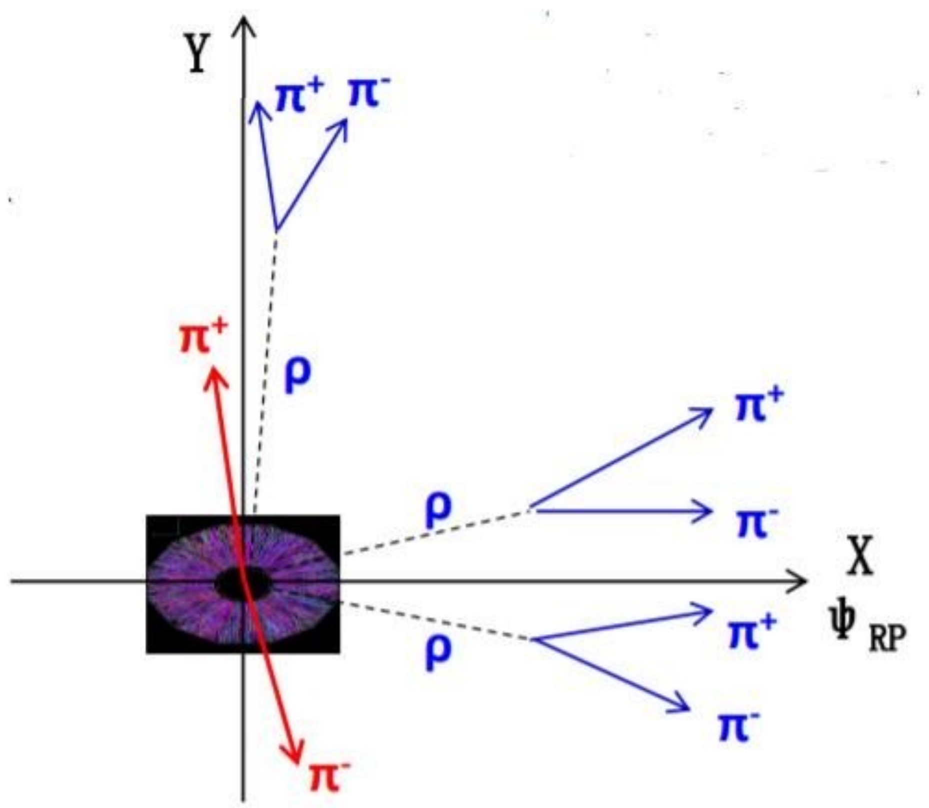

JHEP 09 (2020) 160

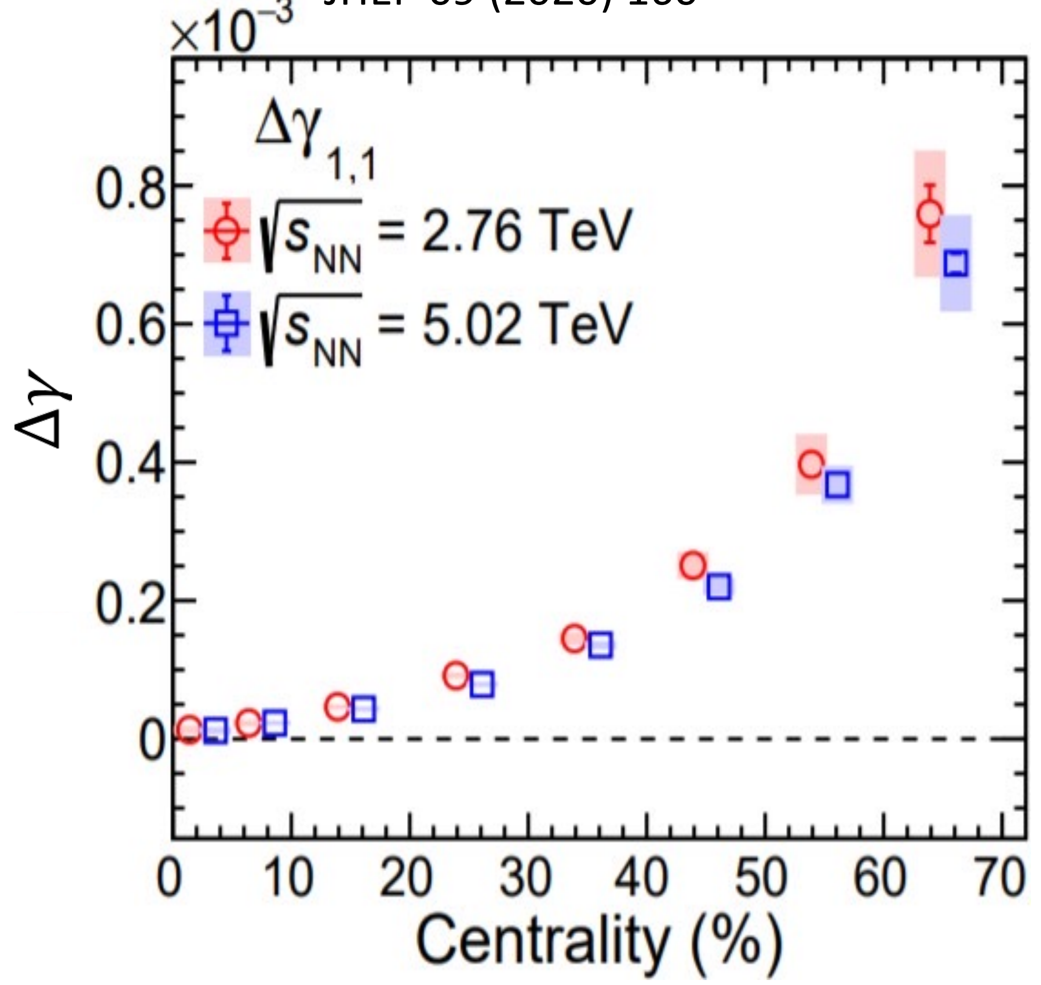

CMS, PRL 118 (2017) 122301

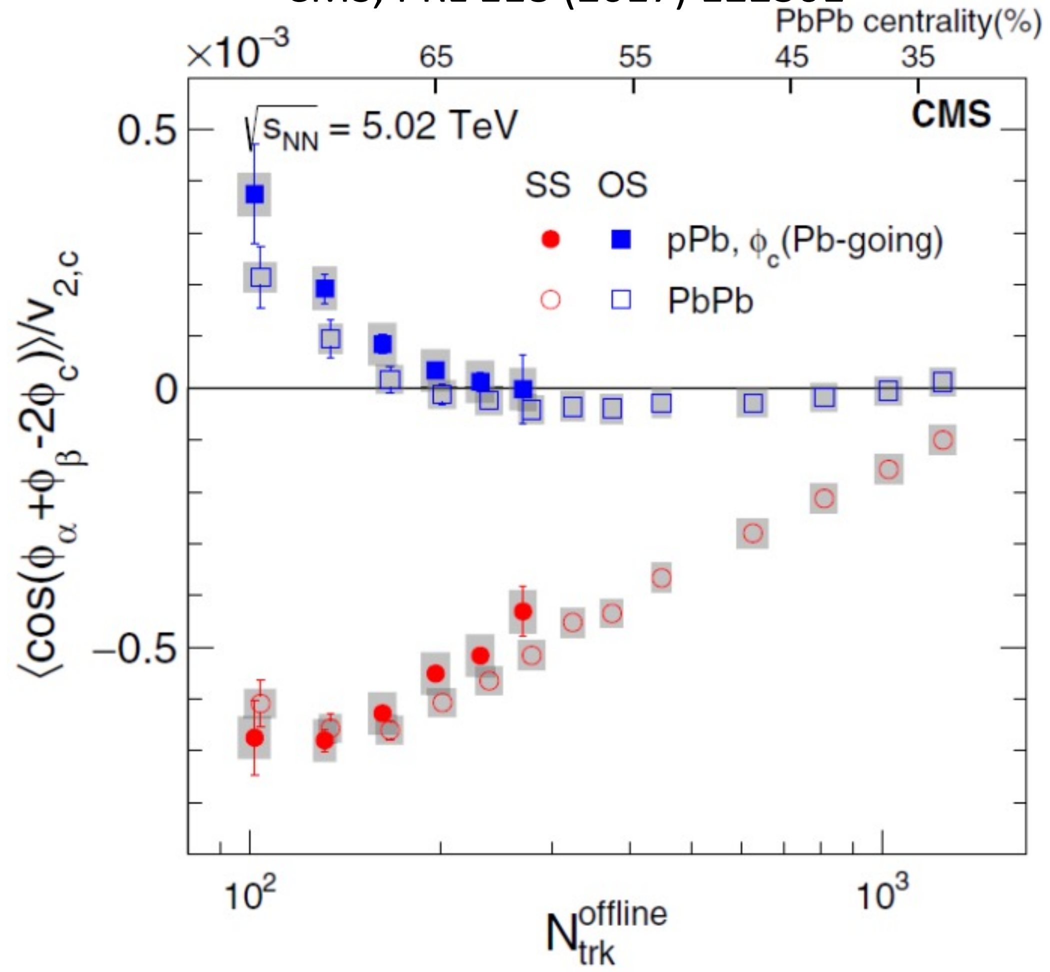

Chiral magnetic effect

- Mix harmonic measurements

$$\Delta\gamma_{112} \equiv \langle \cos(\phi_\alpha + \phi_\beta - 2\psi_2) \rangle \approx \langle \cos(\phi_\alpha - \phi_\beta) \rangle \langle \cos(2\phi_\beta - 2\psi_2) \rangle \approx \kappa_2 \cdot \Delta\delta \cdot v_2 + \text{CME}$$

$$\Delta\gamma_{123} \equiv \langle \cos(\phi_\alpha + 2\phi_\beta - 3\psi_3) \rangle \approx \langle \cos(\phi_\alpha - \phi_\beta) \rangle \langle \cos(3\phi_\beta - 3\psi_3) \rangle \approx \kappa_3 \cdot \Delta\delta \cdot v_3$$

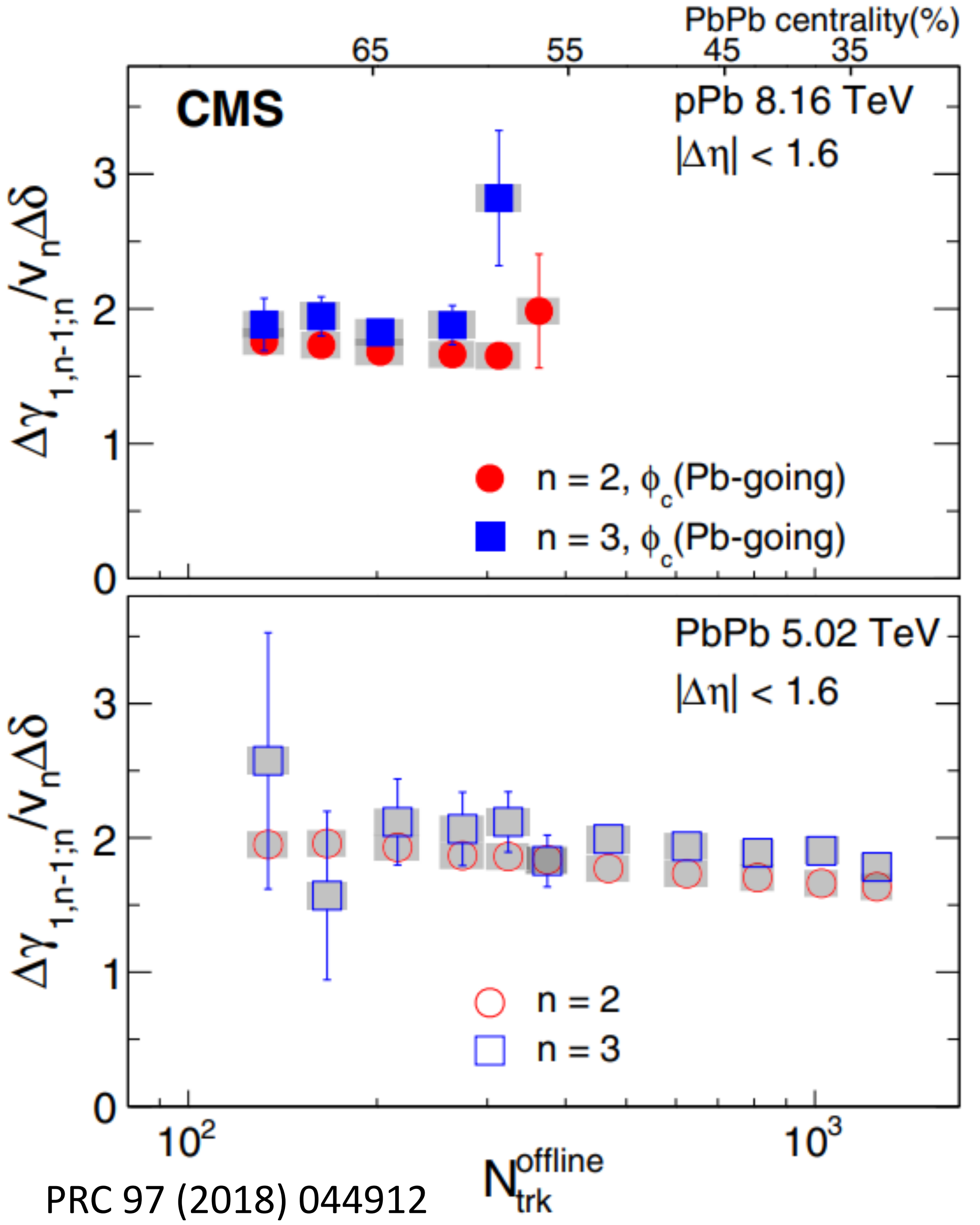

PRC 97 (2018) 044912

- $\kappa_2 = \Delta\gamma_{112}/v_2\Delta\delta$
- $\kappa_3 = \Delta\gamma_{123}/v_3\Delta\delta$
- Assume $\kappa_2 \approx \kappa_3$
- $\Delta\gamma_{1,1}^{\text{Bkg}} \approx \Delta\gamma_{1,2}\dfrac{v_2}{v_3}\dfrac{\kappa_2}{\kappa_3}$

  $\approx \Delta\gamma_{1,2}\dfrac{v_2}{v_3}$

- Upper limit on fraction of CME for each centrality interval from 0-40%
  - ranging from 15-18% at 95% CL
  - ranging from 20-24% at 99% CL

JHEP 09 (2020) 160

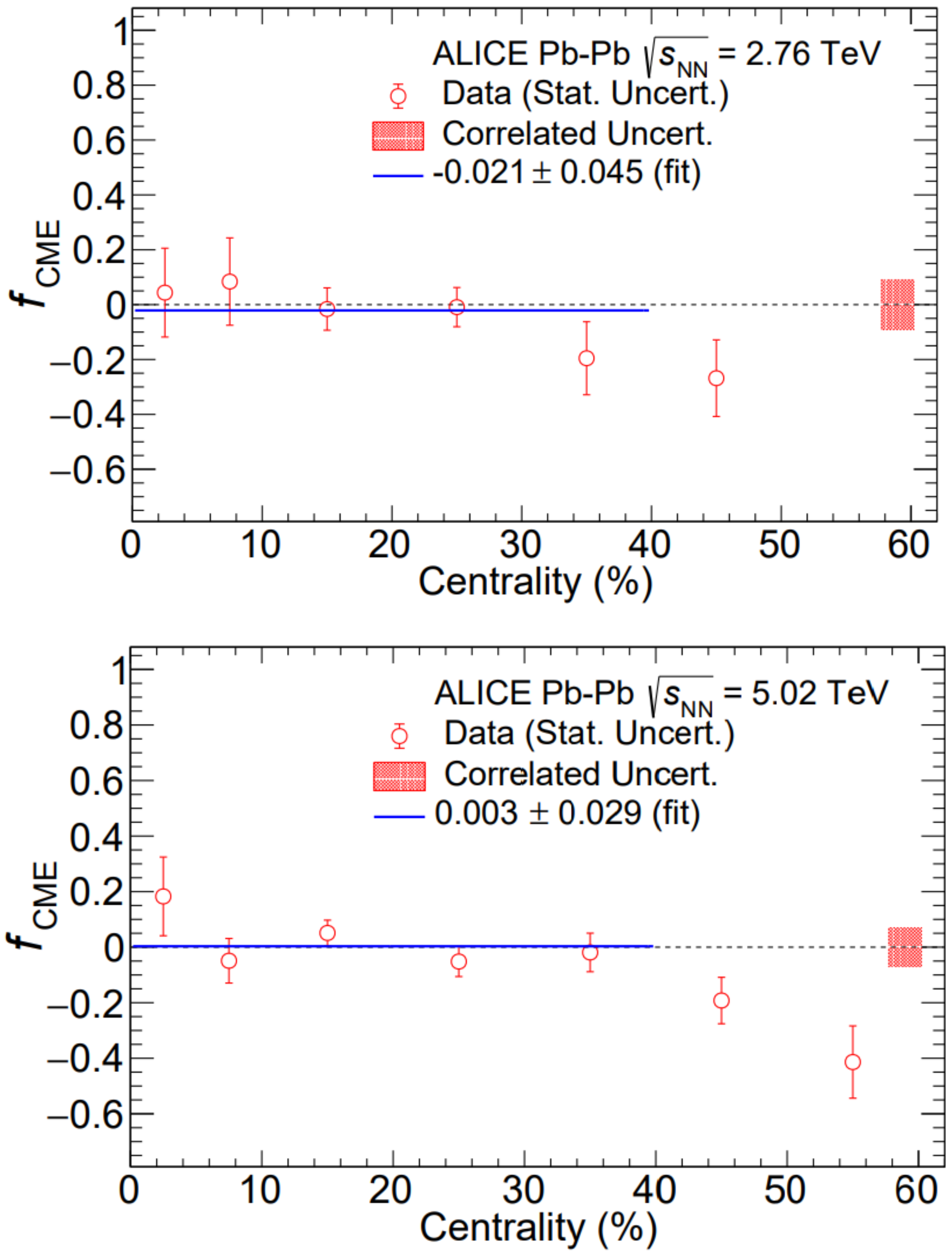

Chiral magnetic effect

- Event-Shape-Engineering
  - Define the second-order reduced flow vector

$$Q_{2,x} = \sum_i^M \cos(2\phi_i)\,, Q_{2,y} = \sum_i^M \sin(2\phi_i)$$

$$q_2 = |\boldsymbol{Q_2}|/\sqrt{M} = \sqrt{Q_{2,x}^2 + Q_{2,y}^2}/\sqrt{M}$$

  - Use q_2 to select different geometry. Use v_2 to quantify event anisotropy
  - A significant CME contribution → non-zero intercepts at $v_2 = 0$ (still the non-zero intercept has background from LCC)

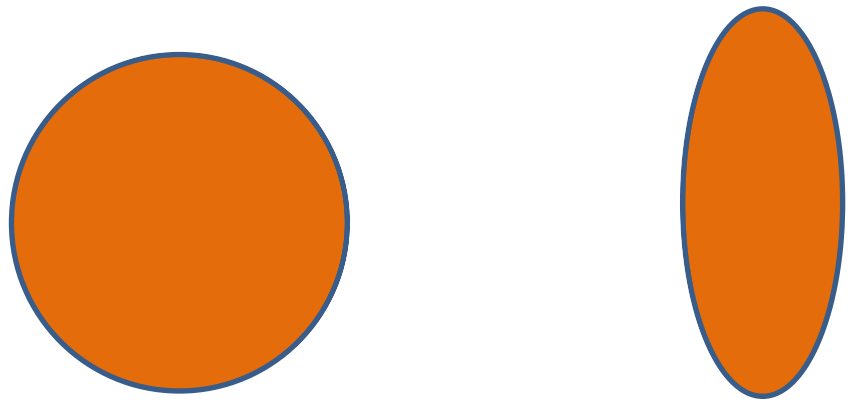

Small q_2 Large q_2

Phys. Lett. B 777 (2018) 151-162

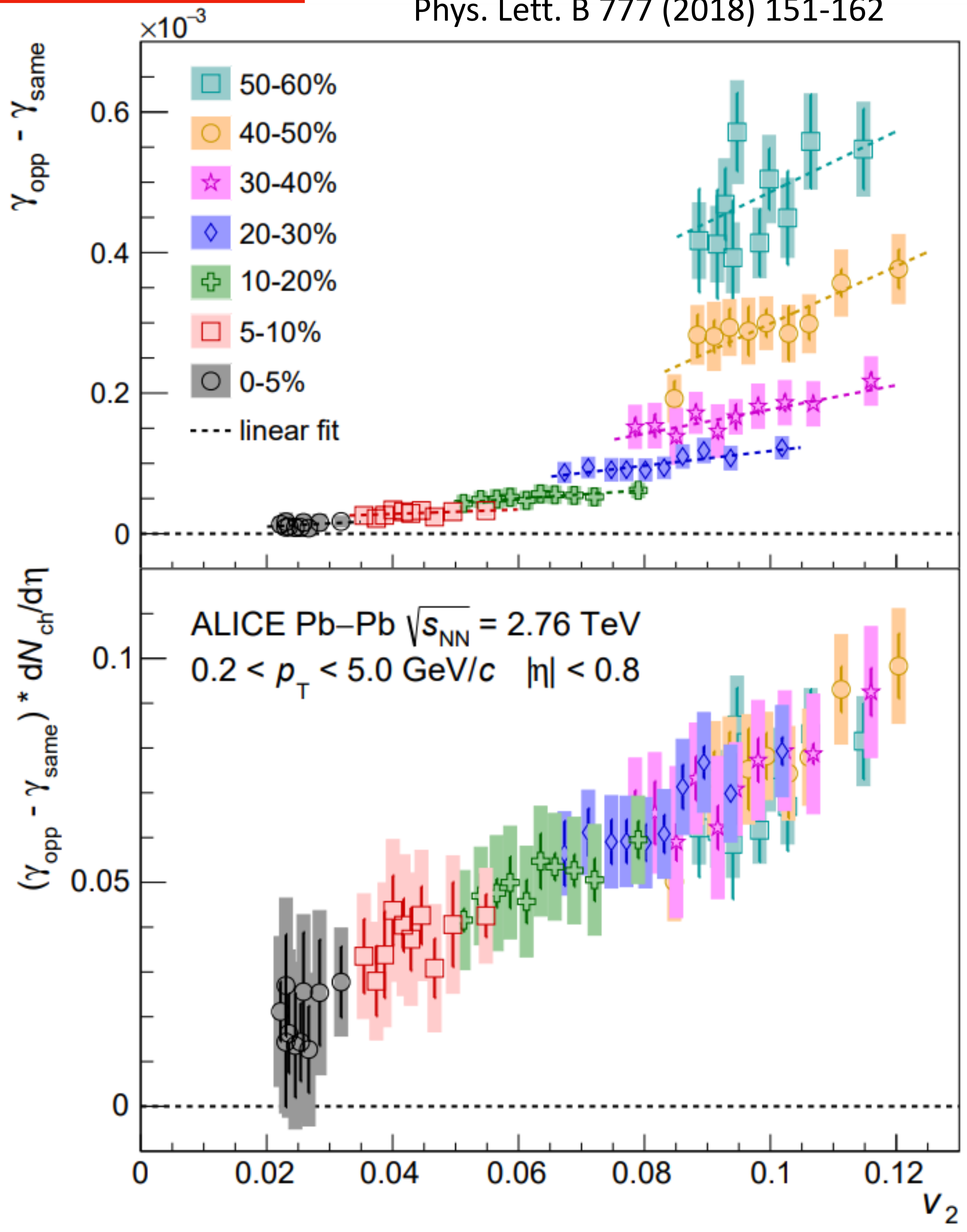

Chiral magnetic effect

- Event-Shape-Engineering
  - Define the second-order reduced flow vector

$$Q_{2,x} = \sum_{i}^{M} \cos(2\phi_i)\,, Q_{2,y} = \sum_{i}^{M} \sin(2\phi_i)$$

$$q_2 = |\boldsymbol{Q_2}|/\sqrt{M} = \sqrt{Q_{2,x}^2 + Q_{2,y}^2}/\sqrt{M}$$

  - Use q_2 to select different geometry. Use v_2 to quantify event anisotropy
  - A significant CME contribution → non-zero intercepts at $v_2 = 0$ (still the non-zero intercept has background from LCC)
  - Using three different initial-state models to estimate the dependence of CME signal to v_2

Phys. Lett. B 777 (2018) 151-162

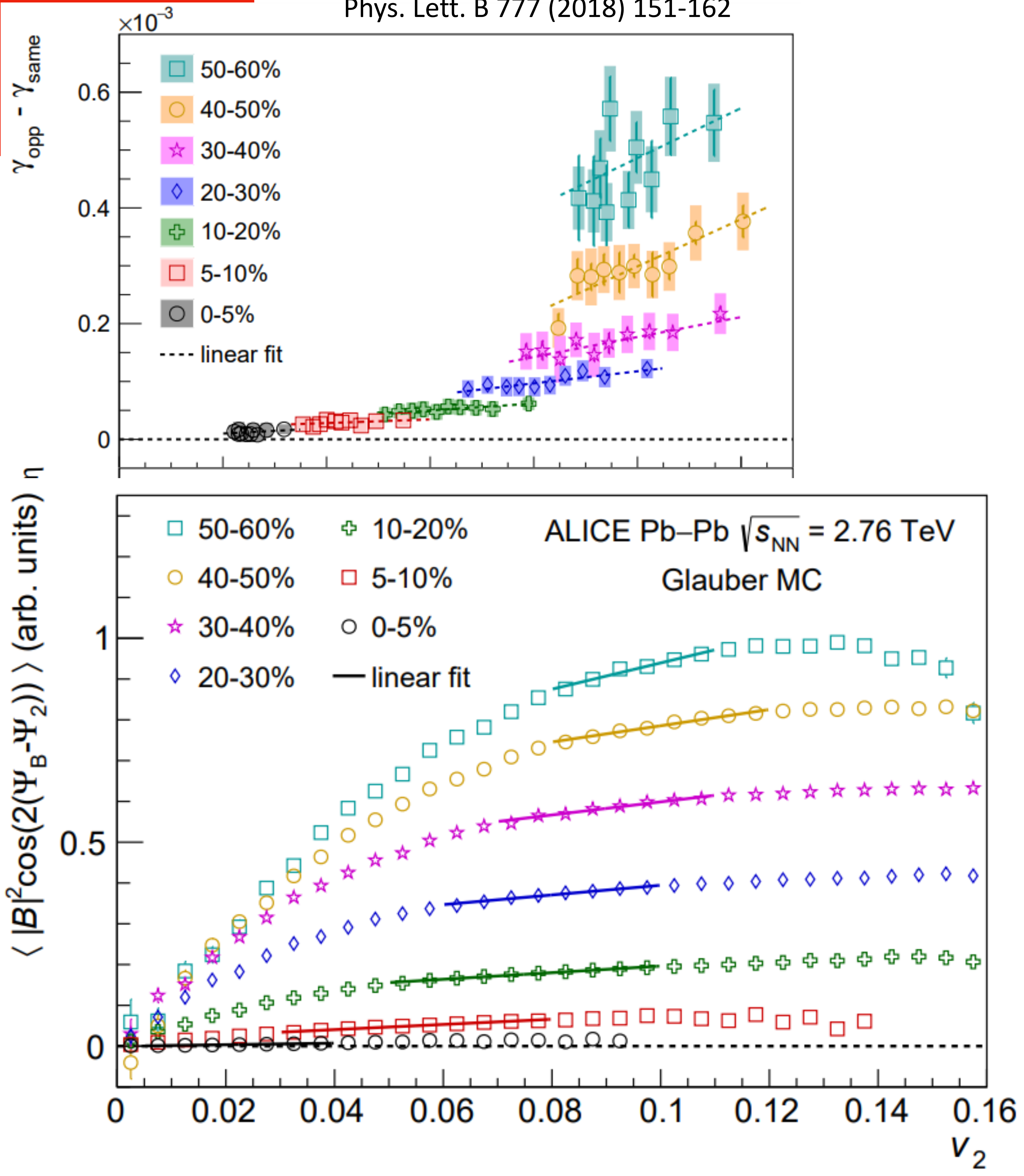

Chiral magnetic effect

Phys. Lett. B 777 (2018) 151-162

- Event-Shape-Engineering
  - Define the second-order reduced flow vector
    $$Q_{2,x} = \sum_i^M \cos(2\phi_i)\,, Q_{2,y} = \sum_i^M \sin(2\phi_i)$$
    $$q_2 = |\boldsymbol{Q}_2|/\sqrt{M} = \sqrt{Q_{2,x}^2 + Q_{2,y}^2}/\sqrt{M}$$
  - Use q_2 to select different geometry. Use v_2 to quantify event anisotropy
  - A significant CME contribution → non-zero intercepts at $v_2 = 0$ (still the non-zero intercept has background from LCC)
  - Using three different initial-state models to estimate the dependence of CME signal to v_2
  - The extracted CME fraction for three models used in the study suggests an upper limit on $f_{\rm CME}$ of 26 to 33% (depending on initial-state models) at 95% CL for the 10-50% centrality interval

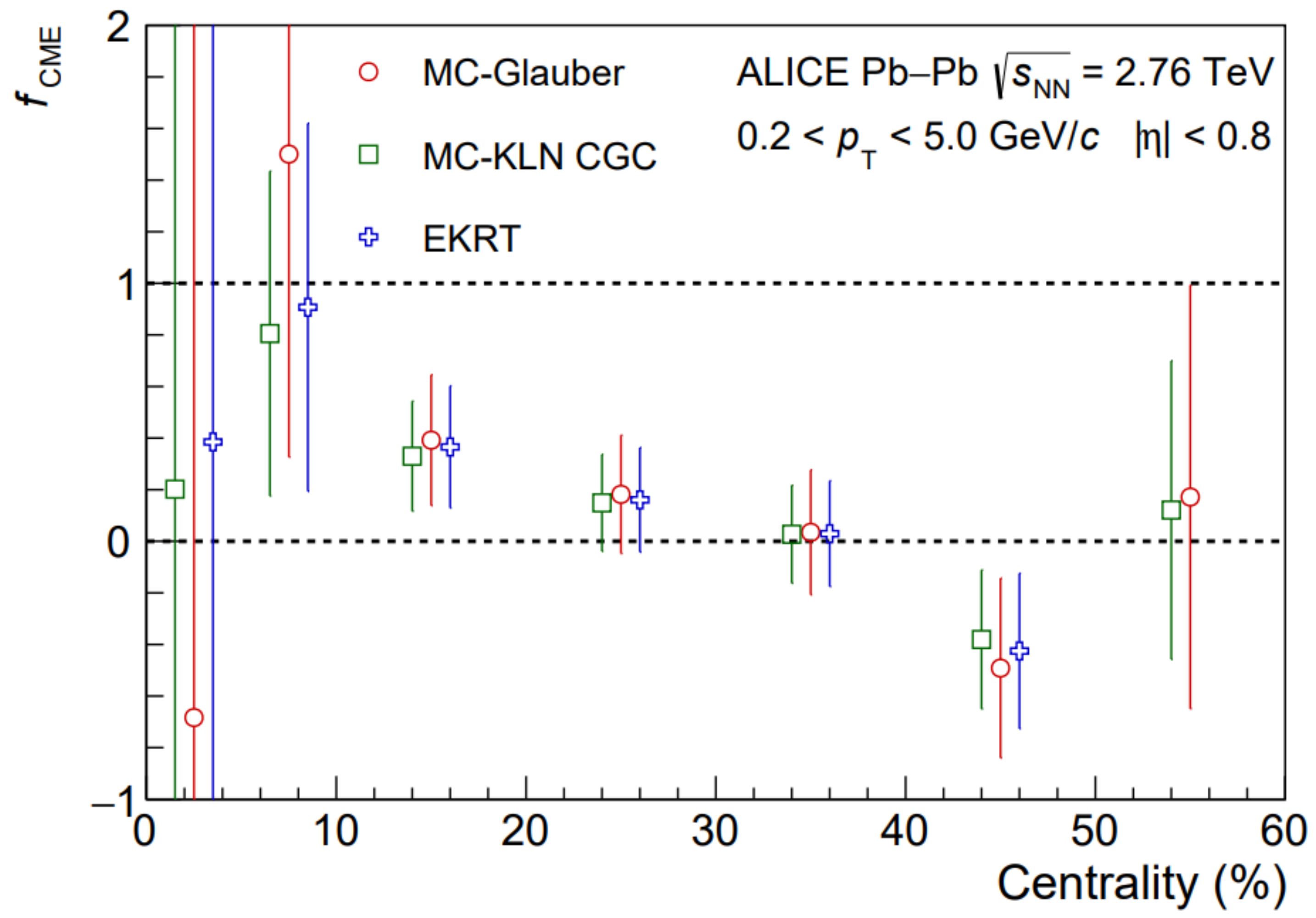

Weak dependence on initial states

Chiral magnetic effect

- A summary of the results for the upper limits for the CME signal at ALICE

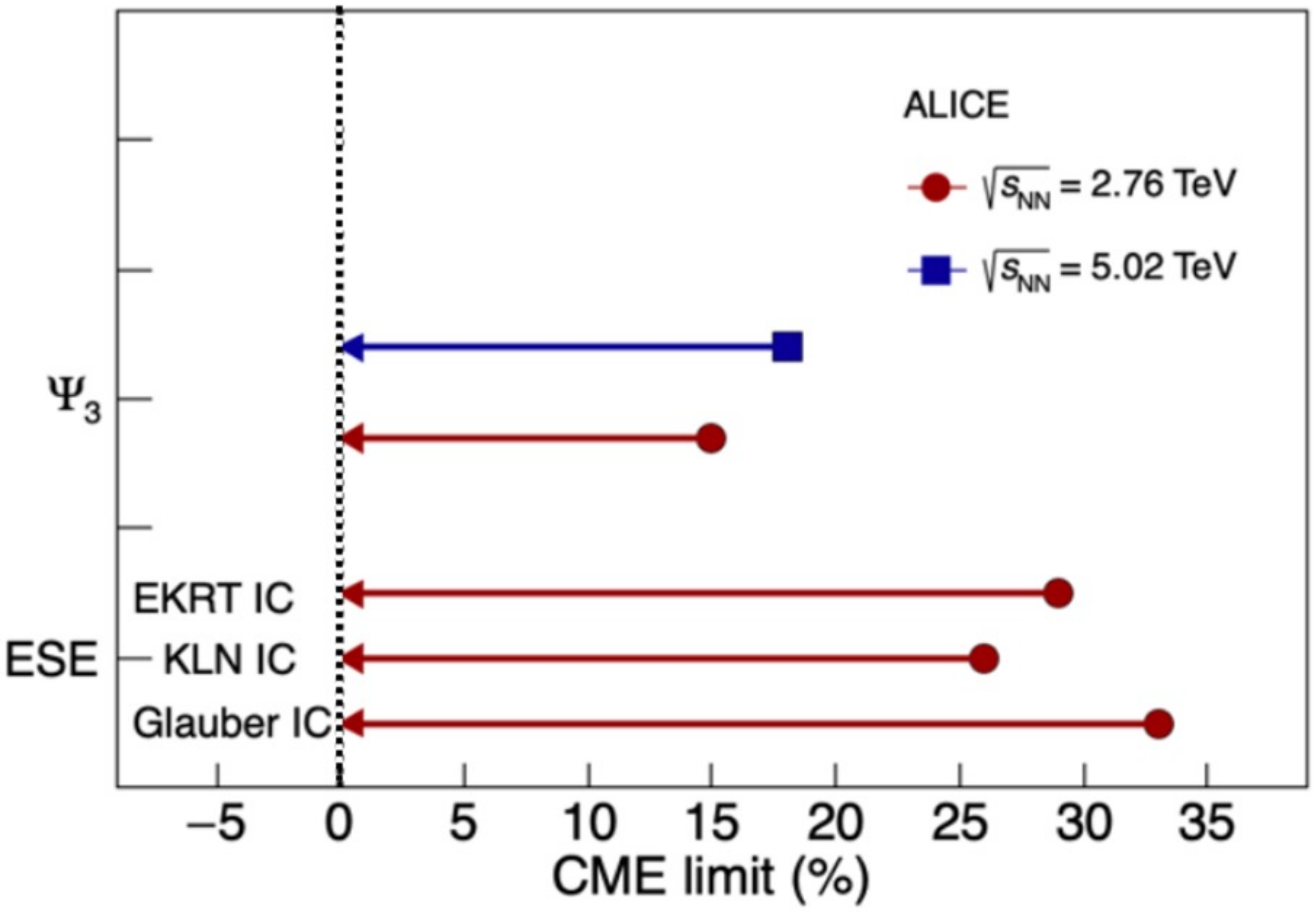

- It is clear that background is dominant
- CME is a very important physics. We have to quantify it
- Currently, the work on using the Spectator/participant planes method is ongoing

PhysRevC.105.024913

Summary

- The early-stage EM field can affect the motion of the final state particles via measurements of directed flow for particles and antiparticles.
- The differences in the measured global polarisation of Λ and $\overline{\Lambda}$ provide an upper limit for the magnitude of the magnetic field
- Direct studies for the existence of the CME in Pb-Pb collisions yielded upper limits of 26 to 33% for ESE and 15-18% at 95% CL for mix harmonic for the 0–40% centrality interval

THANKS

Extra Slides

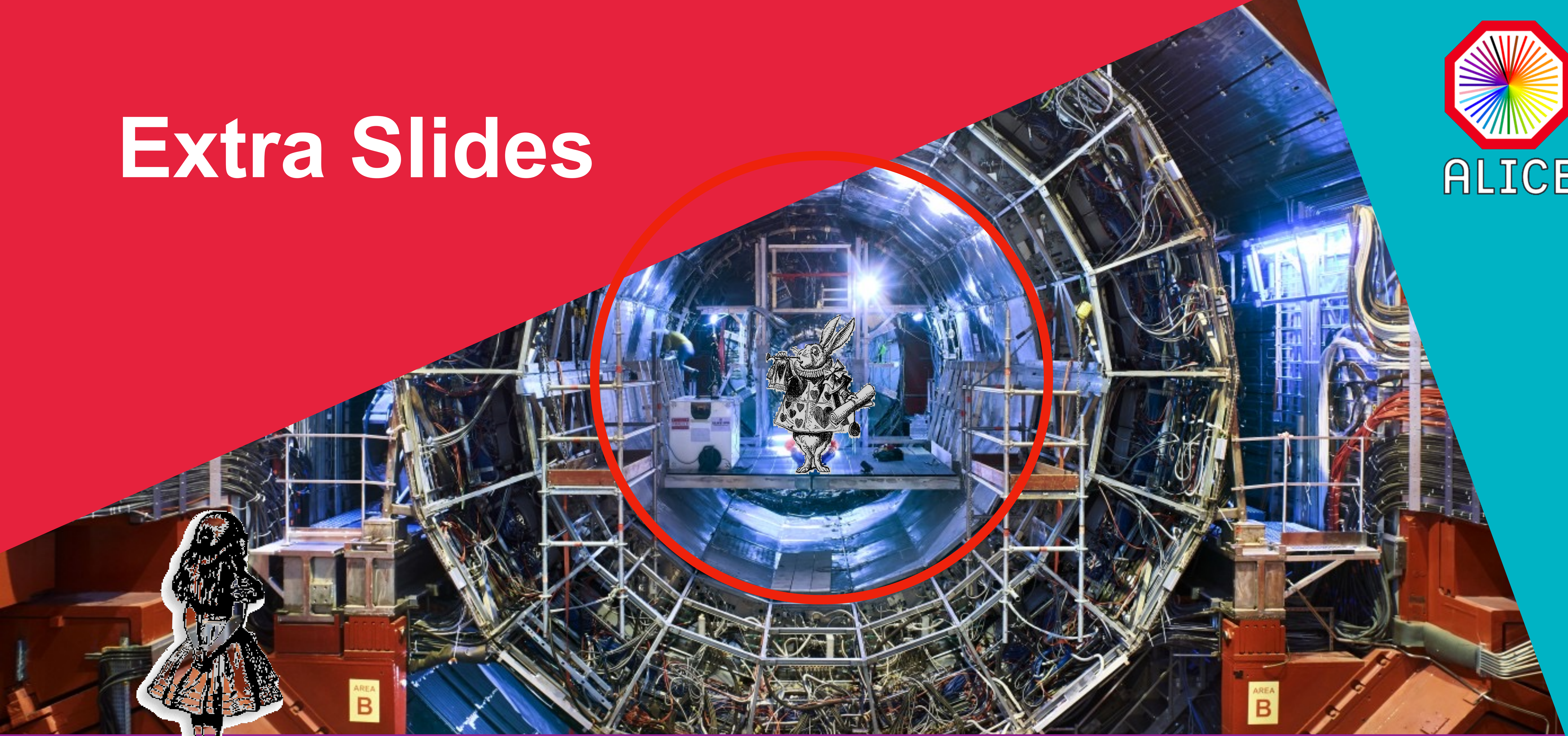

EB field simulation

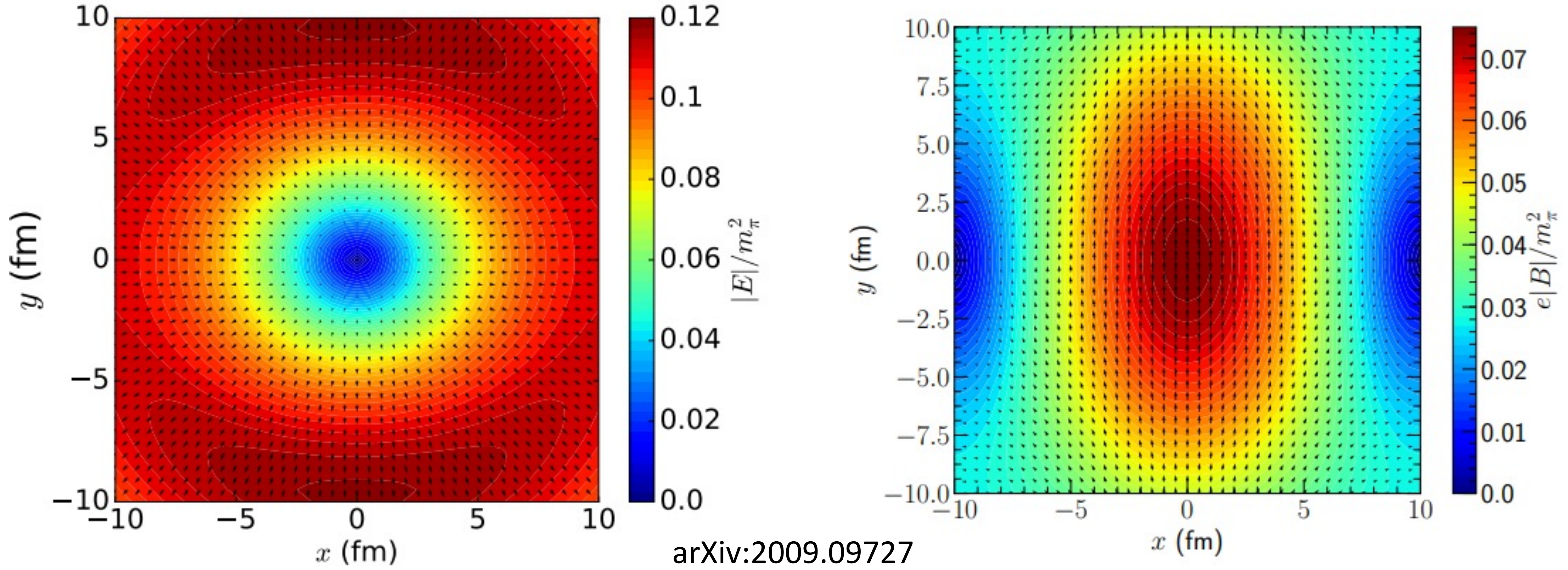

arXiv:2009.09727

Simulation of the electric (left) and magnetic (right) fields in the transverse plane after a Pb–Pb collision at 2.76TeV with 20–30% centrality